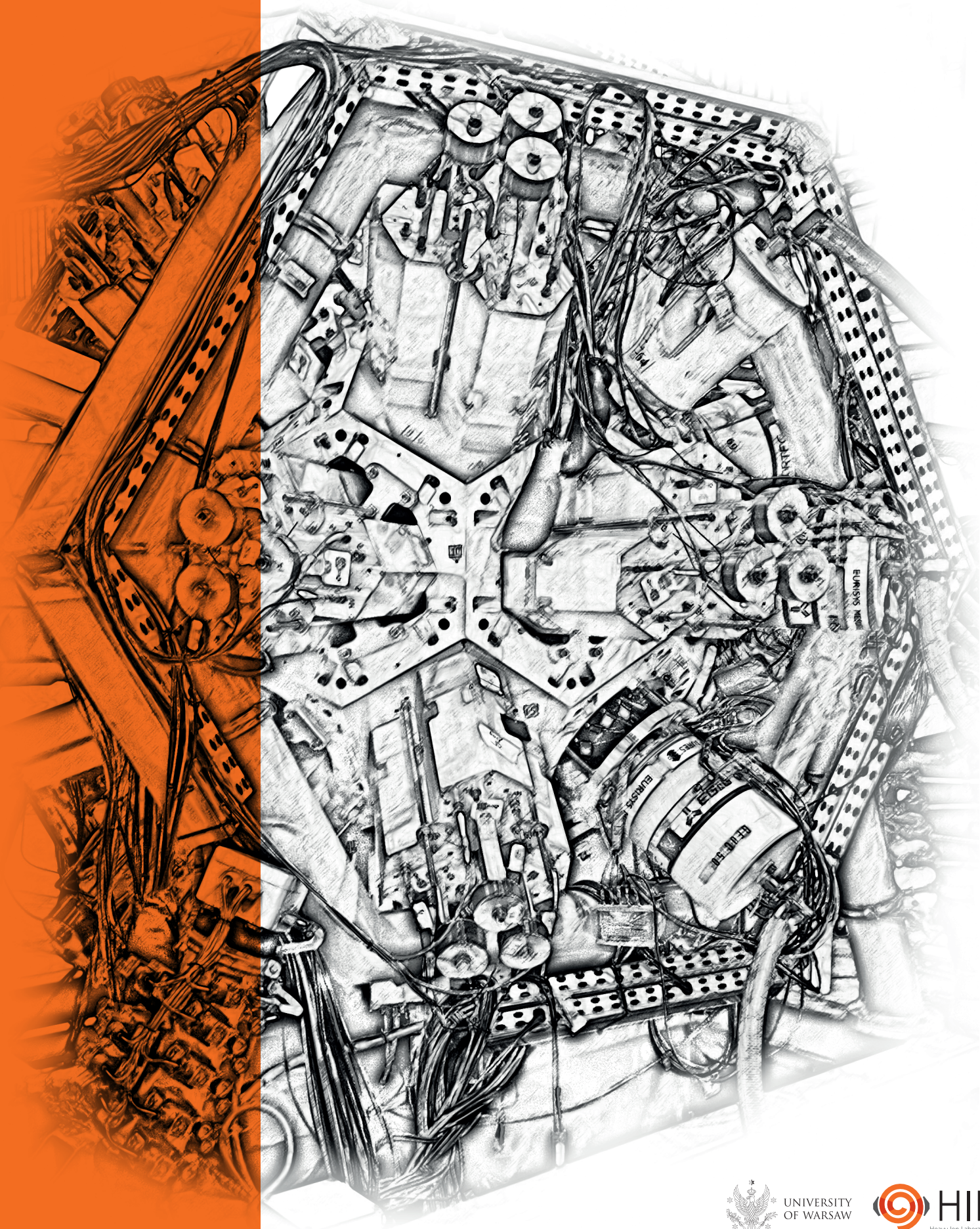


Heavy Ion Laboratory

ANNUAL REPORT 2023



UNIVERSITY
OF WARSAW



Heavy Ion Laboratory
University of Warsaw

ANNUAL REPORT

2023



Warszawa, June 2024

Various information concerning the Laboratory is distributed via the HIL mailing list.
In order to subscribe to the list please visit the page
<http://mail.slcyj.uw.edu.pl/mailman>

Annual Report of the
Heavy Ion Laboratory, University of Warsaw
ul. Pasteura 5a, 02-093 Warszawa, Poland
phone (+48)22-8222123, (+48)22-5546000
fax (+48)22-6592714
<http://www.slcyj.uw.edu.pl>

Editors:

Justyna Samorajczyk-Pyśk, Marzena Wolińska-Cichocka,
Andrzej Tucholski, Nicholas Keeley,
e-mail: raport@slcyj.uw.edu.pl
ISSN 1895-6726

Cover design:

Rafał Klęk

Contents

Introduction	5
A Laboratory overview and technical developments	7
A.1 Cyclotron operation in 2023 including tasks carried out in order to improve the infrastructure and efficiency	9
A.2 Calcium ion beam tests on ECRIS at HIL	11
A.3 Modernization of the spiral inflector	13
A.4 Import of equipment from the Svedberg Laboratory in Uppsala	14
A.5 RF system team activity	17
A.6 New LabVIEW Program to control remotely the XTRD-400K Amplifier	18
A.7 A standalone station with automatic loading, dedicated to the PETtrace cyclotron	19
A.8 Status of the EAGLE array	22
A.9 Preparation of thick isotopic Si target with high efficiency	24
A.10 Polish Workshop on the Acceleration and Applications of Heavy Ions	27
B Research for medical and biological applications	29
B.1 The influence of the presence of polyphenols on the stability of selected selenium compounds	31
B.2 Antioxidant and antibacterial abilities of selenium nanoparticles obtained by green synthesis using herbal extracts.	33
B.3 Synthesis and quality control of porphyrin labelled with ^{64}Cu	35
B.4 Porphyrin complexes of palladium as potential radiopharmaceuticals	38
B.5 Method of mechanical separation of ^{44}Sc from CaCO_3 targets after cyclotron irradiation	40
C Nuclear physics	45
C.1 Towards ^{57}Cu with EAGLE-NEDA-DIAMANT	47
C.2 DIAMANT at HIL – the NEEDI setup	50
C.3 Study of the anomalous behavior of the Coulomb energy difference in the $A = 70$, $T = 1$ izobaric multiplet	52
C.4 Shape coexistence and octupole correlations in the light Xe, Cs and Ba nuclei investigated with the EAGLE+NEDA+Plunger setup	56
C.5 Checking chirality – the lifetime of the 10^+ level in ^{128}Cs	59
C.6 Quasielastic barrier distributions for the $^{20}\text{Ne}+^{92,94,95}\text{Mo}$ systems: Influence of dissipation	62
C.7 The experimental campaign with the Warsaw SilCA(DSSD) array at the IJC Lab, Orsay, France	65
C.8 Low-energy electromagnetic structure of ^{110}Cd studied using Coulomb excitation	68
C.9 Microscopic calculations of collective properties of the even-even $^{180-198}\text{Pt}$ isotopes.	71

C.10	Testing the values of the spectroscopic factors of single-neutron states in ^{11}B and ^{14}C .	74
D	Appendices	77
D.1	List of experiments performed at HIL in 2023	79
D.2	Degrees and theses completed in 2023 or in progress	81
D.2.1	DSc (habilitation) degrees of HIL staff members	81
D.2.2	PhD theses of students affiliated to HIL, of HIL staff members, and supervised by HIL staff	81
D.2.3	MSc and BSc theses supervised by HIL staff members	82
D.3	Publications	84
D.4	Seminars	90
D.4.1	Seminars organised at HIL	90
D.4.2	Seminars co-organised by HIL	91
D.4.3	External seminars given by HIL staff	93
D.4.4	Poster presentations	95
D.4.5	Lectures for students and student laboratories	96
D.4.6	Science popularization lectures	97
D.5	Honours and Awards	99
D.6	Laboratory staff	100
D.7	Laboratory Council	101
D.8	Programme Advisory Committee	102
D.9	External HIL users	103
	List of Authors	105

Introduction

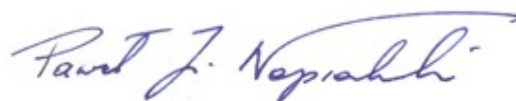
2023 was unequivocally the year of NEDA at the Heavy Ion Laboratory, setting a definitive course for our future endeavors. The majority of our experiments employed this unique neutron detector system. The team led by Dr. Marcin Palacz and Dr. Grzegorz Jaworski did a good job: they not only successfully integrated the NEDA detectors into the EAGLE spectrometer frame but also developed a fully digital data acquisition system and, notably, drew significant interest from numerous European research groups in our experimental campaigns at HIL. The success of the NEEDLE (NEDA+EAGLE) project also facilitated the introduction of a life-time measurement system from the University of Cologne, Germany, and the DIAMAND detector from the ATOMKI Institute, Hungary, to Warsaw. Additionally, scientists from LNL in Italy and IFJ PAN in Kraków played pivotal roles in deploying the digital data acquisition system. In 2023 our lab not only functioned as a User Facility but truly evolved into a hub of collaborative innovation. Their efforts significantly boosted our profile, attracting a multitude of European research groups to participate in our campaigns at HIL.

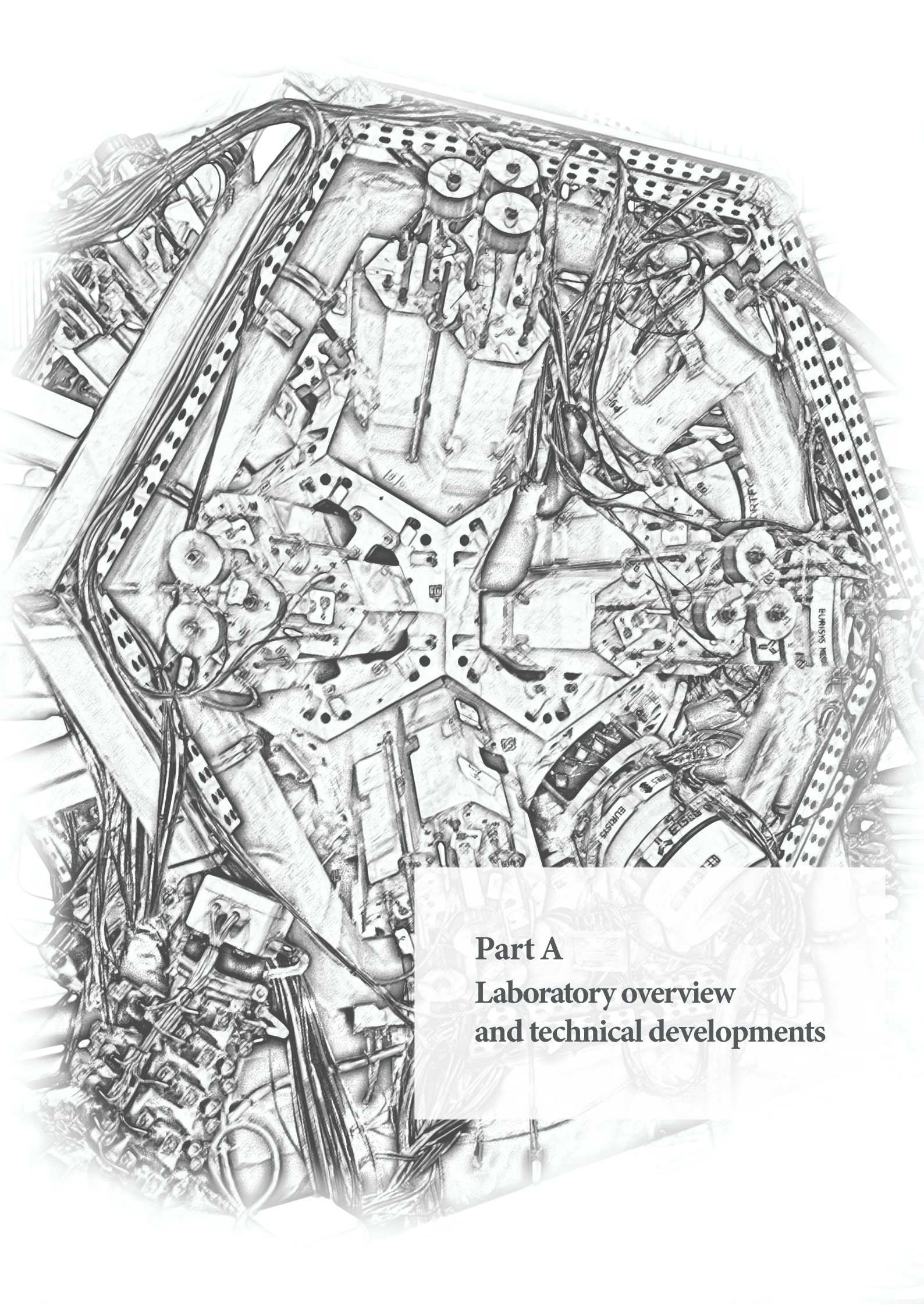
The extensive involvement of our international collaborators in the NEDA experiments at HIL received substantial financial backing from the EURO-LABS program, which commenced in September 2022. The overwhelming interest in these measurements meant that within a single year we nearly accomplished the four-year research support plan.

It comes as no surprise that Drs. Marcin Palacz, Grzegorz Jaworski, and Aleksandra Sentkowska were recognised by the Rector of the University of Warsaw with awards for their outstanding scientific achievements in 2023. Dr. Sentkowska received accolades for her habilitation thesis, heralded as the finest in Poland's field of analytical chemistry. The expansion of the HIL scientific team also highlighted the year.

Furthermore, 2023 saw the promotion of three of our researchers to Assistant Professor. Additionally, three new doctoral students selected our laboratory for their thesis work. The laboratory also welcomed numerous interns who chose to extend their collaboration into their bachelor's and master's theses. We were delighted to host students from across Poland once again for the 17th National Workshop on Heavy Ion Acceleration and Applications, reflecting the growing interest in nuclear physics and research at HIL—a crucial factor as we plan future experimental campaigns post-NEDA.

The achievements of the NEDA project at HIL, coupled with the satisfaction of the international research groups and the enthusiasm of new scholars embarking on their careers at our facility, would not have been possible without the exemplary performance of our accelerator team. Their dedication ensured the stable operation of the Warsaw Cyclotron, marking a third significant triumph for HIL in 2023 and setting the stage for celebrating the 30th anniversary of the first ion beam from the Warsaw Cyclotron in 2024.





Part A
Laboratory overview
and technical developments

A.1 Cyclotron operation in 2023 including tasks carried out in order to improve the infrastructure and efficiency

J. Chojiński, P. Gmaj, A. Bednarek, T. Bracha, P. Jasiński, W. Kalisiewicz, M. Kopka, W. Kozaczka, P. Krysiak, K. Łabęda, K. Makowski, I. Mazur, J. Miszczak, B. Paprzycki, K. Pietrzak, B. Radomyski, O. Nassar, L. Standyło

Heavy Ion Laboratory, University of Warsaw, Warszawa, Poland

Operation:

The basic activity of the technical team was to provide ion beams for experiments recommended by the PAC and approved by the HIL Director. The main effort was put into maintenance of the cyclotron infrastructure and the replacement of worn out elements. However, work related to development of the cyclotron infrastructure was not neglected.

ECR Ion sources:

The 14.5 GHz ECR ion source operated for the needs of the cyclotron and experiments. A new microwave amplifier was purchased and incorporated into the existing ECR control system. More information on this can be found in a dedicated article in this Report. Due to planned modifications of the microwave injection system for the 14.5 GHz source, extensive numerical calculations were carried out. The purpose of the calculations was to find the optimal geometry of the system and optimize the coupling of the microwaves to the plasma chamber. The work is still in progress. Currently, the source is constantly being tested to produce new metallic beams that are necessary for future experiments. The old 10 GHz ECR ion source is not yet in operation. After measurements of its magnetic field in the trap region the permanent magnets lost their magnetization. It is planned to rebuild the complete magnetic trap for the 10 GHz ECR source by buying a new set of magnets in 2024 and prepare a system for the production of metallic beams with this source. A number of mechanical components are ready for assembly, the set of coils is already prepared along with magnetic yokes and a movable platform. Completion of the magnetic trap is planned in the coming months. It will take approximately three months to test the operation of the reconstructed source.

RF system:

In 2023 the RF Generator team was responsible for carrying out current experiments on the cyclotron and maintaining the existing "Chryzolit" amplifier system, as well as testing and commissioning the new system as part of the warranty repair together with the contractor — the "POPEK-Elektronik" company from Zamość, Fig 1.

During the visits of the manufacturer to the HIL premises tests of most components were performed:

- converter anode power supplies for both amplifiers
- screen grid power supply system for both amplifiers
- filament power supply system for both amplifiers

- crowbar circuits to protect both amplifiers against excessive voltage/power
- anode and output circuit tuning systems for both amplifiers

Also, selected tests of the amplifiers connected to dummy load and the actual cyclotron resonators were performed.

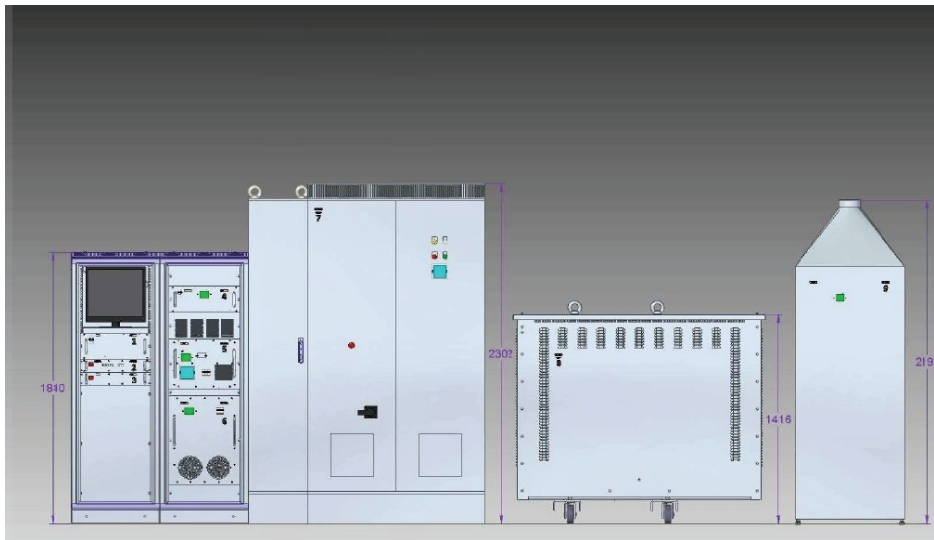


Figure 1: Control, power supply and protection systems of a single amplifier.

By the end of 2023 the manufacturer had still not delivered the control grid power supply for both of the amplifiers. All tests were performed using HIL grid power supplies. While the computer control for the above-mentioned systems works, by the end of 2023 it had not been properly integrated by the contractor into one system constituting the operator's desktop. At the beginning of 2023 we also obtained from the University of Uppsala in Sweden some high power tubes similar to the tubes in our new amplifiers, and some RF components from their decommissioned cyclotron. The tubes obtained have slightly different sockets and max. anode power, but other electrical parameters are identical.

Cyclotron:

The U-200P cyclotron itself required only usual maintenance in 2023. The cyclotron team's main focus was preparing the machine for upcoming experiments. Due to the planned reconstruction of the cyclotron's magnetic field, in order to increase the ion transmission coefficient, intensive tests of the magnetic field measurement system based on search coil technology were carried out. The tests showed an error in the materials used in the construction of the encoder, which resulted in the postponement of the planned field measurement cycle until the appropriate encoder was obtained and installed.

As every year, in October the students' workshop was held, but this time without the actual use of the cyclotron.

A.2 Calcium ion beam tests on ECRIS at HIL

L. Standyło, J. Chojiński, K. Makowski, O. Nassar, K. Sudlitz

Heavy Ion Laboratory, University of Warsaw, Warszawa, Poland

Metallic beam tests were performed on the ECR ion source. Tests included ion beams that have not yet been accelerated in the U-200P cyclotron, but for which there is huge experimental demand. The ion beams were produced using various techniques: ^{40}Ca (oven [1], enlarged crucible — sputtering [2]), ^{56}Fe (MIVOC [3]) and ^{58}Ni (insertion technique — sputtering [4], MIVOC [3], oven [1]). The following report describes research on the production of a ^{40}Ca ion beam with the oven technique. The oven was constructed in the Heavy Ion Laboratory — Fig. 1 — and is constantly being developed. The oven fulfills the temperature and capacity requirements, its maximum operating power is 40 W. Design allows the position of the oven head in relation to the plasma chamber to be changed in the range of 0–25 mm, which affects the intensity of a given beam and changes the tuning of the injected microwave power.

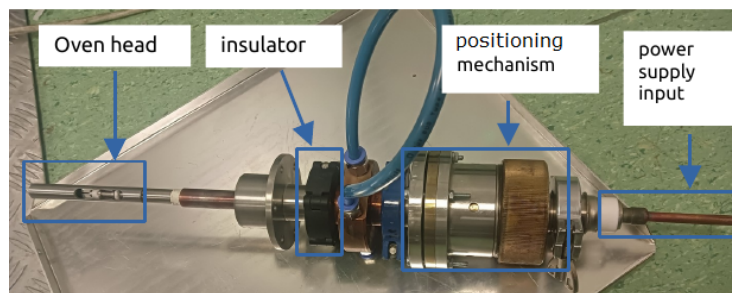


Figure 1: The complete oven structure mounted at the injection part of the ECR source. The oven potential is usually lower than the source potential.

Pure metallic calcium with admixtures of calcium oxide, CaO , of the order of 1%, was used as the material for beam production. The material was heated to temperatures of 600–850 °C, causing its complete evaporation, which proves the thermal efficiency of the oven. The capacity of the crucible in the furnace allows us to place 200–250 mg of calcium in the form of lumps with a diameter of 1–2 mm. The operating parameters of the source for the production of a calcium beam were optimized for a 6^+ charge state. Mainly helium was used as the buffer gas, but some measurements were made with nitrogen. The microwave power was usually in the range of 100–200 W. Several hours of slow heating of the material are needed to ensure the heated material obtains the appropriate conditions for evaporation. The first tests allowed us to obtain a stable $^{40}\text{Ca}^{+6}$ beam with a current of 45 μA for approximately 24 hours. In addition to the charge states of calcium ^{40}Ca (abundance 96.9%), states of the ^{44}Ca isotope (abundance 2.09%) were observed in the spectrum — Fig. 2. For this example (Fig. 2), the charge state distribution has a maximum for state 5^+ ($A/Z=8$).

The next tests enabled a beam to be maintained for 48 hours with a current in the range 45–75 μA (maximum 95 μA with 300 W RF power); the beam current did not remain stable. The maximum of the charge state distribution shifted towards higher states with increasing microwave power — Fig. 3. Unfortunately, higher microwave power results in significant beam instability or a drastic beam drop. The measurements showed that the optimal microwave power for the tested 6^+ charge state was around 180 W.

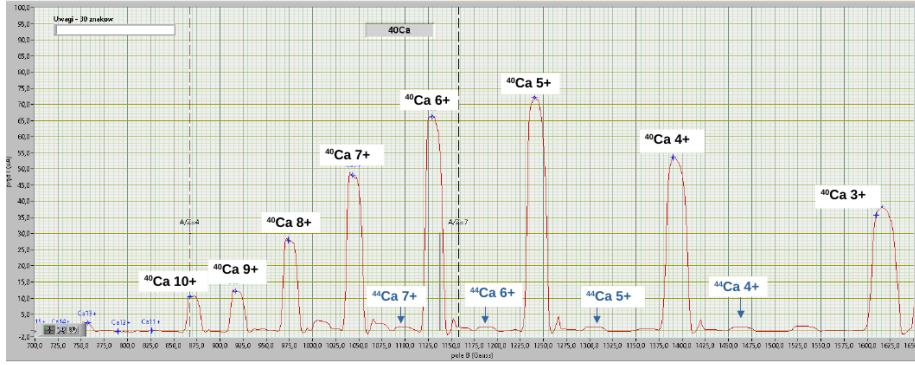


Figure 2: An example of a spectrum for calcium, collected at a power of 140 W. The vacuum at injection was 1.5×10^{-6} mbar and 2×10^{-7} mbar at extraction. The buffer gas was helium. On the vertical axis is the beam current for the specific charge states, and the magnetic field of the analyzing magnet (A/Z) is on the horizontal axis.

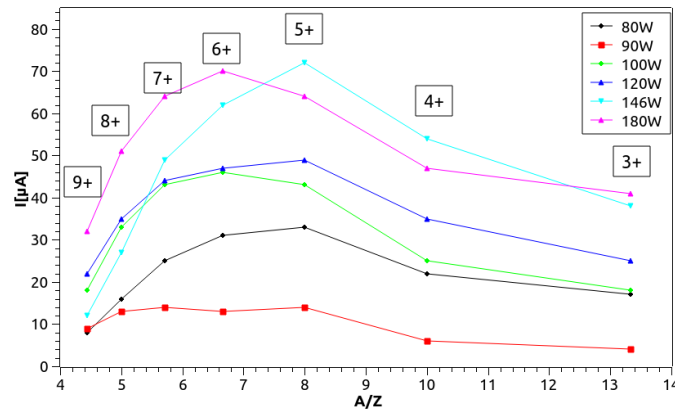


Figure 3: Charge state distribution for ^{40}Ca depending on the microwave power input.

The estimated material consumption was approximately 3–4.5 mg/h and, unfortunately, it was 10 times higher than presented in Ref. [5]. High material consumption was probably caused by a non-optimal oven position relative to the plasma chamber and parasitic heating of the oven head by microwaves. Another factor could be the too high power of the oven, exceeding 30 W. In order to improve the obtained results and further develop the oven technique it is planned to cover the oven structure with a screen to minimize the impact of the microwave power. It is also planned to use another form of heated material, e.g. in the form of pellets. This will allow us to fill the oven volume as completely as possible and slow down the melting time of the material. The goal of the current research is to obtain a stable beam of calcium ions with a material consumption not exceeding 1 mg/h.

Bibliography

- [1] R. Geller *et al.*, Rev. Sci. Instr. **63** (1992) 2795.
- [2] V.N. Loginov *et al.*, Phys. Part. Nucl. Lett. **16** (2019) 30.
- [3] H. Koivisto *et al.*, Nucl. Inst. and Meth. **B 94** (1994) 291.
- [4] T. Nakagawa *et al.*, Proceedings of: 11th International Workshop on Electron Cyclotron Resonance Ion Sources, Groningen, Rep. KVI-996, (1993) 208.
- [5] H. Koivisto *et al.*, AIP Conference Proceedings **600** (2001) 255.

A.3 Modernization of the spiral inflector

*J. Choiński, B. Radomyski, M. Antczak, P. Jasiński, W. Kalisiewicz, R. Kopik,
K. Labęda, B. Paprzycki*

Heavy Ion Laboratory, University of Warsaw, Warszawa, Poland

The positive results from the accumulated experience of operating the modified inflector in 2022 convinced us that further modernization was worth the effort [1]. As first step the power supply system was changed and was connected to the upper part of the inflector's body. The second step concerned the reduction of the inflector's height to receive a space for changing its position in relation to the median plane of the cyclotron, see Fig. 1.

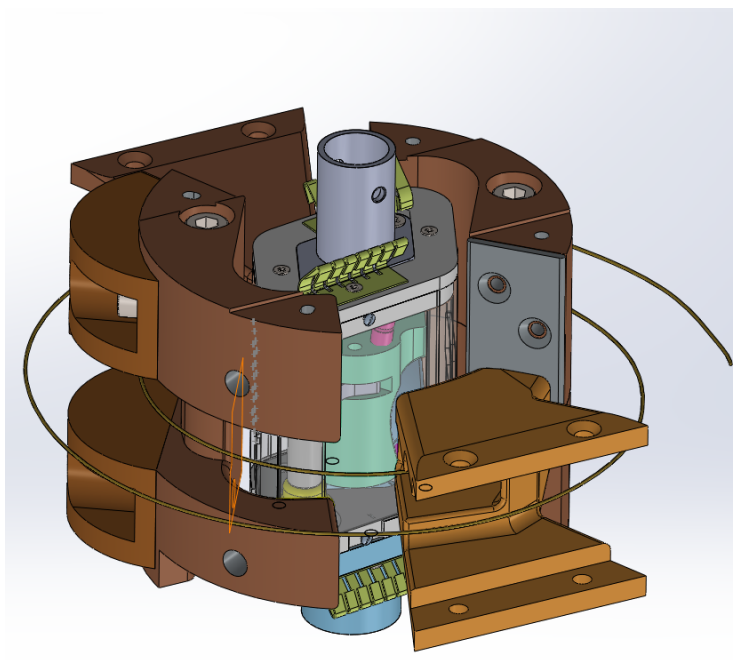


Figure 1: View of the central region with smaller diameter spiral inflector.

The next stage, a new version of the inflector, is now planned. It have a diameter of 55mm, enabling simple installation through the magnet, and will later be equipped with a vacuum lock, so that it can be removed from the cyclotron without breaking the vacuum. The operators will gain an additional degree of freedom, the possibility to rotate the inflector around its vertical axis. Movement of the inflector up and down with rotation will enable the operator to tune much better an injected ion beam to the cyclotron is requirements.

Bibliography

- [1] J. Choiński *et al.*, HIL Annual Report (2022) 11.

A.4 Import of equipment from the Svedberg Laboratory in Uppsala

J. Choiński, M. Antczak, T. Bracha, P. Jasiński, R. Kopik, M. Kopka, P. Krysiak, K. Labęda, M. Matuszewski, J. Miszczak, M. Palacz, R. Ratyński, B. Radomyski, Heavy Ion Laboratory, University of Warsaw, Warszawa, Poland

In June 18, 2018 an e-mail with information that the Svedberg Laboratory (TSL) was being decommissioned was received. In this process much surplus accelerator equipment originating from the Gustaf Werner cyclotron would become available. Additionally, we were informed that the first priority for this equipment would go to labs within Uppsala University, but other labs in Sweden and Europe had already expressed some interest in obtaining some of the equipment. Finally TSL asked us if there was any interest from HIL. Before our first visit to Uppsala we exchanged a number of mails to clarify what surplus equipment was available. We then sent a list of equipment that we were interested in for consultation and approval. Unfortunately, the COVID-19 pandemic suspended our activities for several months. The first visit to TSL took place from December 13 to December 15, 2021. During this visit, a four-person HIL team marked some interesting devices and started dismantling them, Fig. 1.



Figure 1: The HIL team marks devices installed in the cyclotron area.

During the second visit from March 27-31, 2022, the six-person HIL team completed marking the agreed devices and continued their further dismantling, Fig. 2.

During the third visit from May 29 to June 2, 2022, a four-person HIL team finally prepared small and medium-sized equipment for transport on Euro pallets. All Euro pallets, with equipment on them, were stored in dedicated store rooms, Fig. 3.

Necessary information about available loading ramps was also collected. The problem occurred when dismantling and transporting large and very heavy devices. Due to the lack



Figure 2: The HIL team marks agreed devices and continues their dismantling.



Figure 3: Finally prepared equipment for transport on Euro pallet.

of specialized tools at TSL, the HIL team agreed with the TSL team that a professional company would be hired. The transport of these devices will be carried out at the same time as the trucks arrive from Poland. During the fourth visit from January 11 to 14, 2023, a three-person team finished packing the large-sized devices for transport and loaded all the Euro pallets onto two trucks, Fig. 4.



Figure 4: All the Euro pallets with equipment loaded onto two trucks

As a result, HIL received vacuum equipment, ion optics elements, magnet power supplies, and RF components, which significantly reduced the problem of spare parts in the laboratory. We would like to thank the Svedberg Laboratory team from Uppsala for donating the devices and their invaluable help during our visits to the centre.

A.5 RF system team activity

A. Bednarek, T. Bracha, K. Sosnowski

Heavy Ion Laboratory, University of Warsaw, Warszawa, Poland

In 2023, the RF Generator team was responsible for carrying out current experiments on the cyclotron and maintaining the efficiency of the existing "Chryzolit" amplifier system, as well as testing the new system as part of the warranty repair together with the contractor — the "POPEK-Elektronik" company from Zamość. At the beginning of 2023 we also obtained from the University of Uppsala in Sweden high power tubes similar to the tubes in our new amplifiers, and some RF components from their decommissioned cyclotron. The obtained tubes have slightly different sockets and max. anode power, but other electrical parameters are identical. During the visits of the contractor to HIL tests of most components were performed:

- anode high power supply systems for both amplifiers
- screen grid power supply systems of both amplifiers
- filament power supply systems of both amplifiers
- circuits defending both the amplifiers against failure caused by excessive voltage/power (crowbar)
- tuning anode and output circuit systems of both amplifiers
- proper operation tests of both high power tube RF amplifiers

Tests were carried out on the operation of the amplifiers loaded with an equivalent resistor and actual cyclotron resonators. By the end of 2023 the contractor still had not delivered the control grid power supply for both the amplifiers. All test were performed using our grid power supplies as a substitute. While the computer controls for the above-mentioned systems work, by the end of 2023 they had not been properly integrated by the contractor into one system constituting the operator's desktop.

A.6 New LabVIEW Program to control remotely the XTRD-400K Amplifier

T. Abraham, L. Standyło, K. Makowski

Heavy Ion Laboratory, University of Warsaw, Warszawa, Poland

The malfunctioning traveling-wave tube amplifier (TWTA) in the ion source, which delivers ion beams to the U-200P cyclotron, was replaced with an XTRD-400K amplifier produced by Xicom. Most of the devices, including the faulty amplifier, in the ion source are remotely controlled using a LabVIEW program called WHIL Control. In order to continue using WHIL Control to regulate all the ion source subsystems, a new module to manage the TWTA had to be developed. Xicom does not provide LabVIEW drivers for their XTRD-400K; therefore, the first step was to write these drivers. The amplifier responds to commands sent over RS-232 or RS-422/485 interfaces; in this case, RS-232 was chosen. With the drivers ready and tested, the new interface was incorporated into the WHIL Control system (see Figure 1). The interface passed the tests successfully and has been in use since the end of 2023.

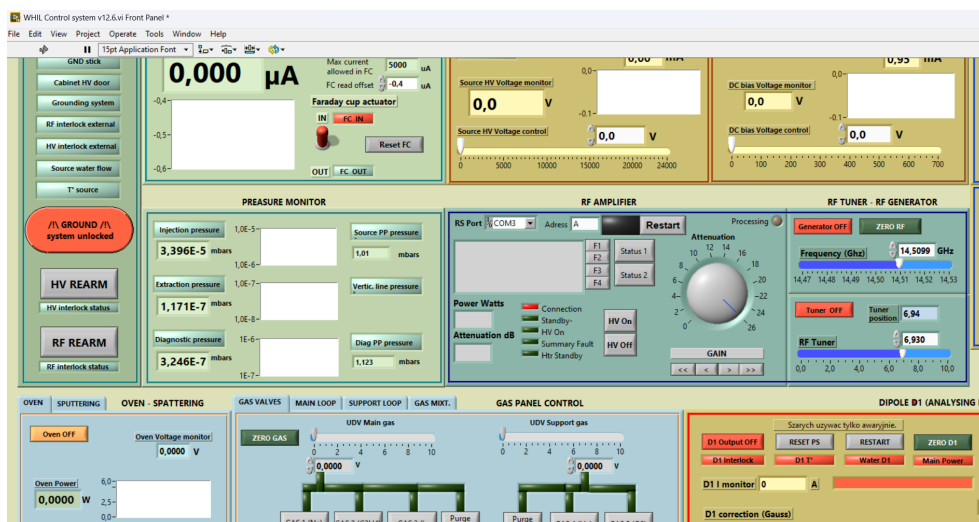


Figure 1: XTRD-400K control panel in WHIL Control ("RF Amplifier" section).

A.7 A standalone station with automatic loading, dedicated to the PETtrace cyclotron

J. Choiński, T. Bracha, R. Kopik, J.A. Kowalska, O. Nassar, B. Radomyski, A. Stolarz, L. Świątek, R. Tańczyk

Heavy Ion Laboratory, University of Warsaw, Warszawa, Poland

The Radiopharmaceutical Production and Research Center was built and launched by the Heavy Ion Laboratory. The Center is leased to an external company and is responsible for daily production of radiopharmaceuticals: fluorodeoxyglucose ^{18}F -FDG and choline based on fluorine ^{18}F . The center is able to produce two other typical radioisotopes for PET scanners, i.e. ^{11}C and ^{15}O using dedicated equipment. In the intervals between regular production of ^{18}F on the PETtrace machine, the HIL team using a dedicated external station for the irradiation of targets in metal and powder form, produces a variety of other radioisotopes for research. They are used for synthesizing/labelling of bio-chemical compounds with potential application as radiopharmaceuticals. For the last two years this research work has been carried on in cooperation with teams from the Institute of Nuclear Chemistry and Technology in Warsaw and the Jagiellonian University, Krakow. This collaboration induced a joint research project entitled "Development of three-photon emitting radiotracers for positronium imaging". The project was launched on 2022/07/21, under the OPUS-2022 edition, contract No. UMO2021/43/B/ST2/02150, where the Jagiellonian University, Faculty of Physics, Astronomy and Applied Computer Science is the leading unit. During the last year, the HIL team was responsible for the task "Development of a methodology for the manufacturing of targets, target holder and target head, Optimization of $^{44\text{m}}\text{Sc}$ production". Production of $^{44\text{m}}\text{Sc}$ is based on a reaction induced by protons on calcium [1–3]. The calcium targets are prepared as tablets formed from CaCO_3 . In the geometry of protons perpendicularly hitting the target, the targets are prepared as an insert of a calcium carbonate tablet into a graphite base (Fig. 1).

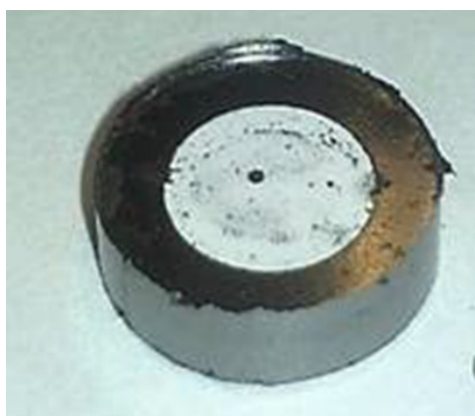


Figure 1: Calcium target (Calcium carbonate pellet of 6 mm diameter) in graphite base (10 mm diameter).

While implementing this task we have designed a new target holder (Fig. 2) allowing application of the target with a 1.5 times larger irradiation surface area compared to the initial target holder (Fig. 3).



Figure 2: View of the new target holder with pressure and twisting rings.



Figure 3: View of the original target holder with (from the left) cover plate, pressure ring and CaCO₃ target.

We have also changed the way the target is fixed to the target holder. In the initial version, the target material embedded in graphite is fixed with three screws. With relatively low activities and use of a dedicated protective station, dismantling the irradiated target can be performed in safe conditions. A certain inconvenience of this solution is the three aluminum screws mentioned above, which need to be separated from the target material. However, in the inclined target holder version, the Calcium target mixed with graphite powder is fastened using an oblique clamp (middle element in Fig. 2) and an Allen key nut (right element in the drawing). This solution significantly facilitates dismantling the irradiated target. Based on the exposures carried out so far, the target material can be irradiated with a proton beam with an energy of 16 MeV and an intensity of approximately 17 mA using the target holder from Fig. 3, without any signs of burning of the target material. In the case of the holder in Fig. 2, a proton beam of the same energy but with a current twice as high, i.e. about 35 mA can be safely applied for target irradiation, producing approximately 2 times greater activity in the same unit of time. The method of water cooling the targets in both holder versions is the same. Changing the target holder, we also redesigned the target closing system in the station in such a way that the system automatically adjusts to a given holder version. This allows the use of both holder solutions for target irradiation depending on requirements. Application of the tilted target holder requires a new shape of target. Production of an ellipse-shape (shape of the proton beam cross section with tilt) can be performed using a newly-purchased die applied to forming the powder. The die (Fig. 4) with dimensions corresponding to the beam cross section was ordered from WEBER in Germany.

Due to the mechanical instability of a calcium carbonate pellet with a thickness corresponding to the proton energy range, having regard to the thickness decrease due to the beam incidence angle, the targets for Sc isotopes production will be prepared with the ad-



Figure 4: Die with shape allowing production of pellets with an elliptical shape.

dition of graphite. The small addition of graphite (2.5-10%) which is chemically inert and should not interfere with further target treatment, significantly improves the mechanical stability of the target. Tests performed so far show that the addition of 5% of Carbon guarantees full mechanical stability of the target (Fig. 5)

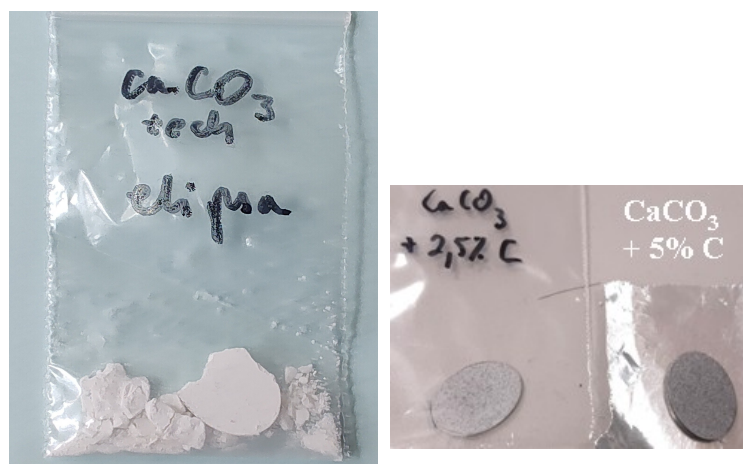


Figure 5: Elliptical shape targets made of: pure CaCO_3 , with the addition of 2.5% C and with 5% C (respectively from left to right)

The following purchases planned in the schedule for 2023 were completed:

1. Electron Beam Gun (e-beam evaporator) with additional equipment
2. Real-time thickness monitor
3. Pressing tool with a non-circular dedicated insert-die for manufacturing powder targets

Bibliography

- [1] J. Choiński et al., HIL Annual Report (2022) 15.
- [2] J. Choiński et al., HIL Annual Report (2021) 18.
- [3] J. Choiński et al., HIL Annual Report (2020) 14.

A.8 Status of the EAGLE array

M. Palacz¹, T. Abraham¹, K. Hadyńska-Klęk¹, G. Jaworski¹, M. Kisieliński¹, M. Komorowska¹, M. Kowalczyk¹, I. Kuti², M. Malinowski^{1,3}, M. Matuszewski¹, J. Molnár², P.J. Napiorkowski¹, W. Okliński¹, S. Panasenko¹, I. Piętka¹, J. Samorajczyk-Pyśk¹, P. Sekrecka¹, A. Špaček¹, A. Tucholski¹, K. Wrzosek-Lipska¹, for the EAGLE collaboration

1) Heavy Ion Laboratory, University of Warsaw, Warszawa, Poland

2) HUN-REN Institute for Nuclear Research (HUN-REN ATOMKI), Debrecen, Hungary

3) Faculty of Physics, University of Warsaw, Warszawa, Poland

The central European Array for Gamma Levels Evaluations (EAGLE) is an array of High Purity Germanium (HPGe) detectors located at HIL [1], see also [2]. Up to 30 HPGe detectors with anti-compton shields can be installed in the EAGLE frame, and the setup can be augmented with various ancillary devices.

The Heavy Ion Laboratory operates a number of HPGe detectors on loan from the GAMMAPOOL [3]. At present, 15 complete sets of a HPGe detector and its anti-compton shield are allocated by GAMMAPOOL to HIL. HIL also owns 19 smaller detectors with anti-compton shields, which may also be installed in the frame of EAGLE. The detectors located at HIL are routinely serviced in-house [4].

In the beginning of 2023 the installation of the NEDA detector in connection with EAGLE [6] was completed, and the setup was commissioned in January. Additionally, in July, the charged particle array DIAMANT was installed inside EAGLE and commissioned [7]. Altogether 5 EAGLE experiments were performed during the year — see separate contributions for details. These projects were entitled:

- “Lifetime measurement of excited states in ^{134}Sm ” (experiment HIL099);
- “Shape coexistence and octupole correlations in the light Xe, Cs and Ba nuclei” (two experiments, HIL097 and HIL106) [8];
- “Single-proton states and $N=Z=28$ core excitations in ^{57}Cu ” (experiment HIL105) [9];
- “Study of the anomalous behavior of the Coulomb energy difference in the $A = 70$, $T = 1$ izobaric multiplet” (experiment HIL115) [10].

In experiments HIL099, HIL097, HIL106, the Köln plunger [5] was also employed together with EAGLE and NEDA, while HIL105 and HIL115 were run using the EAGLE-NEDA-DIAMANT configuration. Fifteen HPGe detectors were used in all the experiments mentioned above.

Acknowledgment

Installation and use of NEDA at HIL is supported by the National Science Centre, Poland under Grant Agreement No. 2020/39/D/ST2/00466.

Bibliography

- [1] J. Mierzejewski *et al.*, Nucl. Inst. and Meth. **A659** (2011) 84.
- [2] M. Palacz *et al.*, HIL Annual Report 2019, page 12.
- [3] T. Abraham *et al.*, HIL Annual Report 2016, page 17.
- [4] T. Abraham *et al.*, HIL Annual Report 2017, page 14.
- [5] C. Fransen *et al.*, HIL Annual Report 2022, page 69, and references therein.

- [6] G. Jaworski *et al.*, HIL Annual Report 2022, page 18.
- [7] I. Kuti *et al.*, this Report, page 50.
- [8] C. Petrache *et al.*, this Report, page 56.
- [9] M. Palacz *et al.*, this Report, page 47.
- [10] M. Matejska-Minda *et al.*, this Report, page 52.

A.9 Preparation of thick isotopic Si target with high efficiency

A. Stolarz¹, J.A. Kowalska¹, M. Palacz¹, M. Strawski²

1) Heavy Ion Laboratory, University of Warsaw, Warszawa, Poland

2) Faculty of Chemistry, University of Warsaw, Warszawa, Poland

Si-28 targets with a thickness of a few mg/cm² were requested for a study of single-proton states and N=Z=28 core excitations in ⁵⁷Cu. Nuclei of interest were produced in a reaction induced by sulphur ions bombarding the ²⁸Si target: ²⁸Si(³²S,p2n γ)⁵⁷Cu.

Production of Si targets of required thicknesses is problematic. Application of Si evaporation in high vacuum or sputtering is questionable as a Si deposit built this way tends to delaminate from the substrate on which the ‘vapour’ is collected when the thickness approaches 1 mg/cm².

Additionally it was expected that the technique used for target preparation would not enhance the content of carbon and oxygen in the final product as detected in 0.5 mg/cm² Si deposits (Fig. 1) prepared by resistive heating evaporation on Ta backing (foils provided by A Blazhev from Köln University).

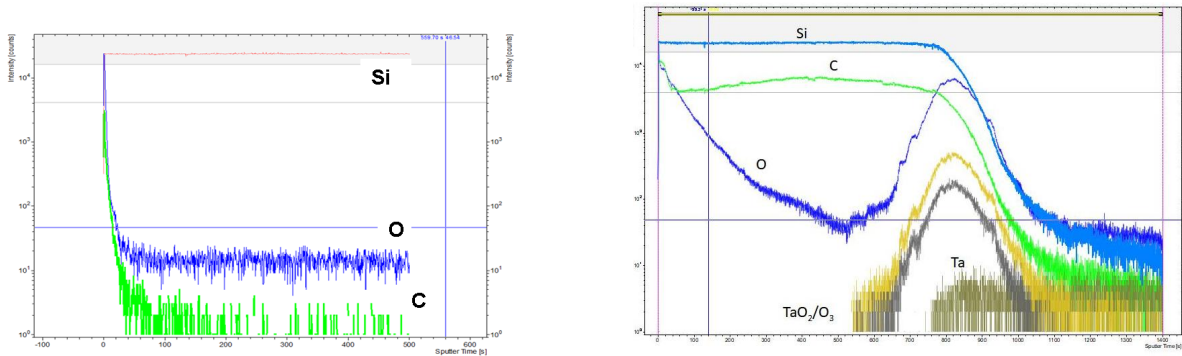


Figure 1: Illustrative results of Secondary Ion Mass Spectrometry (SIMS) analysis of primary natural Si (left) and of the ²⁸Si deposit on Ta backing (right) demonstrating the high content of C and O in the deposited layer (the original starting isotopic material was not available for this measurements so for comparison pure natSi was used).

Thus, taking into account that both elements build up even during evaporation performed from an electron gun in a very high vacuum [1] another technique had to be applied. Formation a self-supporting pellet from silicon powder, although feasible causes problems with final pellet mounting to the frame due to pellet brittleness in the required target thickness range. This brittleness can be overcome by the addition of a binder such as a powder of soft foreign elements (e.g. silver, gold) but this solution may result in reactions interfering with the studied effects. The problem was solved by an innovative combination of the distribution of Si powder on the supporting foil followed by a standard pressing technique used to compact the powder and further adhere it to the backing. The backing foil was selected taking into account the need to avoid reactions that would interfere with the studied effects.

The even distribution of a very small amount (~ 4.5 mg) of Si powder corresponding to the required thickness of the final target over the area of the backing foil (1.13 cm²) was the most challenging step. To achieve a good distribution a very fine Si powder was

applied. The Si pieces were crushed and powdered in an agate mortar and further ground in a pure alcohol environment. After completing the powdering process the Si was left for a dozen hours to enable all the alcohol to evaporate. The fine powder prepared this way was then loaded into a tablet matrix (with a backing Au foil placed on the bottom die) by rubbing through a wire mesh with 25 μm holes. The load was then pressed with a force of 160 bar provided by a hydraulic press. The matrix used at this step (Fig. 2) allows air evacuation before and during powder pressing what minimises the air (and thus oxygen) content in the target.

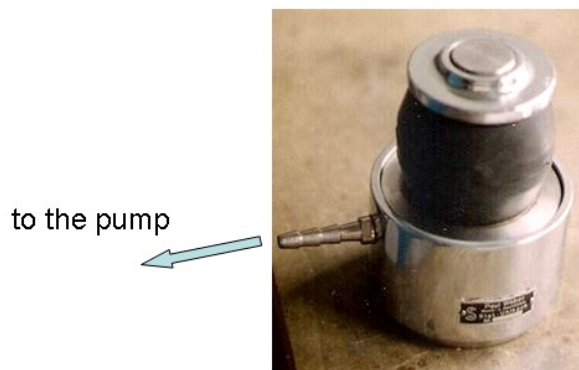


Figure 2: Pellet formation matrix.

The Si layer produced in this way looked relatively smooth and well distributed but the final product was rolled into tubes or shaped into a kind of ‘dome’ (Fig. 3) due to stresses in the Si layer. Nevertheless, the Si layer was mechanically stable, adhering well to the backing foil. This ‘stressy’ effect, although known to appear in evaporated Si layers [2] was unexpected in layers created by powder pressing. This stress appeared regardless of the backing foil thickness or material.

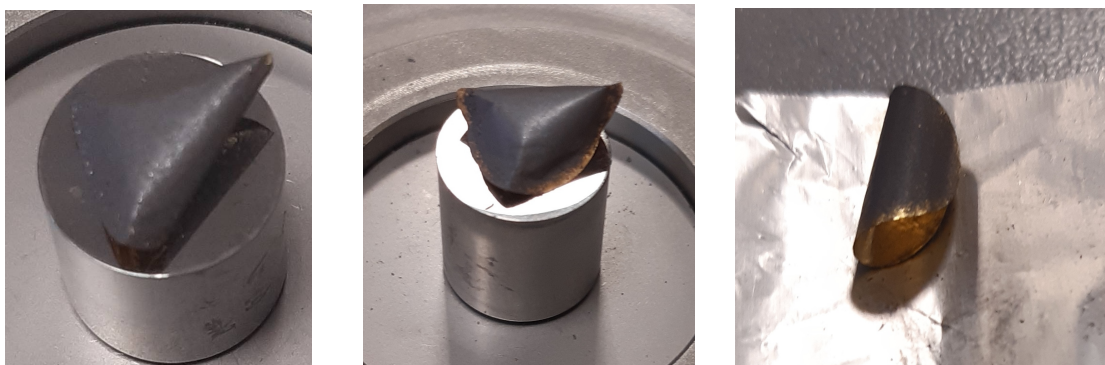


Figure 3: nat-Si target - 3 mg/cm^2 Si on 5 μm Al (left), 4 mg/cm^2 Si on 1.5 μm Au (middle) and 2 mg/cm^2 Si on 6 μm Au (right) backing foil.

Since the targets had to be mounted flat, during stretching cracks appeared in the layer but this does not affect the layer stability. Concerning target stability in beam the targets were vacuum and thermally tested. To check if potential encapsulation of gas residues in the Si layer took place the target was placed in a vacuum container and a vacuum of 10^{-6} bar was maintained for 5 h. Further, the target was left in the vacuum for an additional 24 h. After this treatment there was no damage in the Si layer. To check for possible

damage that might be caused by the heat deposited by ion beam the targets were placed in an oven at up to 500 °C (in 300, 400 and finally 500 °C) for 15–20 min each step and the Si layer looked untouched.

The other attempt of Si powder setting on the backing foil by sedimentation was also undertaken. The Si powder was suspended in 3 different media: alcohol, toluene and chloroform and was left for gravimetric sedimentation using Teflon vessels of 1 cm and 3 cm height. The excess liquid media was evaporated slowly with initial gentle heating with a lamp and when the powder started to become visible the evaporation was completed without the help of further heating. The time needed for the whole process was a dozen hours. The still visibly humid precipitate was transferred to the pellet pressing matrix and left for a dozen hours (usually overnight) to complete drying before powder pressing. Unfortunately, the final product had a non even structure (Fig. 4) independent the suspension medium or the vessel height.



Figure 4: Dry Si deposit from toluene medium in the matrix ready for pressing (left), the deposit after compacting (middle) with clearly visible islands of grouped powder and magnification of the Si powder after press compacting (right). The small voids are already visible in the deposit before compacting (left).

Based on the successful production of natural targets by the procedure of powder rubbing through a wire mesh 14 isotopically enriched ^{28}Si targets were prepared. The described procedure allows target preparation with \sim over 80 % (83–85 %) efficiency. The thickness variations in Si deposits in the range of 15% were irrelevant for the studies conducted. The targets were mechanically stable and the introduction of contaminants potentially interfering with the principal reaction was not detected in the final product during the experiment [3].

Acknowledgment

This work is partly supported by the National Science Centre, Poland under Grant Agreement No. 2020/39/D/ST2/00466.

Bibliography

- [1] A.M.Sandorfi *et al.*, Nucl. Inst. and Meth. **136** (2011) 395.
- [2] J.E. Johnstone *et al.*, Nucl. Inst. and Meth. **A 953** (2020) 163267.
- [3] M. Palacz *et al.*, this Report, page 47.

A.10 Polish Workshop on the Acceleration and Applications of Heavy Ions

J. Samorajczyk-Pyśk¹, G. Colucci¹, P. Chuchała^{1,2}, K. Hadyńska-Klęk¹, G. Jaworski¹, P. Kamińska^{1,2}, M. Kowalczyk¹, K. Kilian¹, U. Kaźmierczak¹, M. Komorowska¹, J.A. Kowalska¹, U. Gryczka³, P.J. Napiorkowski¹, O. Nassar¹, M. Palacz¹, I Piętka^{1,2}, M. Paluch-Ferszt¹, K. Rusek¹, A. Špaček¹, A. Stolarz¹, Z. Szepliński¹, A. Trzcńska¹, M. Wolińska-Cichocka¹

1) Heavy Ion Laboratory, University of Warsaw, Warszawa, Poland

2) Faculty of Physics, University of Warsaw, Warszawa, Poland

3) Institute of Nuclear Chemistry and Technology

The Polish Workshop on the Acceleration and Applications of Heavy Ions has been organised at HIL almost every year since 2005. It is intended for third and fourth year physics students interested in nuclear physics, and offers them a unique opportunity to gain experience in methods of data acquisition and analysis, in operating the cyclotron including beam diagnostics measurements and in charged particle and gamma-ray detection techniques.

The number of willing participants increases every year, but for organizational reasons we can accept only 20 people. We usually receive over twice as many applications as the number of places available. It should also be noted that each year new institutions join the list of universities interested in sending their students to the Workshop. The participants are often interested in continuing their collaboration with HIL in the form of a summer internship or at the BSc and MSc stage. This year, after the workshop, 3 participants continue to cooperate with our laboratory.

During the Workshop participants attend a series of lectures on subjects related to heavy ion physics. The experimental tasks allow them to get acquainted with HIL infrastructure by performing measurements using dedicated apparatus available in the Laboratory. The Workshop is concluded by student presentations – each group prepares a 20 minute talk on their measurements and results.

In 2023 the programme of the lectures was the following:

- HIL in a nutshell (P. Napiorkowski);
- Electron accelerators – properties and use of the beam (U. Gryczka);
- Introduction to heavy ion acceleration and elements of ion optics (O. Nassar);
- Targets for research in nuclear physics (A. Stolarz);
- Radiopharmaceuticals for Positron Emission Tomography (K. Kilian);
- Detection of gamma radiation, charged particles and neutrons (M. Palacz);
- In-beam gamma spectroscopy (K. Hadyńska-Klęk);
- Nuclear reactions (K. Rusek).

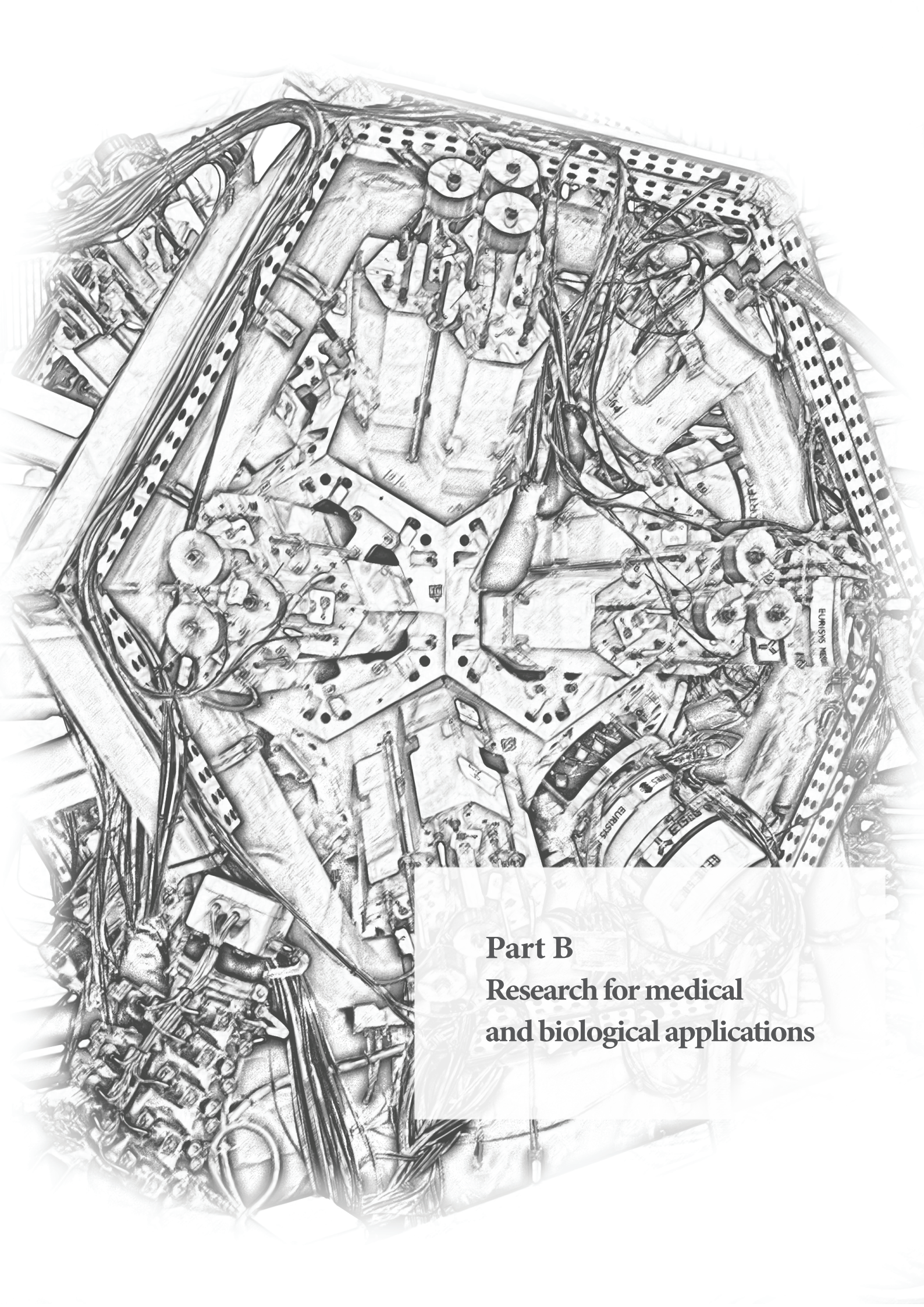
In addition to traditional lectures, students also took part in the 2nd Open Meeting of the Nuclear Physics Section of the Polish Physical Society.

Students took part in the following experimental projects:

- How to measure beam current?
- Gamma spectroscopy with the EAGLE multidetector setup;
- Targets: production and thickness measurements;
- Measurement of ^{137}Cs activity in environmental samples;
- Gamma camera — a medical imaging tool.



Figure 1: Participants of the 17th Polish Workshop on the Acceleration and Applications of Heavy Ions (photo. R. Klęk).



Part B
Research for medical
and biological applications

B.1 The influence of the presence of polyphenols on the stability of selected selenium compounds

A. Sentkowska¹, K. Pyrzyńska²

1) Heavy Ion Laboratory, University of Warsaw, Warszawa, Poland

2) Faculty of Chemistry, University of Warsaw, Warszawa, Poland

Selenium is a key element for the proper functioning of the human body. Deficiency in selenium has been linked to a range of serious conditions such as cardiovascular and inflammatory diseases, diabetes, and many others [1]. Diet is a major source of selenium for humans. Various forms of selenium are present in foods including selenite Se(IV) and selenate Se(VI), and several selenoaminoacids such as selenomethionine (SeMet), selenocysteine (SeCys), selenocystine (SeCys₂), selenohomocysteine (SeHoCys₂), Se-methylselenocysteine (SeMeCys) and c-glutamyl-Se-methylselenocysteine (c-Glu-MeSeCys). However, the selenium content in food tends to reflect the level of this element in soil [2]. Recently, Se-enriched tea, processed from plants grown in seleniferous areas of China and obtained using selenium fertilizers has become increasingly popular due to its more pronounced health-promoting properties [3]. Selenium and green tea both play an important role in antioxidant defence systems and are particularly interesting as a combination because they have potentially complementary mechanisms of action [4]. One of the difficulties in the speciation analysis of selenium is the instability of its compounds. The described research was aimed at checking how the presence of a sample matrix rich in polyphenolic compounds (present in high concentrations in every plant material) affects the stability of selected selenium compounds. High performance liquid chromatography in HILIC mode was used to study the changes in selenium concentration in the presence of green and black tea infusions. The results collected in 36 hours are presented in Figure 1.

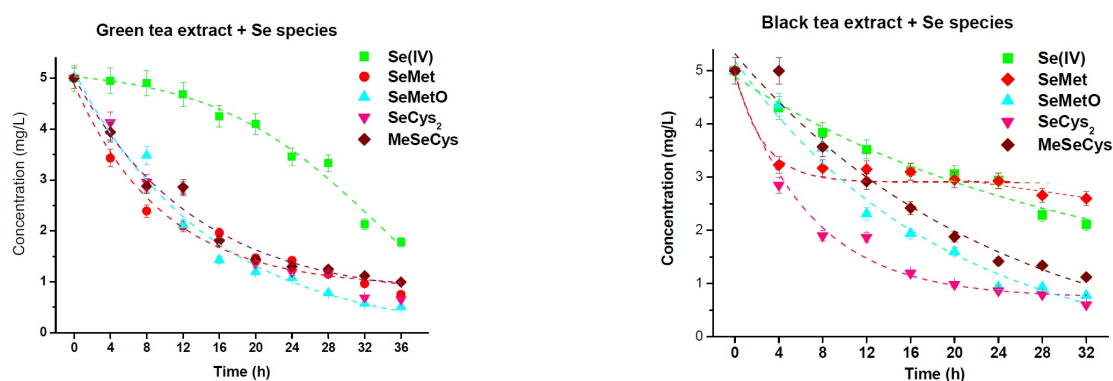


Figure 1: Changes in the concentration of selenium species added to green and black tea infusions [5].

In the presence of both tea infusions, the concentrations of selenium species decreased. This is particularly visible in green tea, where all selenium species, except selenites, gradually decreased during a prolonged time of their mixing. The concentration of Se(IV) was reduced much more slowly. SeMet concentration was reduced faster in the presence of green tea infusion, while in black tea, its concentration was almost stable in the interval time of 4–36 h. After 4 h for black tea and 8 h for green tea, the presence of Se(IV) was also recorded at a concentration equal to 0.80 mg L⁻¹. While Se(IV) concentration with

green tea infusion was almost constant during a prolonged time of storage, in the case of black tea infusion it gradually decreased to 0.16 mg L^{-1} . The compositions of green and black tea infusions differ in terms of polyphenolic content as well as the presence of other substances [6], thus the observed differences in the changes in selenium species concentration in tea infusions. The monomeric catechins and their derivatives are the major polyphenols in green tea, while black tea receives substantial oxidation, which results in the polymerization of catechins into theaflavins and thearubigins. This work investigated the interactions between plant catechins present in tea infusion and selenium species. The results from the conducted experiments were based on changes in the concentration of both reagents, and their stability in aqueous solutions during a prolonged time. Further studies will be undertaken to establish whether interaction between catechin and selenium species interactions alter their bioavailability.

Bibliography

- [1] G. Genchu et al., *Int. J. Mol. Sci.* **24** (2023) 2633.
- [2] M.P. Rayman et al., *Free Rad. Biol. Med.* **127** (2018) 46.
- [3] Y. Ye et al., *Foods* **11** (2022) 2159.
- [4] Y. Hu et al., *PLoS ONE* **8** (2023) e64362.
- [5] A. Sentkowska and K. Pyrzyńska, *Molecules* **28** (2023) 5897.
- [6] A. Sentkowska and K. Pyrzyńska, *Appl. Sci.* **13** (2023).

B.2 Antioxidant and antibacterial abilities of selenium nanoparticles obtained by green synthesis using herbal extracts.

A. Sentkowska¹, J. Konarska², J. Szmytke², A. Grudniak²

1) Heavy Ion Laboratory, University of Warsaw, Warszawa, Poland

2) Faculty of Biology, University of Warsaw, Warszawa, Poland

In recent years, nanoparticles of elemental selenium (SeNPs) have attracted great attention. Green chemistry methods of their synthesis, employing either microorganism or plant extracts have emerged as viable substitutes for chemical synthesis methods [1]. The advantages of green synthesis over the classical methods are among others slower kinetics, environmental compatibility, control over crystal growth and simplicity to scale up. In this study, well-known medicinal herbs such as lemon balm (*Melissa officinalis*), sage (*Salvia officinalis*), blackberry (*Rubus plicatus*), and hop (*Humulus*) were used. Their infusions have been used in folk medicine for many centuries, and the development of knowledge has allowed scientific confirmation of their effects. The obtained SeNPs are presented in Figure 1.

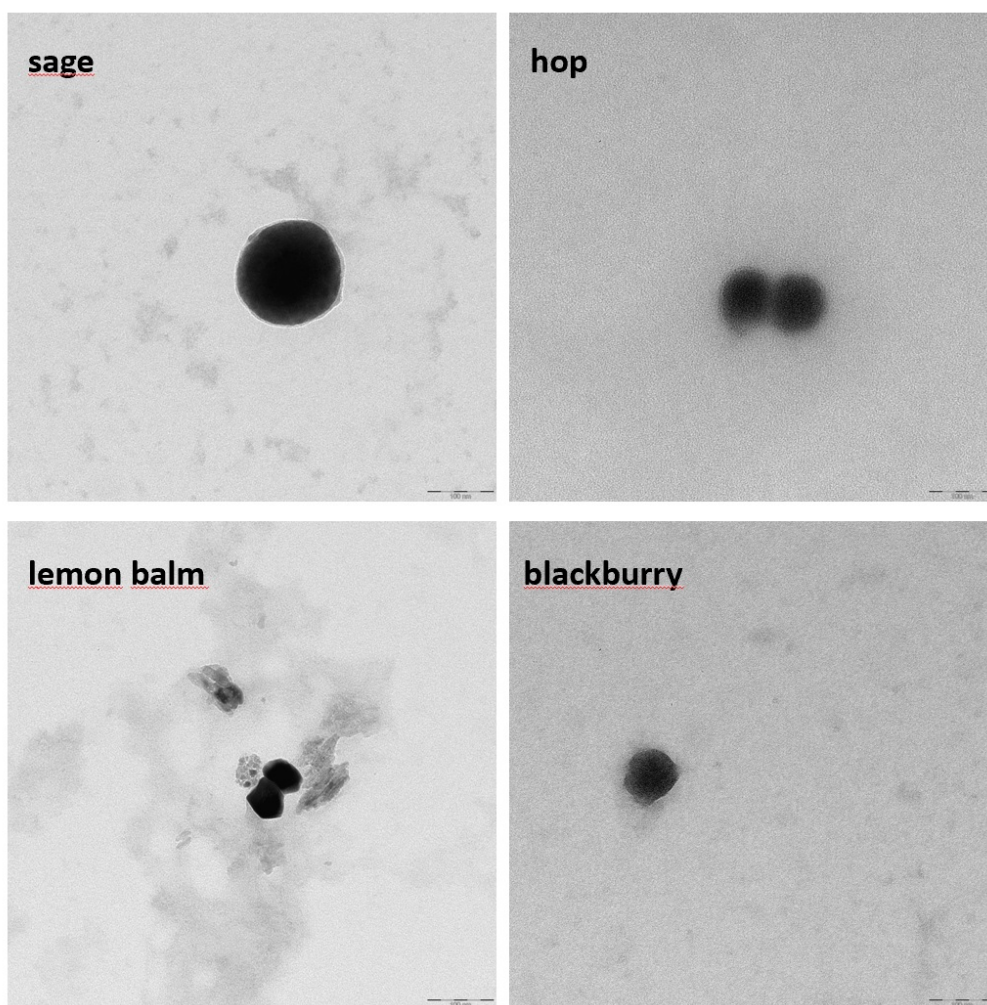


Figure 1: TEM images of SeNPs obtained by green synthesis.

All the obtained SeNPs were characterized by a high ability to neutralize free hydroxyl radicals. The lowest value was obtained for nanoparticles synthesised using sage extract (90.3%), while the highest for those synthesized using blackberry and hops (99%). The analogous value for nanoparticles obtained using lemon balm extract was 98%. The results confirm the great potential of SeNPs in preventing oxidative stress. Furthermore, the antibacterial properties of the obtained nanoparticles were tested by determining the minimum inhibitor concentration (MIC) against two model bacterial species: *Escherichia coli* (gram negative bacterium) and *Staphylococcus aureus* (gram positive bacterium). The SeNPs synthesized with blackberry, hop and sage extracts showed the strongest bactericidal activity against the tested bacteria. The presence of SeNPs in the post-reaction solution resulted in an increased bactericidal effect against *E. coli* and much stronger against *S. aureus*. The probable mechanism of action of the nanoparticles is due to the disruption of mechanisms that enable the removal of free radicals from cells. Further research will be conducted to determine the exact mechanism of action of the obtained SeNPs.

Bibliography

- [1] R. Heydari et al., Chem. Select. **4** (2019) 531.
- [2] B. Ciężki et al., HIL Annual Report 2008, page 51.
- [3] S.E. Arnell et al., Nucl. Inst. and Meth. **A300** (1991) 303.
- [4] A. Tizio et al., Phys. Rev. C **11** (2000) 1111.
- [5] H. Hotel et al., Phys. Rev., in press.

B.3 Synthesis and quality control of porphyrin labelled with ^{64}Cu

M. Pęgier¹, K. Kilian¹, K. Pyrzyńska²

1) Heavy Ion Laboratory, University of Warsaw, Warszawa, Poland

2) Faculty of Chemistry, University of Warsaw, Warszawa, Poland

To assess the usefulness of the method proposed in our previous report [1], the synthesis of Cu complex of meso-tetrakis-4-carboxyphenyl-porphyrin (TCPP) was performed using radioactive ^{64}Cu ($T_{1/2} = 12,7$ h) [2].

^{64}Cu was purchased from a PET radioisotopes manufacturer (Voxel, Cracow, Poland) and was produced in the $^{64}\text{Ni}(p,n)^{64}\text{Cu}$ reaction using an ALCEO solid target system (Comecer, Italy) coupled with a GE PETrace 840 cyclotron (GE Healthcare Technologies Inc., Chicago, USA).

The requested activity was about 200 MBq in the form of dried $^{64}\text{CuCl}_2$ reconstituted on-site with 1 mL of water, acidified with 1 mL of 0.1 mol/L HCl and finally eluted with 0.5 mL of ethanol.

After evaporation near to dryness a small aliquot of PBS was added to reach the expected activity concentration. An Atomlab 500 dose calibrator and wipe tester (Biodex, Shirley, NY, USA) was used for activity determination. In this form, without any purification, the radionuclide was used for labelling according to the procedure developed, achieving a satisfactory yield with good radiochemical purity. $[^{64}\text{Cu}]\text{Cu-TCPP}$ was synthesized at room temperature by mixing 200 μL of $[^{64}\text{Cu}]\text{CuCl}_2$ solution, 400 μL of TCPP and 200 μL ascorbic stock solutions, filled up with a borate buffer up to 5 mL and vortexed. Direct complexation resulted in a 78.7% yield at room temperature immediately.

Further purification using solid phase extraction with an anion exchange column eliminated free ^{64}Cu and increased the radiochemical purity up to 99.0%. For final purification and formulation the solution was loaded onto an anion exchange Waters Sep-Pak Accell Plus QMA column (Waters Corporation, Milford, USA) with an ISM833 Ismatec peristaltic pump (VWR, Radnor, USA) at 1 mL/min, flushed with 5 mL of water at 2 mL/min.

Interesting behaviour was observed during purification on the anion exchange column. The complex could be eluted only in a specific sequence of eluents. After loading of the reaction mixture on the column, deionized water was used to remove the impurities (free $[^{64}\text{Cu}]\text{Cu}^{2+}$, buffers, other metallic contaminants).

Next, a decrease in pH (2 mL 0.1 mol/L HCl) of the column prior to elution was mandatory for quantitative elution of the complex (> 98.5%) with 0.5 mL of ethanol. Using any other sequence of elution led to either retention of the complex on the column or degradation of it. The explanation could be the mixed sorption mechanism. Although the column resin is an anion exchanger and interacts with carboxylic groups, there can also be $\pi - \pi$ interactions between the porphyrin ring and the organic matrix of the column. Acidification breaks the ionic interactions and aprotic solvent releases the complex. Radiochemical purity was analyzed with a Shimadzu AD20 chromatography system with a SPD-M20A UV-Vis photodiode array and radiometric detectors (GabiStar, Raytest, Germany). The separation was done on a Phenomenex Gemini C18 column (150 mm x 4.0 mm i.d., 10 μm), with 40:60 acetonitrile: 0.05 mol/L $\text{CH}_3\text{COOH}/\text{CH}_3\text{COONa}$ adjusted to pH 4.8 as a mobile phase and 1 mL/min flow rate. The purity was confirmed by performing HPLC analysis where free ^{64}Cu ions were eluted in 2.3 min, while $[^{64}\text{Cu}]\text{Cu-TCPP}$ complex was eluted in 4.0 min referring to the radiometric detector signal (Fig. 1).

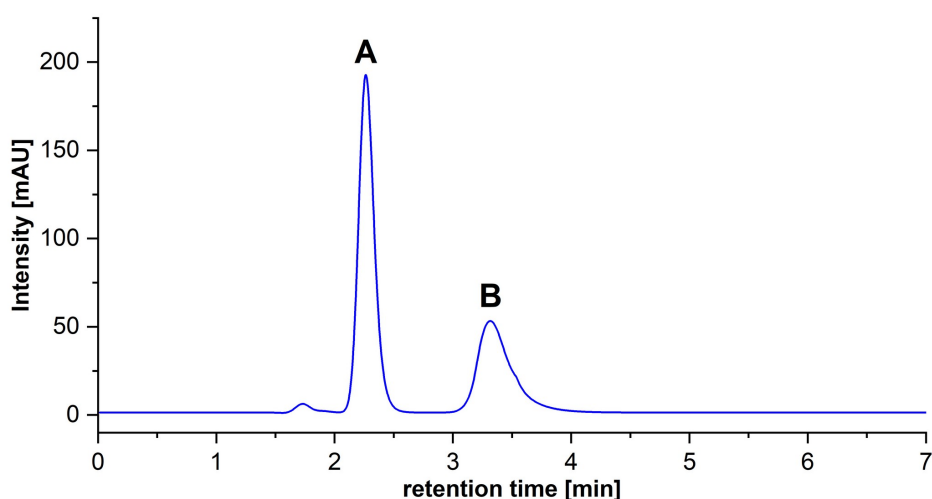


Figure 1: Separation of (A) free TCPP (retention time 2.2 min) and (B) Cu-TCPP complex (retention time 3.3 min).

Peaks were identified according to retention time (Fig. 2) and characteristic spectra (Fig. 3).

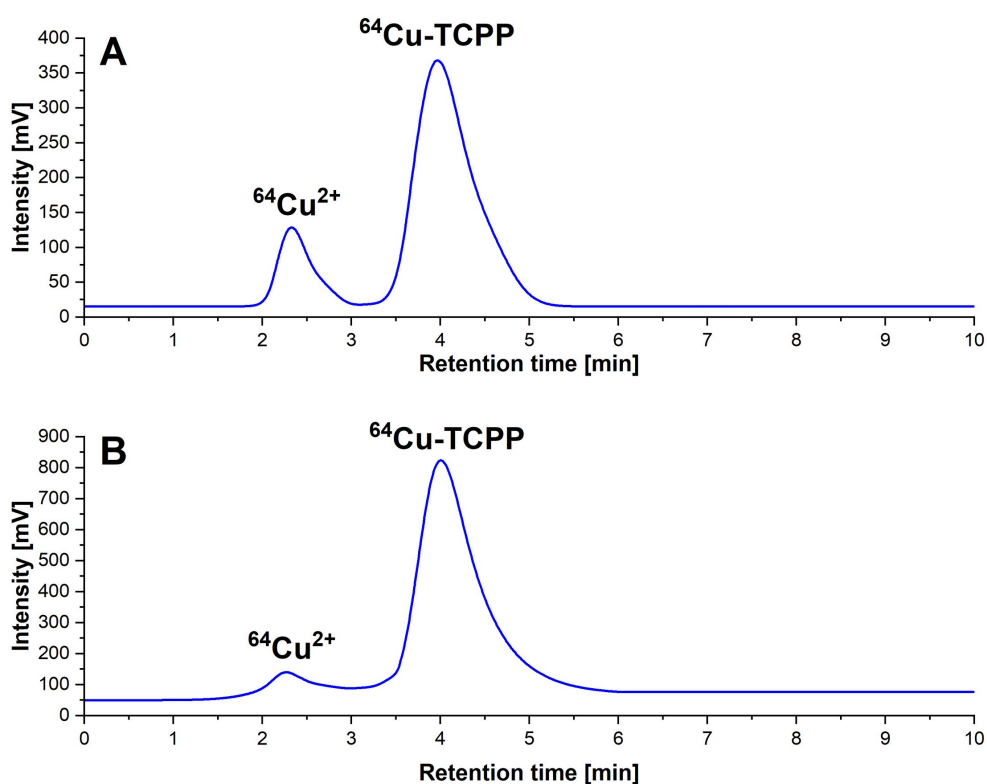


Figure 2: Radio-chromatogram of raw product (A) and purified final product (B).

The HPLC analysis confirmed the presence of ^{64}Cu complex with TCPP and the developed procedure is fast and the reaction occurs within single minutes at pH=9. Another

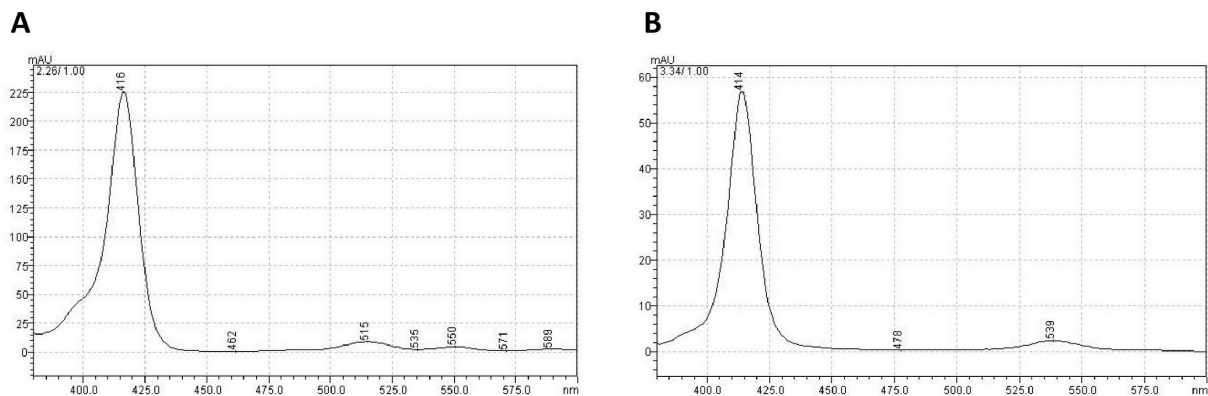


Figure 3: Spectra of (A) TCPP and (B) Cu-TCPP recorded at retention times: 2.2 and 3.3 min respectively.

favourable phenomenon can be observed in the chromatographic separation of the post-reaction mixture. Other divalent metal ions (Ni^{2+} , Zn^{2+}) may compete in the complexation process. The obtained $[\text{}^{64}\text{Cu}]\text{Cu}^{2+}$ solution may contain Ni(II) in a 2-fold excess and Zn(II) ions in an approx. 40-fold excess vs. ${}^{64}\text{Cu}$. As porphyrin ligands are used in the excess they are not competitive. However, due to formal requirements in the development of the radiopharmaceutical, it could be necessary to remove these metal ions. The proposed HPLC method also allows for the separation of impurities in the form of Ni-TCPP and ZnTCPP complexes.

Bibliography

- [1] M. Pęgiel, K. Kilian, K. Pyrzyńska, HIL Annual Report 2022, page 45.
- [2] M. Pęgiel, K. Kilian, K. Pyrzyńska, *Molecules* **28** (2023), 2350.

B.4 Porphyrin complexes of palladium as potential radiopharmaceuticals

M. Pęgier¹, K. Kilian¹, K. Pyrzyńska²

1) Heavy Ion Laboratory, University of Warsaw, Warszawa, Poland

2) Faculty of Chemistry, University of Warsaw, Warszawa, Poland

Porphyrins are promising agents that can be used as ligands for both positron emission tomography (PET) and radiotherapy. They are able to act as bifunctional ligands that can effectively coordinate the radionuclide of interest, serve as a targeting molecule themselves for tumor detection and can be linked to other targeting molecules [1].

Porphyrin complexes are normally present in the human organism (as iron complex in heme, or cobalt complex in cobalamin). The palladium radioisotope ^{103}Pd ($T_{1/2}=16.99$ days) is a promising agent for radiotherapy. It is already used in the clinical procedure of brachytherapy as metal seeds. In recent years ^{103}Pd has gained more attention as it has also been proposed for targeted Auger electron radiotherapy [2]. It emits Auger electron while decaying to $^{103\text{m}}\text{Rh}$ ($T_{1/2}=56.1$ min), which is another Auger electron emitter decaying to stable ^{103}Rh , so ^{103}Pd can serve as an in vivo generator of this radionuclide. This radionuclide can be synthesized in a cyclotron via the $^{103}\text{Rh}(p,n)^{103}\text{Pd}$ reaction.

Another radionuclide of palladium that is potentially interesting for radiopharmaceutical applications is ^{109}Pd ($T_{1/2}=13,70$ h), which undergoes β^- decay to $^{109\text{m}}\text{Ag}$ ($T_{1/2}=39.6$ s) which in turn emits a cascade of conversion and Auger electrons, which makes ^{109}Pd on in vivo generator of $^{109\text{m}}\text{Ag}$ [3]. In this study complexes of palladium(II) with porphyrin were synthesized. The hydrophilic anionic porphyrin meso-tetrakis(4-sulfonatophenyl)porphyrin (TSPP) was used (Fig. 1).

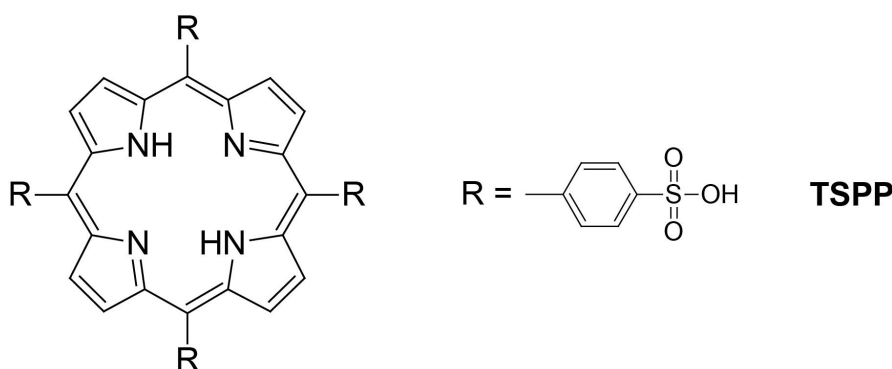


Figure 1: Structure of TSPP.

The reaction was conducted in three different pH buffers (acetate pH 4, phosphate pH 7, borate pH 9) and monitored using a UV-VIS spectrophotometer (Fig. 2).

The reaction in pH 4 led to formation of Pd-TSPP complex, while pH 7 and pH 9 showed no signs of a reaction. The spectrum after reaction confirms the formation of the complex, as characteristic changes occur; the Soret band is shifted from 434 nm for free TSPP to 410 nm for Pd complex and a new peak at 520 nm in the Q-band is formed with

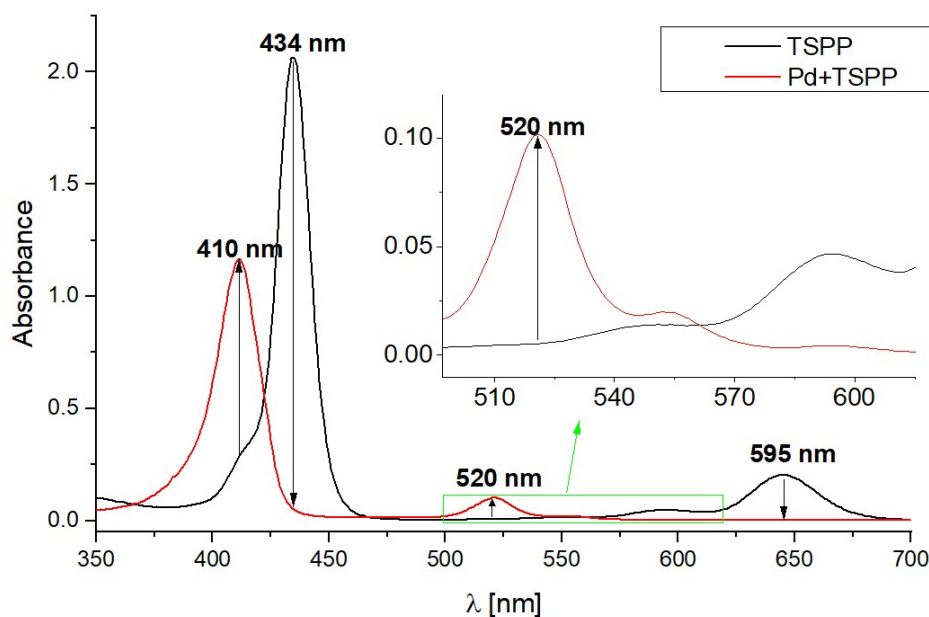


Figure 2: Changes in the UV-VIS spectra after formation of Pd-TSP complex.

the simultaneous disappearance of the free porphyrin bands. Similarly to Cu(II) complexes with porphyrins to increase the reaction rate synthesis using sitting-a-top complex would be the natural method to increase the reaction rate [2]. The only pH value in which the Pd complex was formed was pH 4. At this pH value the porphyrin complexes of large ions (Cd^{2+} , Pb^{2+} , Hg^{2+}) could not be synthesized.

The complexes of porphyrins with Pd(II) are promising models for further development of Auger electron therapeutic radiopharmaceuticals, but further studies to improve the reaction kinetics are needed.

Bibliography

- [1] K. Pyrzyńska, K. Kilian, M. Pęgier, *Molecules* **27** (2022), 3311.
- [2] F D. Filosov, E. Kurakina, V. Radchenko, *Nuclear Medicine and Biology* **94-95** (2021), 1-19.
- [3] J. Pineau et al., *Chemistry A European Journal* **28** (2022), e202200942.
- [4] K. Kilian, M. Pęgier, K. Pyrzyńska, *Spectrochim. Acta A Mol. Biomol. Spectrosc.* **159** (2016) 123-127.

B.5 Method of mechanical separation of ^{44}Sc from CaCO_3 targets after cyclotron irradiation

R. Walczak¹, P. Koźmiński¹, K. Mastowska¹, N. Razzaq¹, E. Gniazdowska¹, A. Bilewicz¹, J. Chojiński², T. Bracha², J.A. Kowalska², O. Nassar², A. Stolarz², L. Świątek², R. Tańczyk²

1) Institute of Nuclear Chemistry and Technology, Warszawa, Poland

2) Heavy Ion Laboratory, University of Warsaw, Warszawa, Poland

In 2023 the close cooperation between HIL and INCT begun over a decade ago was continued. The last years of joint research were focused on: the production of specific radionuclides, the processes of their separation from irradiated targets, and the search for radiolabeling procedures for molecules acting as isotope carriers. For radioisotope production proton beams accelerated in a cyclotron were used. The appropriate targets were produced at the Heavy Ion Laboratory and then irradiated with a beam of protons from the PETtrace cyclotron on a special stand connected to the cyclotron. The thicknesses of the targets were selected in such a way that the proton beam was completely stopped in the target. After irradiation the targets were transported to the Institute of Nuclear Chemistry and Technology for further processing.

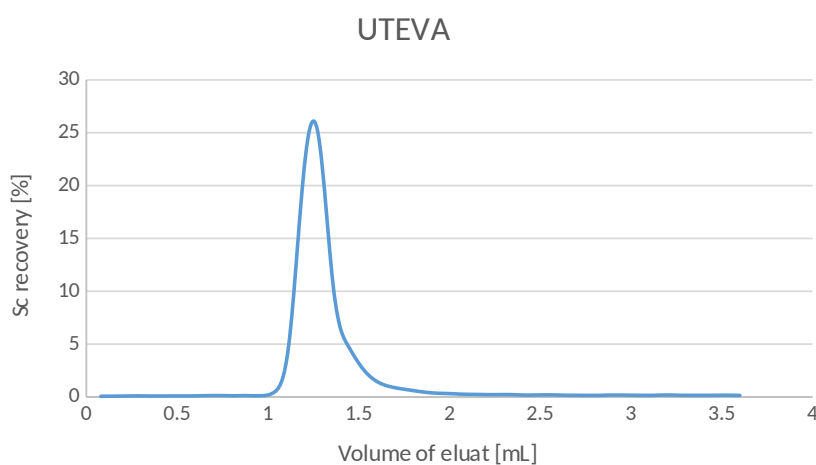


Figure 1: Calcium target (Profile of Sc elution from UTEVA resin).

In our previous work, we developed an efficient method of production of ^{44}Sc via the $^{44}\text{Ca}(p,n)^{44}\text{Sc}$ reaction. Application of highly enriched $^{44}\text{CaCO}_3$ (94,8% ^{44}Ca) allowed us to produce tens of GBq of ^{44}Sc [TTY: (pE: 21.8 \rightarrow 0 MeV) 1030 ± 50 MBq/ μAh for CaCO_3 300 mg $\cdot\text{cm}^{-2}$ target]. While such high efficiency is very appealing for the synthesis of diagnostic radiopharmaceuticals, it also presents risks for the scientists responsible for the separation of the radionuclide from the target material. The most effective means of safeguarding the laboratory crew from radiation is through the automation of the separation method. However, the initial step towards automation involves designing equipment for a mechanical process that imitates and utilizes the same components as future automatic solutions. Two two-step methods of separation of Sc from CaCO_3 targets were selected for automation.

Method 1.

The first method is based on UTEVA extraction resin. After irradiation, the target material was dissolved in 10 M HCl and then loaded onto a column filled with 200 mg of UTEVA resin, which had been activated for 12 hours in 10 M HCl. The filtrate, containing the target material, was collected for recovery. Subsequently, the column was washed with 10 mL of 10 M HCl to remove residual calcium cations. The wash solution was combined with the previously collected filtrate. Scandium was eluted using 3.5 mL of water. In this method, the total recovery of Sc was $74.4 \pm 2.2\%$ [Fig. 1].

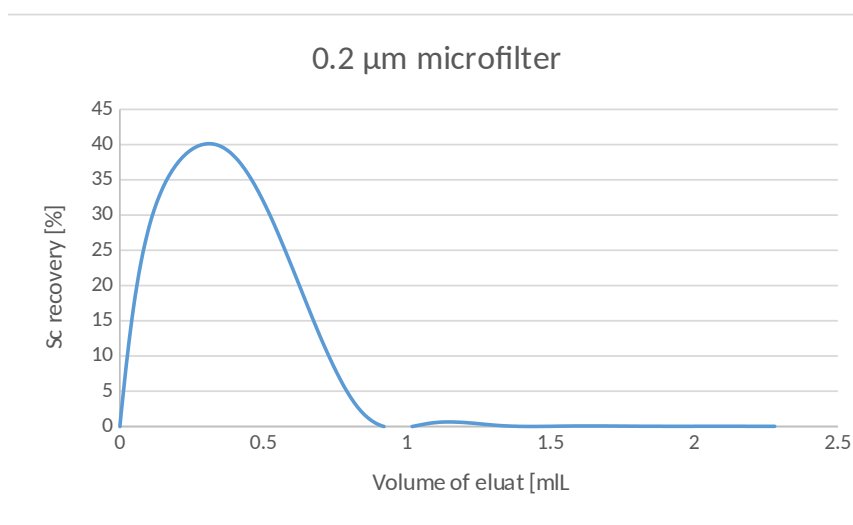


Figure 2: Profile of Sc elution from a 0.2 μm microfilter.

Method 2.

In the second method, we exploit the differences in the chemical properties of calcium and scandium in basic solutions. After dissolving the target material in 1 M HCl, the resulting solution was alkalized to pH 10 using 25% ammonia water. Under these conditions, calcium cations remained in a dissociated form, while scandium formed insoluble $\text{Sc}(\text{OH})_3$. To separate scandium hydroxide from the target material solution, a 0.22 μm porous filter was used. After loading the suspension onto the filter, it was washed with 10 mL of water to remove residual calcium. The filtrate from this wash and the previous solution were combined and collected for target material recovery. Scandium was then removed from the filter using 2 mL of 0.5 M HCl with an efficiency of $95.8 \pm 1.7\%$ [Fig. 2].

The second step of the separation process is identical for both methods. In this phase, the solution containing Sc was loaded onto 200 mg of Dowex50wx4 cation exchange resin to transition the solution from HCl to sodium acetate buffer. Prior to loading, the resin was conditioned with 1 M acetate buffer for 12 hours. Following the loading of the Sc solution, the resin was washed with 5 mL of water to remove the hydrochloric acid. Subsequently, Sc was eluted with 2 mL of 1 M sodium acetate buffer at pH 4.5. The recovery of scandium was $74.0 \pm 2.9\%$ [Fig. 3].

For both methods, a mechanical procedure was designed and constructed [Fig. 4 and Fig. 5]. Peristaltic pumps were utilized for transporting solvents in the case of UTEVA and Dowex50wx4 resins, while a syringe pump was used for the microfilter, where higher pressure was required. Solutions were moved at a rate of 1 mL/min. The construction of

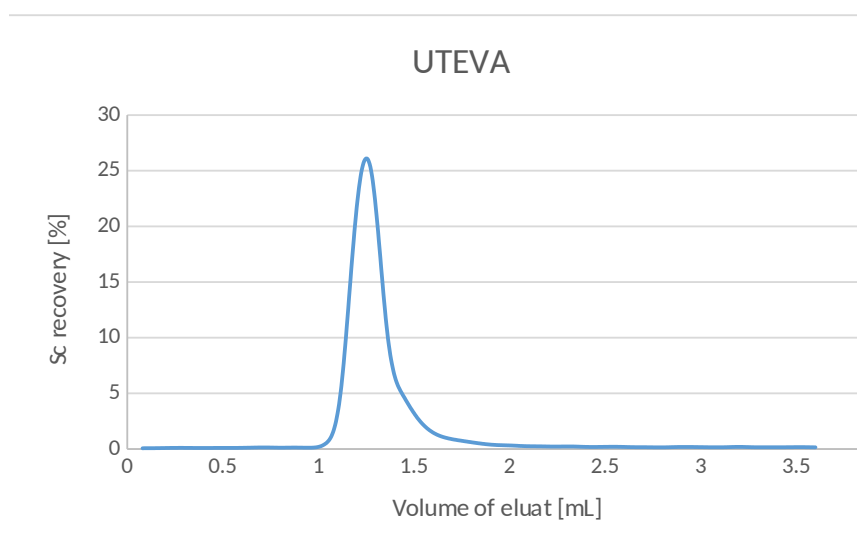


Figure 3: Profile of Sc elution from Dowex50wx4 resin.

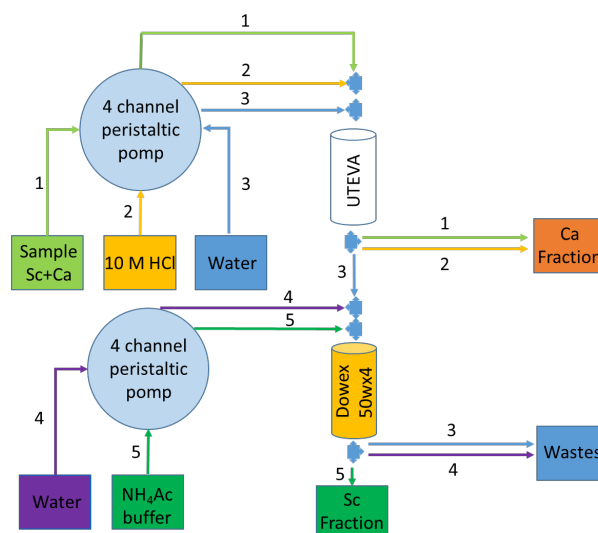
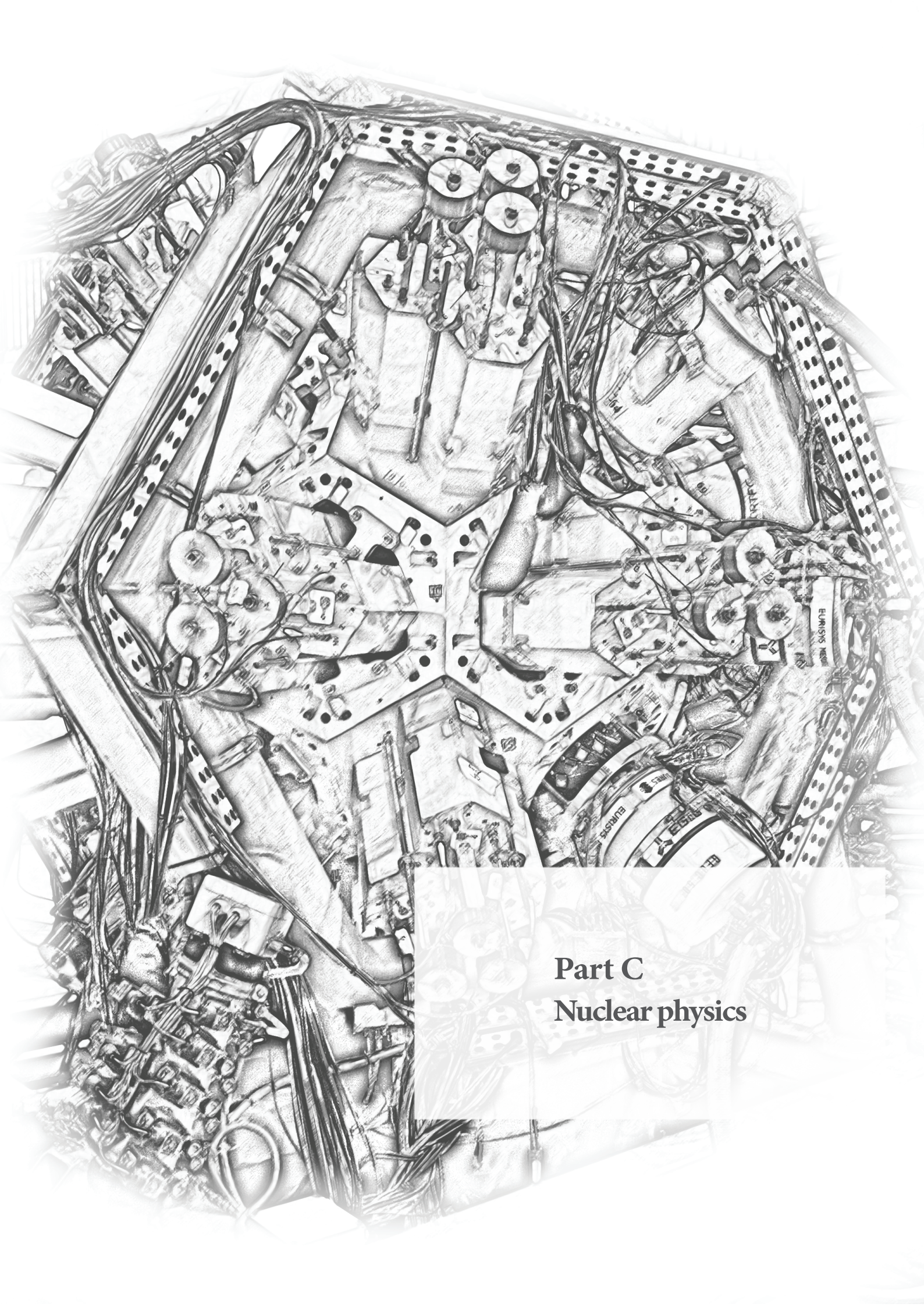


Figure 4: Schematic view of the automation for separation of Sc with the UTEVA/Dowex50wx4 method.

the apparatus involved the use of 5 mm inner diameter tubing, three-way valves, columns, and connectors resistant to acids and bases.

The mechanized UTEVA/Dowex50wx4 separation method was employed for the preparation of the ^{44}Sc solution used in the labeling of Peptide and Peptidomimetic Conjugates. The results of this synthesis were published in [1].

The modules will also be utilized in the realization of the current NCN grant: OPUS-22, 2021/43/B/ST2/02150 entitled "Development of three-photon emitting radiotracers for positronium imaging." They will be employed for the separation of ^{44}Sc from CaCO_3 targets and, following reconstruction, for the separation of cobalt radionuclides from metallic iron targets.



Part C
Nuclear physics

C.1 Towards ^{57}Cu with EAGLE-NEDA-DIAMANT

M. Palacz¹, A. Fijałkowska², G. Jaworski¹, M. Komorowska¹, M. Kowalczyk¹, I. Kuti³, M. Malinowski², J. Molnár³, M. Regulska², P. Sekrecka¹, E. Ahlgren Cederlöf^{4,5}, P. Bednarczyk⁶, M. Ciemala⁶, G. Colucci¹, A. Goasduff⁷, M. Górski⁸, J. Grębosz⁶, V. Guadilla², K. Hadyńska-Klęk¹, C. Hiver⁹, Y. Hrabar¹⁰, M. Kisieliński¹, A. Korgul², J.A. Kowalska¹, A. Krakó³, B. Kruzsic³, P. Kulesa^{1,7}, M. Matejska-Minda⁶, M. Matuszewski¹, C. Mazzochi², K. Miernik², A. Nałęcz-Jawecki¹¹, W. Okliński¹, S. Panasenko¹, I. Piętka¹, J. Samorajczyk-Pyśk¹, A. Špaček¹, A. Stolarz¹, G. Szymanek², N. Toniolo⁷, A. Tucholski¹, K. Wrzosek-Lipska¹

1) Heavy Ion Laboratory, University of Warsaw, Warszawa, Poland

2) Faculty of Physics, University of Warsaw, Warszawa, Poland

3) HUN-REN Institute for Nuclear Research (HUN-REN ATOMKI), Debrecen, Hungary

4) Department of Physics and Astronomy, Uppsala University, Uppsala, Sweden

5) KTH Royal Institute of Technology, Stockholm, Sweden

6) Institute of Nuclear Physics Polish Academy of Sciences, Kraków, Poland

7) INFN, Laboratori Nazionali di Legnaro, Legnaro, Italy

8) GSI Helmholtz Center for Heavy Ion Research, Darmstadt, Germany

9) Laboratoire de Physique des 2 infinis Irène Joliot-Curie – IJCLab, Orsay, France

10) Lund University, Lund, Sweden

11) National Centre for Nuclear Research, Otwock, Poland

The EAGLE-NEDA-DIAMANT [1] set-up was employed in an experiment aimed at observation of γ -ray radiation emitted from excited states of ^{57}Cu . This nucleus has only 1 valence proton outside the doubly-magic, self-conjugate $N = Z = 28$, ^{56}Ni core. Assuming a rigid core, its ground state (g.s.) and low lying excited states should thus be well described by very pure Shell Model configurations, with the valence proton placed in $p_{3/2}$, $f_{5/2}$, $p_{1/2}$ and $g_{9/2}$ orbitals, corresponding to states with spin and parity $3/2^-$, $5/2^-$, $1/2^-$, $9/2^+$, respectively. Evidence is however available that the $N = Z = 28$ core is relatively soft, and its excitations are highly collective. This was for example discussed in the recent work of Ref. [2] in which the lifetimes of the 4^+ and 6^+ states of ^{56}Ni were determined. Thus an interplay of single-particle and collective effects should also be manifested in the excited states of ^{57}Cu . The core ^{56}Ni nucleus has a half-life of 6.08 days and forms a key waiting point in the astrophysical rp-process. The $^{56}\text{Ni}(p,\gamma)\text{Cu}$ reaction is in particular crucial for the flow of material up the proton drip-line, so is the competing proton-capture $\text{Cu}(p,\gamma)^{58}\text{Zn}$ reaction with the β^+ decay of ^{57}Cu . Moreover, proton capture in stars happens in very high temperature environments (above 10^9 K), so that the protons have sufficient energy to overcome the Coulomb barrier. The product nuclei are thus created in excited states. In this context knowledge of the shell structure and properties of excited states in ^{57}Cu are essential for the production of heavier elements in the universe, see for example Ref. [3] and references therein.

The present knowledge concerning states of ^{57}Cu is summarised in Fig. 1. The ground state spin of ^{57}Cu has been determined in β decay work [4]. The lowest 2 excited states at 1028(4) and 1106(4) keV were identified in γ -ray spectroscopy measurements [3, 5]. The g.s. as well as these two excited states are interpreted as pure single-particle $p_{3/2}$, $f_{5/2}$ and $p_{1/2}$ Shell Model configurations, respectively. Gamma rays emitted from the 2398(10) keV state were also seen in the work of reference [5], but not in [3]. States at 2520(25), 3510(25) and 5710(25) keV were observed as resonances in transfer reactions [6], while states at 3280(50) and 5350(50) keV were identified via spectroscopy of protons emitted after the ^{57}Zn β^+ decay.

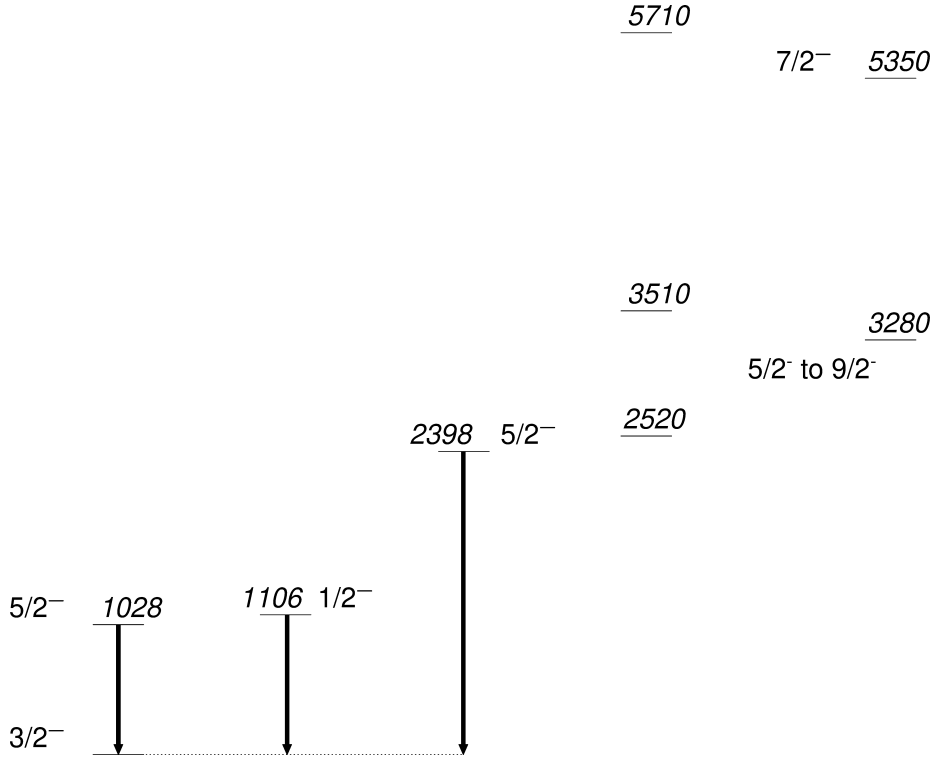


Figure 1: Known states of ^{57}Cu [3–6]. All energies are given in keV.

The present project aims at:

- identification of the $7/2_1^-$ state and confirmation of the $5/2_2^-$ state;
- identification of higher lying states in the possible yrast negative parity cascade, above $7/2_1^-$;
- identification of the $9/2^+$ state.

An 82 MeV beam of ^{32}S was used to bombard ^{28}Si targets. In this reaction one proton and 2 neutrons (p2n) should be emitted from the compound nucleus ^{60}Zn to reach ^{57}Cu . The average beam intensity was about 3 pA and data were collected during about 260 hours. The targets were produced by an innovative combination of ^{28}Si metallic powder distribution over a Au backing, followed by compacting and ‘adhering’ the powder to the backing using a hydraulic press. As a result, a 3.5 mg/cm^2 thick layer of ^{28}Si on a 7.3 mg/cm^2 thick backing could be obtained [7]. The ^{28}Si material was 99.99751(2)% isotopically enriched. The backing was thick enough to stop the evaporation residues.

A growing deposit of ^{12}C was observed during the run, and for this reason targets were changed at regular intervals. Altogether 10 targets were used. The chosen beam energy was only slightly higher than the Coulomb barrier energy for this reaction and this results in a relatively low reaction rate. All events in which at least 1 Compton unsuppressed γ -ray was registered in the HPGe detectors could be accepted by the trigger condition.

The reaction is dominated by reaction channels associated with the emission of 2 or 3 protons, possibly together with 1 neutron. The cross section for the p2n reaction channel leading to ^{57}Cu is expected to be in the 0.1 mb range, which in relative terms corresponds to about $3 \cdot 10^{-4}$ of the total fusion cross section. Use of the NEDA and DIAMANT detectors was thus essential to select events of interest. The isotopic and chemical purity of the

targets was also of primary importance, as in possible reactions on heavier Si isotopes, or on contaminants, cross sections for the emission of neutrons could be orders of magnitude higher than in the reaction on ^{28}Si . Such reactions would thus severely hamper tagging on rare neutron emission.

Analysis of the collected data is in progress.

Acknowledgment

This work is partly supported by the National Science Centre, Poland under Grant Agreement No. 2020/39/D/ST2/00466.

Bibliography

- [1] M. Palacz, *et al.* this Report, page 22, and references therein.
- [2] K. Arnsward, *et al.* Phys. Lett. **B820** (2021) 136592.
- [3] D. Kahl, *et al.* Phys. Lett. **B797** (2019) 134803.
- [4] D. F. Sherman, M. S. Zisman, R. A. Gough, and J. Cerny Phys. Lett. **B60** (1976) 261.
- [5] X. G. Zhou, *et al.* Phys. Rev. **C53** (1996) 982.
- [6] E. Stiliaris, *et al.* Zeitschrift für Physik **A326** (1987) 139.
- [7] A. Stolarz, *et al.* this Report, page 24.

C.2 DIAMANT at HIL — the NEEDI setup

*I. Kuti¹, J. Molnár¹, G. Jaworski², M. Palacz², A. Goasduff³, M. Matuszewski²
on behalf of DIAMANT and EAGLE collaborations.*

1) HUN-REN Institute for Nuclear Research (HUN-REN ATOMKI), Debrecen, Hungary

2) Heavy Ion Laboratory, University of Warsaw, Warszawa, Poland

3) INFN, Laboratori Nazionali di Legnaro, Legnaro, Italy

The DIAMANT light-charged-particle detector system [1, 2] was connected to EAGLE and NEDA [3–5] for the first time during its commissioning. The combination of the three detector arrays – NEEDI – was used in two experiments during the first physics campaign with the new arrangement.

DIAMANT is a light-charged-particle detector system, operated by the HUN-REN Institute for Nuclear Research (HUN-REN ATOMKI, Debrecen, Hungary). Over the past decades, DIAMANT has been effectively integrated with γ -detector arrays, contributing to various physics projects [6–9]. Recently, the front-end electronics and the mechanical structure of DIAMANT were extensively redesigned, the latter allowing for partial- or full-geometry configurations, also employing a pass-through target loader.

DIAMANT at HIL includes 72 detectors. Sixty-four detectors are mounted on a flexible PCB (printed circuit board) around the target, and eight detectors on a separate part further downstream. The main element of each detector unit is a 3 mm thick CsI(Tl) scintillator crystal, which is coupled to a PIN photodiode through a 5 mm thick plexiglass optical light guide. All detectors are equipped with charge-sensitive preamplifiers that operate in vacuum.

The signal processing is entirely digital and carried out in NUMEXO2 units [10], using custom, DIAMANT-specific firmware. The particle discrimination process is carried out in the FPGA units of NUMEXO2. The parameters PID (Particle ID), Energy, and Time are stored. The reaction channels of interest can be identified by applying gates on the PID values, or on two-dimensional distributions such as PID vs Energy or PID vs Time.

The acquisition systems have a common clock, provided by the GTS (Global Triggering System). The readout process and data collection of EAGLE-NEDA and DIAMANT is performed independently, data files are merged offline.

In 2023 two experiments (HIL105, HIL115) were performed successfully [11] with the NEEDI setup.

Acknowledgment

This work is partly supported by the National Science Centre, Poland under Grant Agreement No. 2020/39/D/ST2/00466.

Bibliography

- [1] J. Sheurer *et al.*, NIM A **385** (1997) 501.
- [2] J. Gál *et al.*, NIM A **516** (2004) 502.
- [3] J.J. Valiente-Dobon *et al.*, NIM A **927** (2019) 81.
- [4] G. Jaworski *et al.*, Acta Phys. Pol. **50(3)** (2019) 585.
- [5] J. Mierzejewski *et al.*, NIM A **659** (2011) 84.
- [6] J. Timár *et al.*, Phys. Rev. Lett. **122** (2019) 062501.
- [7] B. Cederwall *et al.*, Nature **469** (2010) 68.

- [8] A. Ertoprak *et al.*, The European Physical Journal A volume **56** (2020) 291.
- [9] B. Cederwall *et al.*, Phys. Rev. Lett. **124** (2020) 062501.
- [10] F.J. Egea-Canet *et al.*, IEEE Trans. Nucl. Sci. **62** (**3**) (2015) 1056.
- [11] M. Palacz *et al.*, this Report, page 47.

C.3 Study of the anomalous behavior of the Coulomb energy difference in the $A = 70$, $T = 1$ isobaric multiplet

*M. Matejska-Minda*¹, *P. Bednarczyk*¹, *M. Ciemala*¹, *G. Jaworski*², *I. Kuti*³, *M. Palacz*², *G. de Angelis*⁴, *T. Cap*⁵, *N. Cieplicka-Oryńczak*¹, *I. Dedes*¹, *K. Gajewska*¹, *J. Grębosz*¹, *K. Hadyńska-Kleńk*², *L. Iskra*¹, *M. Kmiecik*¹, *M. Komorowska*², *M. Kopeć*⁶, *M. Kowalczyk*², *J.A. Kowalska*², *A. Krakó*³, *B. Krzysic*³, *M. Loriggiola*⁴, *A. Malinowski*⁶, *M. Matuszewski*², *K. Mazurek*¹, *J. Molnár*³, *P.J. Napiorkowski*², *A. Otręba*⁶, *W. Poklepa*⁶, *M. Regulska*⁶, *J. Samorajczyk-Pyśk*², *P. Sekrecka*², *A. Stolarz*², *A. Špaček*², *J. Towers*⁷

1) Institute of Nuclear Physics Polish Academy of Sciences, Kraków, Poland

2) Heavy Ion Laboratory, University of Warsaw, Warszawa, Poland

3) HUN-REN Institute for Nuclear Research (HUN-REN ATOMKI), Debrecen, Hungary

4) INFN, Laboratori Nazionali di Legnaro, Legnaro, Italy

5) National Centre for Nuclear Research

6) Faculty of Physics, Warsaw University of Technology, Warszawa, Poland

7) Department of Physics, University of York, York, UK

In the $A \approx 70$, $N = Z$ nuclei, lying far off the stability line, a particularly strong proton-neutron correlation may occur due to the occupation of the same orbitals by nucleons of both types. In the structure of low and high-spin nuclear states in this region, the isovector ($J = 0$, $T = 1$) and the isoscalar ($J = 1$, $T = 0$) pn pairing may play a particular role [1]. In this region, different particle configurations drive a nucleus towards various deformed shapes: prolate, oblate, octupole, or non-axial [2]. Shell model calculations limited to the $f_{5/2}p_{1/2}g_{9/2}d_{5/2}$ active orbitals have shown that the configuration change along the $N = Z$ line may strongly influence the macroscopic properties of these medium-light nuclei, such as the moment of inertia [3]. A sharp change in the moment of inertia, that occurs around the $N = Z = 35$ nucleus ^{70}Br [3], suggests a qualitative structural change between nuclei with $N = Z \leq 35$ and $N = Z > 36$, and was attributed to a phase transition from a spherical to a deformed mean field. Since no nuclei sit in between, it implies that the structure change with nucleon number is sudden. The total energy surfaces for the $N = Z$ ^{68}Se and ^{72}Kr nuclei calculated using phenomenological mean-field theory [4] are presented in Fig. 1. The ^{68}Se nucleus in its ground state is prolate deformed, while the map for ^{72}Kr shows oblate (collective and non-collective) as well as triaxial minima. The coexistence of the prolate and oblate shapes is here a typical phenomenon, it was investigated recently for example in the selenium and krypton isotopes [5]. Moreover, nuclei lying close to the $N = Z$ line are of special interest because the effects of the isospin-symmetry breaking can manifest themselves through structural changes in this vicinity. The charge independence of nuclear forces requires that isobaric analog states in an isospin multiplet are degenerate. The only term breaking the isospin symmetry is the Coulomb interaction between protons. It was demonstrated that the Coulomb energy difference (CED) between $T = 1$ analog states is sensitive to structural changes in a nucleus gaining angular momentum through the alignment of nucleons [6]. Such a difference gives information on the nucleon alignment at the backbending, the evolution of the nuclear radii along the band, as well as on the isospin non-conserving terms in the residual interactions [7]. In the $N = Z$, $T_z = 0$ member of the $T = 1$ multiplet, one expects stronger pn pair correlations with respect to the like-nucleon pairing [7]. In contrast, in the $T_z = 1$ isobar proton-proton (besides neutron-

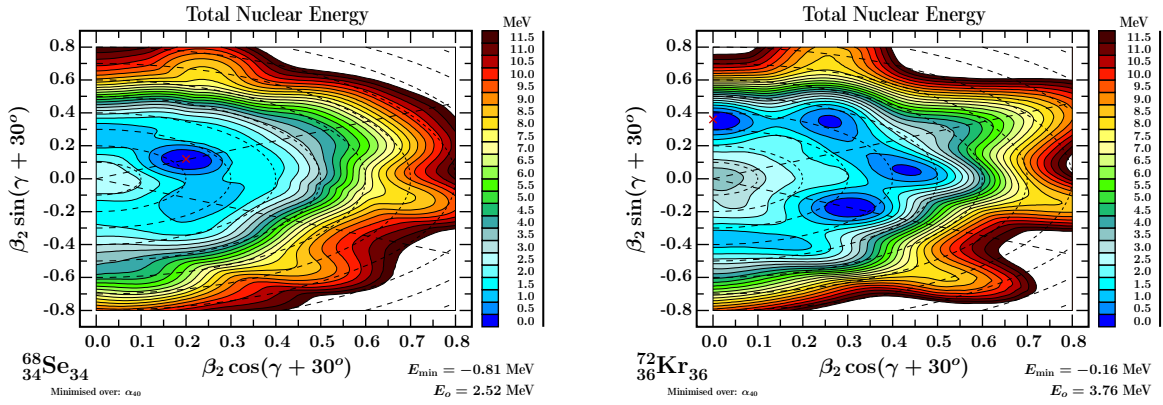


Figure 1: Total energy surface for the $N = Z$ ^{68}Se and ^{72}Kr nuclei calculated using mean-field theory [4], in the form of the (β_2, γ) representation, where at each point the energy was minimized over the hexadecapole deformations. The ^{68}Se nucleus in its ground state is prolate deformed, while the map for the ^{72}Kr shows oblate minima (collective and non-collective) as well triaxial ones.

neutron) correlations dominate, thus increasing the Coulomb energy. Yet, with growing angular momentum, due to Coriolis antipairing, alignment of protons takes place and the Coulomb repulsion gradually reduces. Therefore, in general, a rise of CED between $T = 1$, $T_z = 0, 1$ pairs with spin is observed, however, in the $^{70}\text{Br}/^{70}\text{Se}$ pair this trend is reversed [11]. As discussed in Ref. [11], a negative CED might arise if a significant change in the elongation of the nucleus with increasing spin can modify the Coulomb energy. It was pointed out in [11] that ^{70}Se exhibits an oblate shape in the ground state and a rather unstable prolate deformation ($\beta \sim 0.3$), extracted from lifetime measurements [9], in the low spin excited states $J^\pi < 8^+$. Studies of ^{70}Se at high spins [12] suggested that the prompting of the crossing observed in the $T = 1$ yrast band may be caused by an increase of prolate deformation. Furthermore, very recently ^{70}Kr has been investigated by Wimmer et al., [13], where the dramatic change found in the $B(E2; 0_{g.s.} \rightarrow 2_1^+)$ value between ^{70}Se and ^{70}Kr was interpreted as the result of a possible change of shape between the mirror partners, indicating a larger deformation in ^{70}Kr than in ^{70}Se .

To date knowledge of the level structure of ^{70}Br is based on two experimental works [10, 14]. Some hints about the possible structure of ^{70}Br may also be found in the work devoted to the spectroscopy of ^{70}Kr [8]. In the discussed works [10, 14], the fusion-evaporation reactions $^{40}\text{Ca}(^{32}\text{S}, \text{pn})$ and $^{40}\text{Ca}(^{36}\text{Ar}, \alpha\text{pn})$ were used to populate the excited states in ^{70}Br . The two resulting level schemes agree at low spins, but some discrepancies at higher angular momentum appear. The most important difference, as regards the $T = 1$ isobaric analog band in ^{70}Br is the presence of the weak 963 keV ($6^+ \rightarrow 4^+$) and 1025 keV ($8^+ \rightarrow 6^+$) transitions which are observed in the (pn) evaporation channel [14] but not in the (αpn) one [10]. From a comparison with the level scheme of ^{70}Se such transitions could correspond to the $8^+ \rightarrow 6^+ \rightarrow 4^+$ decay sequence (see [14]). Under this assumption the CED in the $^{70}\text{Br}/^{70}\text{Se}$ pair at spins above $4\hbar$ shows negative behavior. The investigations of the CED revealed that the $A = 70$ nuclei show a different (negative) trend than all other cases studied so far in the pf shell. A possible explanation for this unexpected behavior is related to the rapid evolution of nuclear shapes in these nuclei. This anomaly in CED between the isospin $T = 1$ states in the odd-odd $N = Z$ nucleus ^{70}Br and the analog states in its even-even partner ^{70}Se is a puzzle.

An experiment to study the $A \approx 70$, $N = Z$ nuclei, in particular the $^{70}\text{Br}/^{70}\text{Se}$ pair, was performed at HIL UW in December 2023 using the EAGLE-NEDA-DIAMANT setup [15]. A ^{32}S beam of 86-MeV energy impinged on a ^{40}Ca target. The target was made of 0.8 mg/cm^2 enriched ^{40}Ca material on a 12 mg/cm^2 Au backing, and to avoid fast oxidation of the target material it was covered with a thin $100 \text{ }\mu\text{g/cm}^2$ Au layer. The use of the NEDA and DIAMANT detectors is essential to select events of interest populated in this fusion-evaporation reaction. As can be seen in the spectrum presented in Fig. 2, setting the condition of 3 protons eliminates the background resulting from contamination like: target oxidation, scattering on the gold, as a result lines from the 3p reaction channel leading to the ^{69}As are very well seen. Analysis of the collected data is ongoing.

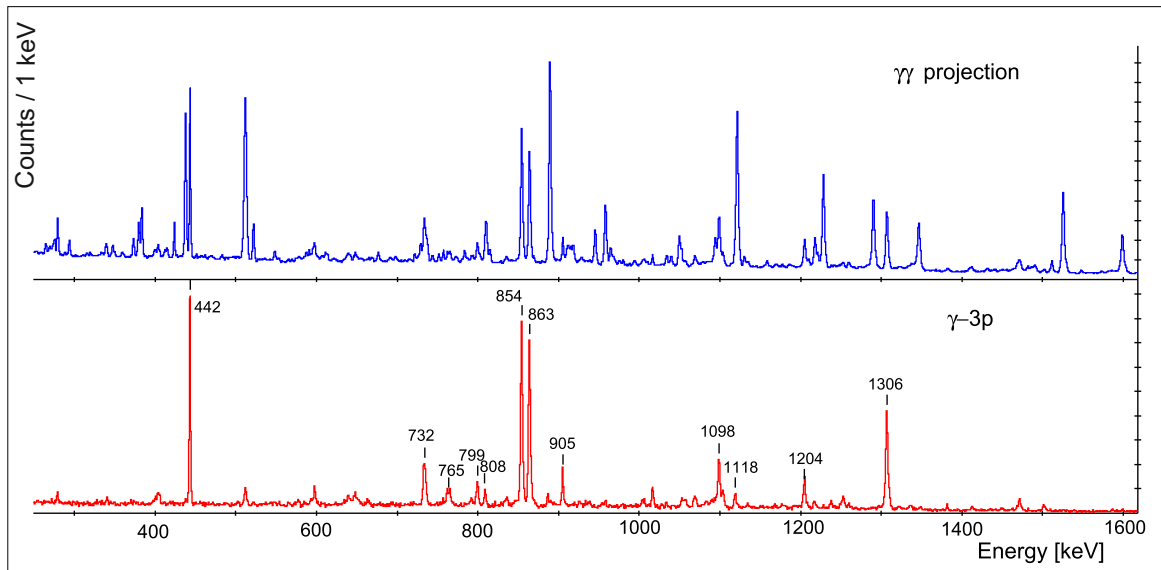


Figure 2: Gamma-ray energy spectra obtained in the fusion reaction of 86-MeV ^{32}S with a ^{40}Ca target (HIL115 experiment). The upper spectrum displays the $\gamma\gamma$ projection with no condition on particles, while lower one presents the γ -3p coincidence condition, which clears the spectrum from contamination like: target oxidation, scattering on the gold, and selects lines from the ^{69}As evaporation residue exclusively.

Acknowledgment

This work was supported by the National Science Centre, Poland under Grant Agreement No. 2023/50/E/ST2/00621, and 2020/39/D/ST2/00466. This project received funding from the European Union's Horizon Europe Research and Innovation programme under Grant Agreement No. 101057511 (EURO-LABS). The European Gamma-Ray Spectroscopy Pool (GAMMAPOOL) is acknowledged for providing HPGe detectors. I.K. acknowledges the support of the International Visegrad Fund under project no. 62320200.

Bibliography

- [1] W. Nazarewicz, et al. Nucl. Phys A 435 (1985) 397.
- [2] A.V. Afanasjev and S. Frauendorf Phys. Rev. C 71 (2005) 064318.
- [3] M. Hasegawa, et al. Phys. Lett. B 656 (2007) 51.
- [4] A. Gaamouci, et al., Phys. Rev. C 103, (2021) 054311.
- [5] J. Ljungvall et al., PRL 100, (2008) 102502.
- [6] C.D. O'Leary et al., Phys. Lett. B 525 (2002) 49.
- [7] M.A. Bentley, S.M. Lenzi, Prog. Part. Nucl. Phys. 59 (2007) 497.

- [8] D. M. Debenham, et al., *Phys. Rev. C* 94 (2016) 054311.
- [9] J. Heese, et al., *Z. Phys. A* 325 (1986) 325.
- [10] D.G. Jenkins et al., *Phys. Rev. C* 65 (2002) 064307.
- [11] B.S. Nara Singh et al., *Phys. Rev. C* 75 (2007) 061301.
- [12] G. Rainovski et al., *J. Phys. G: Nucl. Part. Phys* 28 (2002) 2617.
- [13] K. Wimmer et al., *Phys. Rev Letters* 126, (2021) 072501.
- [14] G. de Angelis et al., *Eur. Phys. J A* 12 (2001) 51.
- [15] M. Palacz, et al. this Report, and references therein.

C.4 Shape coexistence and octupole correlations in the light Xe, Cs and Ba nuclei investigated with the EAGLE+NEDA+Plunger setup

C.M. Petrache¹, A. Astier¹, P.M. Jodidar¹, G. Jaworski², M. Palacz²,
 K. Hadyńska-Klęk², M. Komorowska², M. Kowalczyk², K. Krutul-Bitowska²,
 P.J. Napiorkowski², J. Samorajczyk-Pyśk², J. Srebrny², A. Tucholski²
 K. Wrzosek-Lipska², M.M Palkowski³, W. Poklepa³, C. Fransen⁴, M. Beckers⁴,
 F. Dunkel⁴, L. Kornweibel⁴, F. von Spee⁴, C. Lakenbrink⁴, B.F. Lv⁵, K.K. Zheng⁵,
 S. Guo⁵, E. Grodner⁶, A. Nałęcz-Jawecki⁶, J. Grębosz⁷, E. Uusikyla⁸, T. Grahn⁸,
 J. Sarén⁸, J. Uusitalo⁸, Nuclear Spectroscopy Group⁸, A. Briscoe⁹, A. McCarter⁹,
 N. Macdonalds¹⁰, A. Krakó¹¹, I. Kuti¹¹, D. Sohler¹¹, C. Andreoiu¹², P. Spagnolett¹²,
 F. Wu¹²

1) Institut de Physique Nucléaire, CNRS/IN2P3, Université Paris-Saclay, Orsay, France

2) Heavy Ion Laboratory, University of Warsaw, Warszawa, Poland

3) Faculty of Physics, University of Warsaw, Warszawa, Poland

4) Institute for Nuclear Physics, University of Cologne, Germany

5) Institute of Modern Physics, Chinese Academy of Science, Lanzhou, China

6) National Centre for Nuclear Research

7) Institute of Nuclear Research, Kraków, Poland

8) Department of Physics, University of Jyväskylä, Finland

9) Oliver Lodge Laboratory, University of Liverpool, Liverpool, UK

10) Department of Physics, University of Surrey, Guildford, UK

11) HUN-REN Institute for Nuclear Research (HUN-REN ATOMKI), Debrecen, Hungary

12) Department of Chemistry, Simon Fraser University, Burnaby, Canada

In proton-rich $A \approx 120$ nuclei with the number of valence neutrons close to the maximum $N = 66$ outside the closed $Z, N = 50$ major shells, the proton-neutron interactions are predicted to lead to significant quadrupole deformation of $\beta_2 \approx 0.3$, enabling additionally Nilsson intruder and extruder states emanating from the $1h_{11/2}$ and $1g_{9/2}$ spherical sub-shell, respectively, to appear near the Fermi level [1]. The nuclei in this region of the nuclide chart are predicted to present pronounced octupole correlations, which are favoured at particle numbers near $N = Z = 56$ [2], primarily due to strong $d_{5/2}$ - $h_{11/2}$ correlations. Calculations with the quadrupole-octupole collective Hamiltonian relativistic Hartree-Bogoliubov (QOCH-RHB) model for ^{120}Ba and $^{116,118,120}\text{Xe}$ extracted from Ref. [3] are shown in Figs. 1 and 2.

Another interesting phenomenon in these nuclei is shape coexistence [4], which is predicted to occur due to the presence close to the proton Fermi surface of the low- Ω $h_{11/2}[550]1/2^-$ and high- Ω $h_{11/2}[505]11/2^-$ Nilsson orbitals for prolate and oblate deformations, respectively. Potential energy surfaces for ^{119}Cs and ^{120}Ba calculated with different interactions exhibiting wide minima in the γ direction are shown in Fig. 3. Very recently we succeeded in identifying a low-lying band based on an oblate shape in the strongly deformed ^{119}Cs nucleus in a MARA+JUROGAM experiment, which is predicted to have a lower quadrupole deformation than the prolate band [5]. A measurement of the lifetimes of the states in the two coexisting bands would bring solid support to the proposed interpretation.

The experimental determination of detailed properties in these nuclei will enable direct tests of theoretical calculations in extended model spaces, density functional theory predictions and also other shell model or cluster models, providing crucial information for the

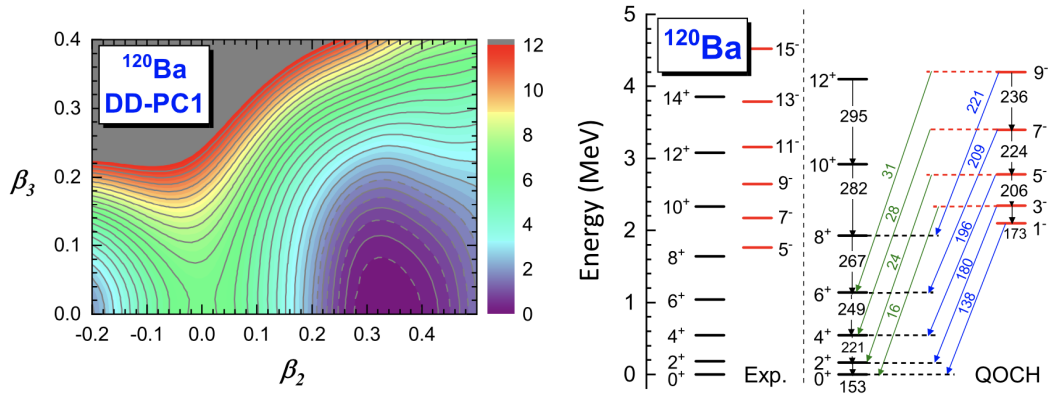


Figure 1: Deformation energy surface of ^{120}Ba in the $\beta_2 - \beta_3$ deformation plane, calculated with the QOCH-RHB model with the DD-PC1 density functional. The corresponding calculated excitation spectrum compared with the experimental one, as well as calculated intra-band $B(E2)$ (W. u.), inter-band $B(E1)$ ($\times 10^{-5}$ W. u.) and $B(E3)$ (W. u.) values of ^{120}Ba .

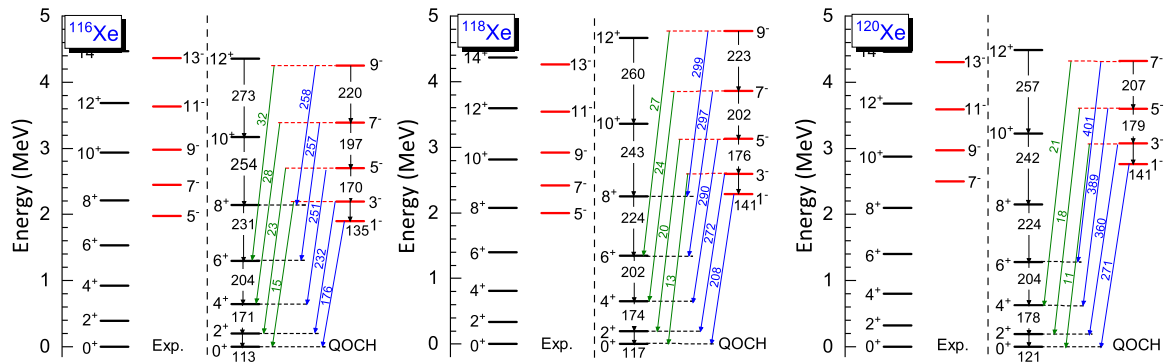


Figure 2: The excitation spectrum, intraband $B(E2)$ (W. u.), interband $B(E1)$ ($\times 10^{-5}$ W. u.) and $B(E3)$ (W. u.) values of $^{116-120}\text{Xe}$ calculated with the QOCH model based on DD-PC1 relativistic density functional, compared to experimental results.

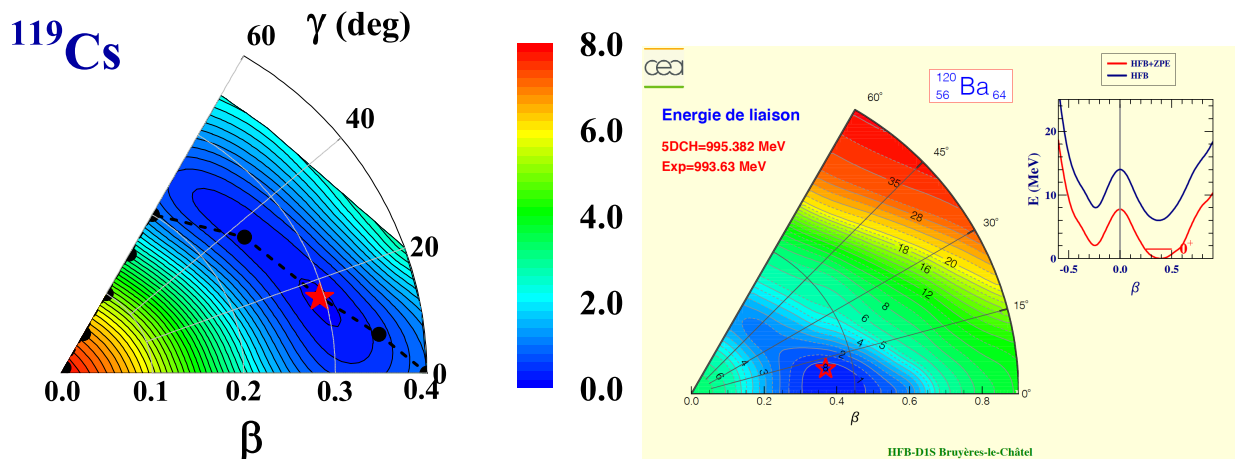


Figure 3: PES from TAC-CDFT calculations for ^{119}Cs [5] showing a wide minimum in the γ direction, and from the CEA Bruyère-le-Château website for ^{120}Ba showing the calculated oblate and prolate minima separated by ≈ 2 MeV.

understanding of the development of deformation and collective excitations close to the drip line.

Two successful experiments, each lasting two weeks, were performed with the NEEDLE setup in March and June 2023. The main aims of the experiments were to measure the lifetimes of low-lying excited states in light Xe, Cs and Ba nuclei using the complex EAGLE+NEDA array for the detection of photons and neutrons, coupled with the Köln plunger for measuring lifetimes in the picoseconds range. This powerful detection system can be used not only to enhance or select very weak reaction channels populated through the evaporation of several neutrons by exploiting the NEDA detectors for neutrons, but also to determine with high precision lifetimes of low-lying states using the performant plunger designed, constructed and implemented in the HIL detection system by the Köln group.

With such a powerful detection system, we will be able to establish essential quantities like transition probabilities from which we can deduce the deformations, which will confirm or not the prolate-oblate shape coexistence and chiral bands recently discovered in ^{119}Cs . We will also be able to extract separately the $B(E2)$ and $B(E1)$ transition probabilities, which, in contrast to the $B(E1)/B(E2)$ ratios of transition probabilities, will directly give the experimental information on the collectivity and deformation of the negative-parity bands via in-band $B(E2)$ values, as well as experimental information on the strength of the octupole correlations via the out-of-band $B(E1)$ values of the transitions from the negative-parity bands and the ground state band.

In the first experiment performed in March 2023, we used the ($^{106}\text{Pd}+^{16}\text{O},\alpha xnyp$) reaction with an ^{16}O beam of 80 MeV and intensity between 1 and 2 pnA. We measured at 8 plunger distances of 3, 6, 10, 20, 50, 100 and 500 microns, 1-1.5 days for each distance. In the second experiment performed in June 2023, we used the ($^{92}\text{Mo}+^{32}\text{S},\alpha xnyp$) reaction with a ^{32}S beam of 155 MeV and intensity between 1 and 2 pnA. We measured at 9 plunger distances of 1, 3, 6, 10, 20, 50, 100 and 500 microns, 1-1.5 days for each distance. The data analysis is in progress.

Acknowledgment

This work is partly supported by the National Science Centre, Poland under Grant Agreement No. 2020/39/D/ST2/00466.

Bibliography

- [1] P. Möller, *et al.*, *At. Data and Nucl. Data Tabl.* **94** (2008) 758.
- [2] J. Skalski *Phys. Lett.* **B 238** (1990) 6.
- [3] B.F. Lv *et al.*, *Phys. Rev. C* submitted.
- [4] B. Aggarwal, *et al.*, *Phys. Rev. C* **89** (2014) 024325.
- [5] K.K. Zheng *et al.*, *Phys. Lett.* **B 822** (2021) 136645.

C.5 Checking chirality – the lifetime of the 10^+ level in ^{128}Cs

A. Nałęcz-Jawecki¹, E. Grodner¹, J. Srebrny², M. Kowalczyk², Ch. Droste³, A. Stolarz³, J. Samorajczyk-Pyśk², G. Jaworski², M. Paluch-Ferszt², M. Palacz², T. Abraham², A. Tucholski², A. Kwiatkowska³, O. Smolira³, I. Skwira-Chalot³, A. Podwysocka³, J. Orliński³, C. Fransen⁴, C. Lakenbrink⁴, M. Beckers⁴, F. Spee⁴, Q.B. Chen⁵

1) National Centre for Nuclear Research, Poland

2) Heavy Ion Laboratory, University of Warsaw, Warszawa, Poland

3) Faculty of Physics, University of Warsaw, Warszawa, Poland

4) Institut für Kernphysik, University of Koln, Germany

5) Department of Physics, East China Normal University, Shanghai 200241, China

Introduction

In July 2022 an experiment was performed, which aimed to verify the chiral nature of the 10^+ state in ^{128}Cs . It is a first step to determine how nuclear chirality emerges with increasing spin [1-7]. The Recoil Distance Method (RDM) [8] was used to determine the lifetime of the 10^+ state. The PLUNGER device was set initially for 17 distances. Quick analysis during the experiment showed that we should focus on the range below $60\ \mu\text{m}$, in which we set 5 distances for longer acquisition.

The most efficient reaction was chosen, which is $^{10}\text{B}(^{122}\text{Sn},4n)^{128}\text{Cs}$ with 400 mb cross-section. Beam with an energy of 54 MeV was provided by the cyclotron of the Heavy Ion Laboratory of Warsaw University. More information on the setup and motivation can be found in last year's report [9].

The analysis is now nearly completed. Results show that the lifetime of the 10^+ state is $9 \pm 4\ \text{ps}$, which proves that there is a change in structure in comparison to higher, chiral levels.

Methodology

As stated before, the goal was to measure the lifetime of the 10^+ state in ^{128}Cs with RDM. The only transition from this state is 143 keV, which is lower than usually measured with RDM, because of its low Doppler shift. As the velocity of the recoil nuclei was $0.6\%c$, the shift was only 0.75 keV, which is less than the resolution of the LOAX detector used (about 1 keV). Therefore, the shifted (FLIGHT) peak was not separated from the non-shifted (STOP) and a special method was developed.

The method included 2 additional measurements during the experiment to get the shapes (i.e. gaussian width and position) of pure FLIGHT and pure STOP peaks. Pure FLIGHT was measured by setting a distance much higher than the lifetime of the 10^+ state. Measuring pure STOP was achieved by turning around the target. As the Sn target was originally on the a Au backing, after the turn the Sn part was facing the beam and the Au stopped (in $<1\ \text{ps}$) all the recoil nuclei, so the Doppler effect was seen.

STOP and FLIGHT positions are used for fitting the combined peak of the 10^+ to 9^+ transition. The result is very sensitive to these positions values – simulation shows that displacement of 0.1 keV changes the amplitude ratio by 30% when the amplitudes of STOP and FLIGHT peaks are similar, and even by 200% when one amplitude is 10 times smaller. Therefore, a very precise calibration, up to 0.01 keV, is needed.

Analysis

To maximize the resolution at 143 keV one LOAX detector was used. No X-ray shield was used to maximize the amount of 143 keV photons measured. The intensity of X-ray

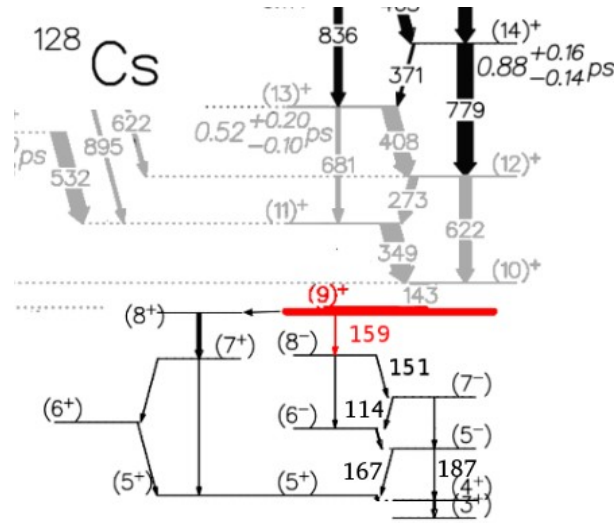


Figure 1: Relevant part of the ^{128}Cs decay scheme. The 10^+ to 9^+ transition of 143 keV was measured. The 114, 151, 159, 167, and 187 keV transitions, all below the 9^+ isomeric state, were used for coincidences to clean the 145 keV double X-ray peak and other background noise from the spectrum.

photons from Au, from which the beam dump and stopper were made, was so high that measuring 2 X-ray photons was at a similar rate as measuring a single gamma from ^{128}Cs . This caused an additional peak of 145 keV, too close to 143 keV peak of interest. The problem was overcome by using coincidences with 5 energies of transitions below the 9^+ isomeric state (see Fig 1) observed by 14 HPGe detectors in the EAGLE setup, which were provided by the European GAMMAPOOL.

A digital data acquisition system [10, 11] provided a nearly perfect linear calibration. Therefore for calibration, only 2 peaks were used. One, 67 keV, was an X-ray from Au and the second, 279 keV, from Coulomb excitation of Au. Both were much higher than any other peak. The 151 keV calibrated position was checked for every measurement and it was identical during the whole experiment with 10 eV accuracy.

During the analysis it was found that the 622 keV peak, which is the fast transition from the 12^+ to the 10^+ state, see Fig. 1, was not fully shifted even for the longest (600 μm) PLUNGER distance. The most probable cause is that some of the tin from the target diffused into the gold backing.

The target used was supposed to be 0.3 mg/cm^2 Sn on 5 mg/cm^2 Au backing. The velocity distribution of the recoil nuclei was supposed to be narrow. Simulating different velocity distributions and comparing them with the shapes of short-lived high-energy transition peaks, we discovered that the velocity distribution was much wider. Around 30% of cesium nuclei were produced too far inside the target so that they did not leave it. The wide velocity distribution also affected the time of flight. The simplest approximation that $t_{\text{average}} = d/v_{\text{average}}$ was no longer valid. Different times of flight for different velocities were calculated for better accuracy.

Results

The results show that the lifetime of the 10^+ state is 9 ± 4 ps. The uncertainty should be lowered after measuring the lifetimes of the 11^+ and 12^+ states, as they decay to the

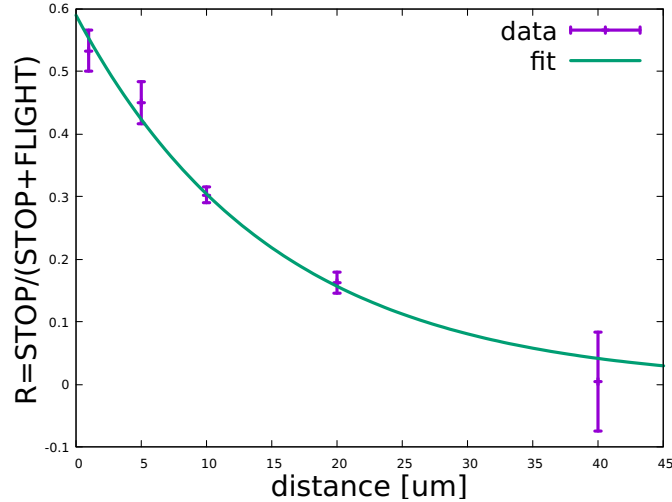


Figure 2: Dependence of the ratio $R = \text{STOP} / (\text{STOP} + \text{FLIGHT})$ on the PLUNGER target-stopper distance. If the feeding time is negligible the dependence should be exponential, as was fitted here. The fitted lifetime is 9 ± 4 ps.

10^+ state and are not negligible in comparison with 9 ps. These lifetimes might be up to 6 ps, but due to their low recoil velocity (around $0.6\%c$) and the minimum distance that could be set in the PLUNGER ($17 \mu\text{m}$), the time of flight for the shortest distance was about 10 ps. Therefore, most of the nuclei had already decayed below the 11^+ state, so the FLIGHT peaks of these transitions were already small and prone to inaccuracies. The way to measure these lifetimes is to use a beam of heavier nuclei, so that the recoil velocity will be faster. An experiment with a ^{22}Ne beam has already been proposed and accepted by the HIL PAC.

To interpret the lifetime in terms of chiral structure, one must compare it to previous experiments [7, 13]. The bandhead isomeric 9^+ state was found to be not chiral by measurements of the g-factor. States with spin 13 and higher were found to be chiral. Extrapolating properties from states with spin 13 and higher, the lifetime of the 10^+ state should be ≥ 60 ps. The lifetime at a level of around 10 ps suggests that the structure changes between spin ≥ 13 and 10 – the 10^+ state properties do not fit the properties of an ideal chiral structure with $\gamma = 30^\circ$.

Bibliography

- [1] S. Mukhopadhyay *et al.*, Phys. Rev. Lett. **99** (2007) 172501.
- [2] T. Marchlewski *et al.*, Acta Physica Polonica **B 11** (2018) 87.
- [3] Wu Xiaoguang *et al.*, Plasma Science and Technology **14** (2012) 526.
- [4] T. Marchlewski *et al.*, Acta Physica Polonica **B 46** (2015) 60.
- [5] P. Olbratowski *et al.*, Phys. Rev. Lett. **93**(2004) 052501.
- [6] T. Koike *et al.*, Phys. Rev. Lett. **93** (2004) 172502.
- [7] E. Grodner *et al.*, Phys. Rev. Lett **97** (2006) 172501.
- [8] A. Dewald *et al.*, Progress in Particle and Nuclear Physics, **67** (2012) 786.
- [9] A. Nałęcz-Jawecki *et al.* HIL Annual Report 2022, page 72.
- [10] T. Abraham *et al.*, HIL Annual Report 2018, page 51.
- [11] M. Palacz *et al.*, HIL Annual Report 2020, page 10.
- [12] J. Mierzejewski *et al.*, The COMPA manual.
- [13] E. Grodner *et al.*, Front. Phys. **19** (2024)34202.

C.6 Quasielastic barrier distributions for the $^{20}\text{Ne} + ^{92,94,95}\text{Mo}$ systems: Influence of dissipation

G. Colucci¹, E. Piasecki¹, A. Trzcińska¹, M. Wolińska-Cichocka¹, B. Zalewski¹, M. Kisieliński¹, M. Kowalczyk¹, E. Geraci², B. Gnoffo², K. Hadyńska-Kleńka¹, G. Jaworski¹, P. Koczoń³, J.A. Kowalska¹, Y. Leifels³, B. Lommel³, F. Risitano², J. Samorajczyk-Pyśk¹, A. Stolarz¹, M. Trimarchi², W. H. Trzaska⁴, A. Tucholski¹, C. Zagami^{5,6}

1) Heavy Ion Laboratory, University of Warsaw, Warszawa, Poland

2) INFN Sezione di Catania, Catania, Italy

3) GSI Helmholtz Center for Heavy Ion Research, Darmstadt, Germany

4) Department of Physics, University of Jyväskylä, Finland

5) Dip. di Fisica e Astronomia, Univ. di Catania, Catania, Italy

6) INFN-LNS, Laboratori Nazionali del Sud, Catania, Italy

Determination of the barrier distributions (BD) is an excellent tool for revealing details in the energy dependence of the measured fusion cross sections at energies close to the Coulomb barrier. During fusion reactions the excited states of the projectile and target nuclei are populated in a complex manner, and their relative motion couples with them. The study of the influence of a small number of projectile and target collective excitations on near- and sub-barrier fusion was successfully addressed by the Coupled Channels (CC) method [1–3].

The CC calculations reproduced experimental results of fusion excitation functions for many systems, explaining the enhancement of sub-barrier fusion cross sections and the observed structures in the barrier distributions. However, there are mechanisms whose influence on the fusion still needs to be better understood: weak (non-collective) excitations and transfer reaction channels. There are hypotheses that they can be responsible for the smoothing of the BD observed experimentally in some systems.

A measurement of the BD for the $^{20}\text{Ne} + ^{92,94,95}\text{Mo}$ systems was proposed and performed at the Heavy Ion Laboratory of Warsaw University. The experiment aimed to study the influence of dissipation on fusion via measurements of quasielastic barrier distributions under well-controlled conditions by choosing isotopes of the same element that differ by single particle level densities. In this perspective, the target nuclei were chosen to minimize the influence of transfers and maximize the difference between the single-particle (s.p.) level densities.

The ^{20}Ne beam (of 65 MeV, 70 MeV, and 73 MeV) was accelerated by the U200-P Cyclotron. The beam current was ~ 25 enA. The ~ 0.5 MeV energy steps were obtained by employing a set of degraders (thin $^{\text{nat}}\text{Ni}$ and $^{\text{nat}}\text{Au}$ foils). The targets, ^{92}Mo , ^{94}Mo , and ^{95}Mo of thicknesses 160 - 180 μ/cm^2 , were prepared from MoO_3 on a C backing of 40 μ/cm^2 thickness. The compact CUDAC3 chamber was used. It was equipped with an array of 30 silicon detectors (PIN diodes) placed at backward angles, viz. 145, 135, and 125 degrees and four PIN diodes at the forward angle of 35 degrees. The backward detectors allow us to determine the energy and number of the backscattered projectiles. The forward ones were used for beam energy determination and gave information on the Rutherford cross section. The energy resolution (resulting mainly from the beam properties) was also monitored and was equal to 1.5 MeV, 2.2 MeV, and 1.3 MeV for $^{92,94,95}\text{Mo}$, respectively, in the center-of-mass system.

The barrier distributions were extracted for the three systems. Preliminary results are shown in Fig. 1, where the experimental barrier distributions are compared with the theo-

retical predictions. The theoretical calculations performed within the standard CC method (dashed lines) [4] included the rotational coupling to the first three excited states of ^{20}Ne and vibrational couplings up to the two-phonon excitations of the first quadrupole and octupole excited states of the $^{92,94}\text{Mo}$ isotopes. In the case of the odd ^{95}Mo isotope, the couplings to the one phonon excitation of the $3/2^+$ and the one and two phonon excitations of the $5/2^+$ excited states were included by treating them as quadrupole and octupole excitations, respectively. The results of the calculation performed with the CC+RMT [5] model are also shown (solid lines).

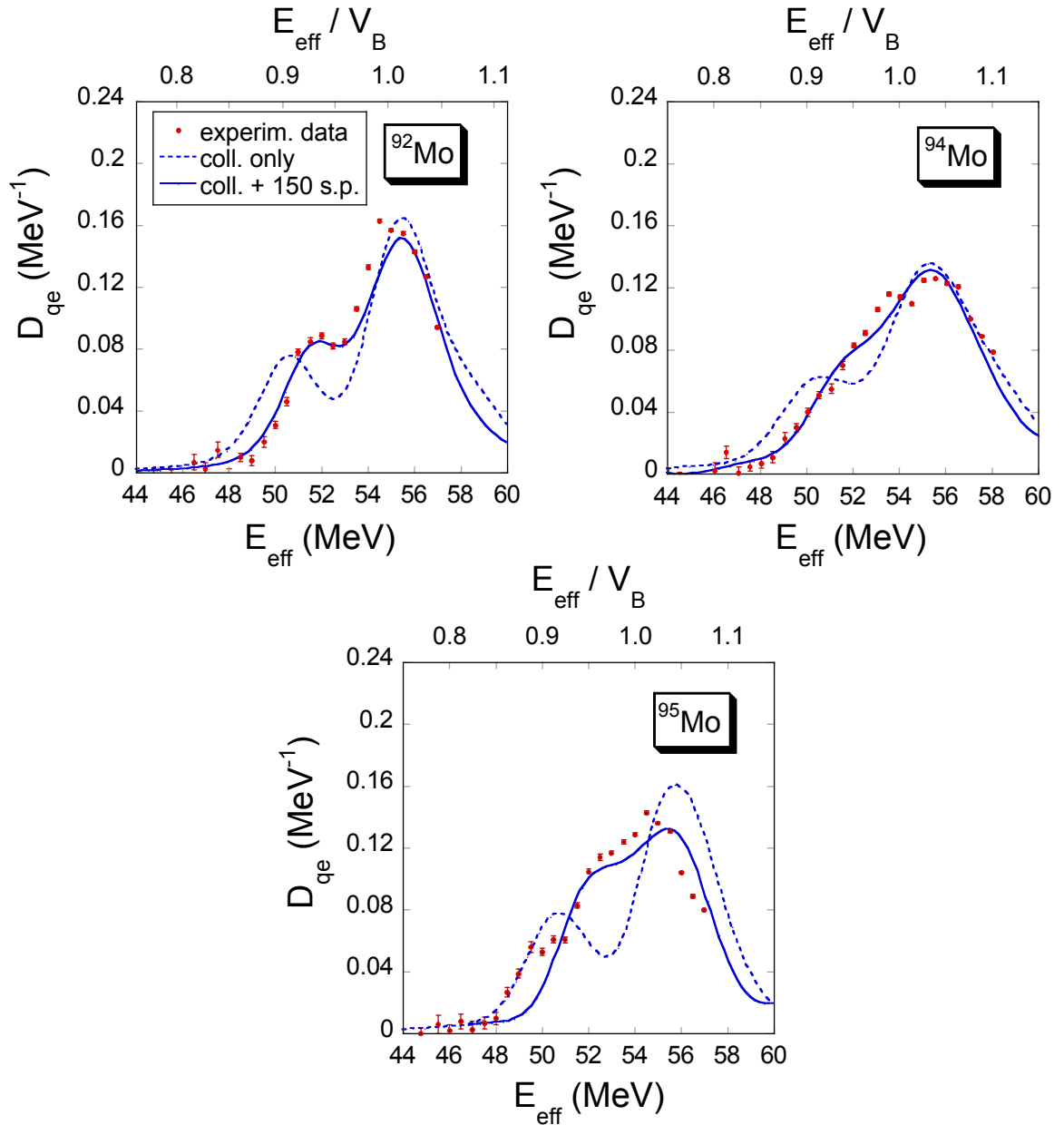


Figure 1: Quasielastic barrier distributions of the $^{20}\text{Ne}+^{92,94,95}\text{Mo}$ systems. The experimental data are compared with predicted barrier distributions, with (solid lines) and without (dashed lines) including dissipation due to non-collective excitations. The energy resolution for the three systems was taken into account by folding the calculated distributions with a Gaussian function with a corresponding FWHM.

The study of the $^{20}\text{Ne}+^{92,94,95}\text{Mo}$ systems indicates the influence of dissipation due to coupling to non-collective excited states on the shape of the barrier distributions. It reveals the smoothing out of the barrier distribution with respect to the CC prediction. It is stronger for the heavier Mo isotopes, with higher level density. The theoretical calculations performed within the CC+RMT model agree with the experimental data, supporting the hypothesis that non-collective excitations can alter the structure of the barrier distributions. In the case of nuc95Mo , the experimental BD is slightly wider than the theoretical prediction. Another dissipation mechanism could cause this: projectile-target transfers of light particles. This hypothesis will be checked in a separate experiment planned for 2024.

Bibliography

- [1] M. Dasgupta *et al.*, *Annu. Rev. Nucl. Part. Sci.* **48** (1998) 401.
- [2] T. Tamura, *Rev. Mod. Phys.* **37** (1965) 679.
- [3] G. Montagnoli, A. Stefanini, *Eur. Phys. J. A* **59** (2023) 138.
- [4] K. Hagino and N. Rowley (unpublished).
- [5] E. Piasecki *et al.*, *Phys. Rev. C* **100** (2019) 014616.

C.7 The experimental campaign with the Warsaw SilCA(DSSD) array at the IJC Lab, Orsay, France

K. Hadyńska-Klęk¹, P. Napiorkowski¹, C. Hiver², G. Pasqualato², J.N. Wilson², on behalf of the ν -ball2+SilCA(DSSD)+PARIS campaign in 2023 at the IJC Lab, Orsay, France.

1) Heavy Ion Laboratory, University of Warsaw, Warszawa, Poland

2) Irene Joliot Curie Laboratory, Orsay, France

The SilCA versatile scattering chamber was designed and built at the Heavy Ion Laboratory in Warsaw to accommodate an annular DSSD array (Double-Sided Silicon Strip Detector) [1]. It was vacuum tested and shipped to the Irene Joliot-Curie Laboratory, Orsay, France in Autumn 2022. The array was equipped with a motorised and automated rotating target changer (3D-printed) and in analogue camera with LED illumination, see the right panel of Fig.1. The SilCA(DSSD) chamber was coupled to the ν -ball2 HPGe clover array [2] and the PARIS LaBr₃ (CeBr) + NaI phoswich high-energy γ scintillator calorimeter [3], see Fig. 1.

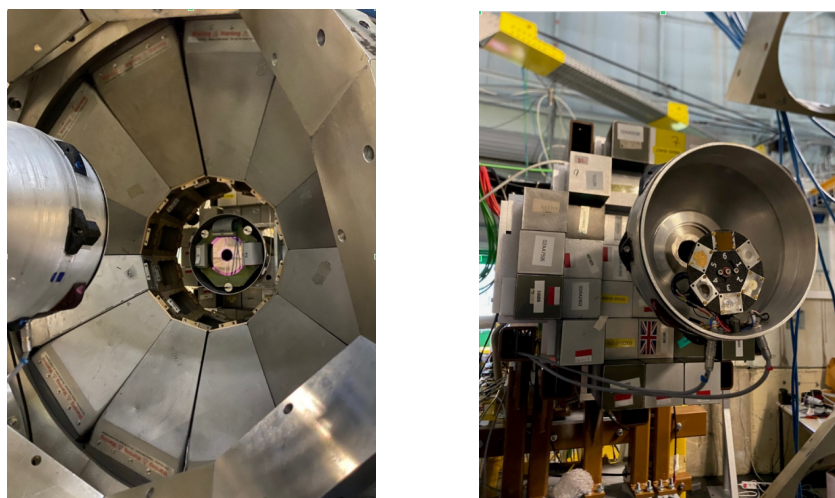


Figure 1: The Warsaw DSSD detector in the SilCA scattering chamber, placed in the ν -ball2 frame. View of the backward (left panel, the DSSD array is shown) and the forward (right panel, the target changer is presented) hemispheres.

The setup was in-beam commissioned at the ALTO facility in December 2022. A Coulomb excitation reaction with a 66 MeV ^{16}O beam scattered from a ^{197}Au target was successfully tested. The commissioning experiment was followed by a campaign of measurements with the ν -ball2+SilCA(DSSD)(+PARIS) setup:

1. *Evidence for enhanced collectivity in ^{58}Fe examined through Coulomb excitation* (spokespersons: G. Pasqualato (IJC Lab, Orsay, France), J. Ljungvall (IJC Lab, Orsay, France), A. Stuchbery (Australian National University, Canberra, Australia));
2. *Coulomb excitation of the super-deformed band in ^{40}Ca* (spokespersons: P. Napiorkowski (Heavy Ion Laboratory University of Warsaw, Poland), A. Maj (Henryk Niewodniczański Institute of Nuclear Physics PAN, Kraków), F. Azaiez ((IJC Lab, Orsay, France)));

3. *Emergence of collectivity near magic nuclei: Coulomb-excitation of ^{62}Ni*
(spokespersons: K. Hadyńska-Klęk (Heavy Ion Laboratory University of Warsaw, Poland), M. Rocchini (INFN Sezione di Firenze, Florence, Italy), N. Marchini (INFN Sezione di Firenze, Florence, Italy));
4. *Investigation of high spin structures in ^{44}Ti and ^{42}Ca via discrete and continuum gamma spectroscopy using ν -ball2, PARIS and OPSA setup*
(spokespersons: M. Matejska-Minda (Henryk Niewodniczański Institute of Nuclear Physics PAN, Kraków), K. Hadyńska-Klęk (Heavy Ion Laboratory University of Warsaw, Poland));
5. *Search for the fission shape isomer in ^{232}Th*
(spokesperson: C. Hiver (IJC Lab, Orsay, France));
6. *$^{194,196}\text{Hg}$ fission studies*
(spokesperson: K. Miernik (Faculty of Physics, University of Warsaw, Poland));
7. *Detailed spectroscopy of fission isomers in uranium isotopes*
(spokesperson J. Wilson (IJC Lab, Orsay, France)).

In the first three experiments the DSSD array was used to register back-scattered heavy ions following Coulomb excitation. It should be noted that in experiment number 3 (Coulomb-excitation of ^{62}Ni), due to problems with the beam, the beam was changed from ^{62}Ni to ^{60}Ni and scattered on a ^{197}Au target. The online spectrum, Doppler-corrected for the ^{60}Ni velocity, is presented in Fig. 2.

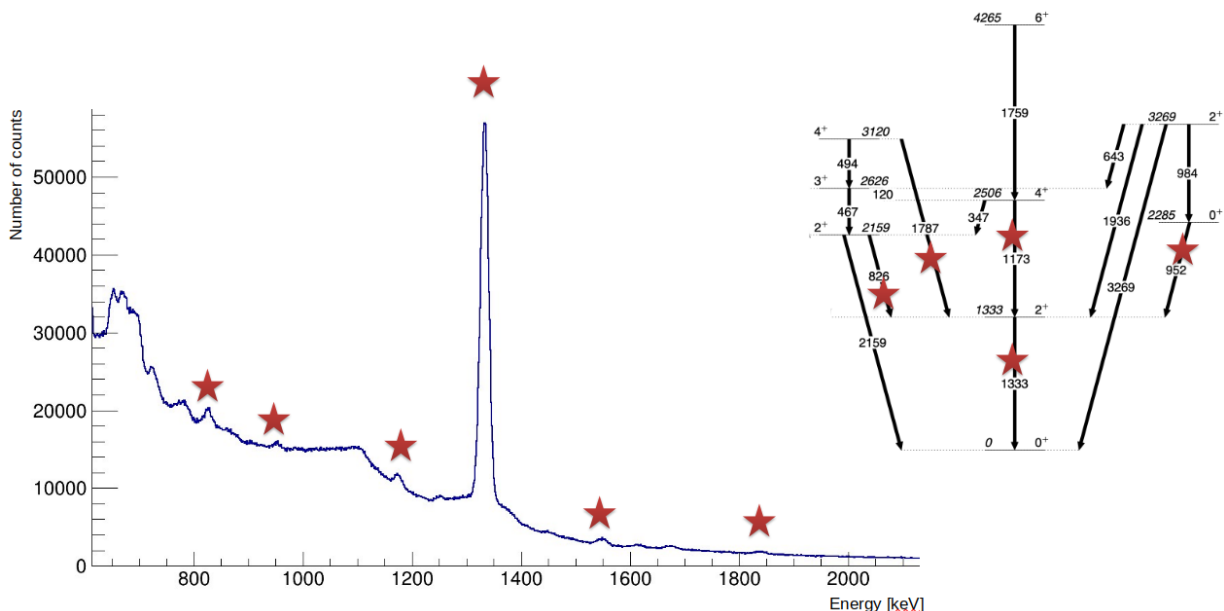


Figure 2: The on line ^{60}Ni Coulomb-excited spectrum, collected with a ^{197}Au target, Doppler-corrected for the ^{60}Ni velocity. Inset: level scheme of ^{60}Ni .

In experiments 5, 6 and 7, the DSSD array was shielded against emitted fission fragments with aluminum foil, and the detector was used to register light ions exclusively (protons, deuterons, and alpha particles). In experiment 4 the DSSD array replaced the initially proposed OPSA detector and measured the light ions emitted after the fusion-evaporation reaction. The analysis of all the listed experiments is currently ongoing.

After the campaign, in the Autumn of 2023, the SilCA chamber was shipped back to Warsaw. In February 2024 an ^{241}Am α source was used to test the properties of the DSSD array after its return from maintenance performed at the University of Lund, Sweden. The SilCA array was placed in the frame of the EAGLE spectrometer [4] and tested with CAEN V1725SB digitizers using the COMPASS [5] and XDAQ CERN-LNL software. The SEAGLE (SilCA(DSSD)+EAGLE) setup will be commissioned in-beam in June 2024 using Coulomb excitation of ^{104}Pd with ^{32}S projectiles delivered from the Warsaw cyclotron.

The chamber is currently in the process of redesigning to accommodate a set of side detectors mounted in the forward hemisphere, extending from around 90 degrees towards lower angles.

Bibliography

- [1] K. Hadyńska-Klęk et al., *SilCA – Silicon Coulomb excitation Array at the Heavy Ion Laboratory*, HIL Annual Report 2022, page 20.
- [2] M. Lebois et al. Nucl. Inst. and Meth. **A 960** 163580 (2020).
- [3] A. Maj *et al.*, The PARIS project, Acta Phys. Pol. **B 40** (2009) and F. Camera and A. Maj, PARIS White Book, ISBN 978-83-63542-22-1 (2021) 565.
- [4] J. Mierzejewski *et al.*, Nucl. Inst. and Meth. **A 659**, 84, (2011).
- [5] COMPASS – Multiparametric DAQ Software for Physics Applications (<https://www.caen.it/products/compass/>).

C.8 Low-energy electromagnetic structure of ^{110}Cd studied using Coulomb excitation

I. Piętka¹, K. Wrzosek-Lipska¹, L. Próchniak¹, P.E. Garrett², M. Zielińska³, P.J. Napiorkowski¹ on behalf of HIL094 collaboration

1) Heavy Ion Laboratory, University of Warsaw, Warszawa, Poland

2) University of Guelph, Guelph, Canada

3) IRFU, CEA, Université Paris-Saclay, Gif-sur-Yvette, France

For several decades, stable even-mass Cd isotopes have been considered to be textbook examples of multiphonon spherical vibrators [1] based on the excitation energy pattern of their low-lying states. However, in the isotopes near the neutron mid-shell, “additional” 0^+ and 2^+ states were found in the vicinity of the presumed two-phonon states that were initially unexplained [2]. A study of the β decay of ^{110}In established a rotational-like band built on the 0_2^+ level in ^{110}Cd , indicating the presence of deformed intruder states [3]. Gamma-ray spectroscopy of stable even-even Cd isotopes (summarized in Refs. [4–6]) revealed consistent and systematic discrepancies between a number of the measured $B(E2)$ values and the model predictions, even if mixing of the intruder and vibrational states was invoked. These discrepancies were perhaps the most clearly delineated in ^{110}Cd , for which a recent measurement of ^{110}In β decay [6] observed a number of transitions between the low-lying excited states, or established upper limits on them. Subsequent investigation of ^{110}Cd and ^{112}Cd using the symmetry-conserving configuration-mixing (SCCM) method [7, 8] and the General Bohr Hamiltonian (GBH) approach [9] suggested the presence of multiple shape coexistence in these isotopes. To verify the shape-coexistence scenario and establish the shapes of low-lying 0^+ states in $^{110,112}\text{Cd}$, complete sets of transitional and diagonal $E2$ matrix elements, including their relative signs, are needed. This key experimental information can be obtained using the low-energy Coulomb-excitation technique [10].

The first step in this investigation, focused on the lowest-lying states in ^{110}Cd , involved their Coulomb excitation with 91-MeV ^{32}S [9] and 34.7-MeV ^{14}N [11] beams delivered by the cyclotron at the Heavy Ion Laboratory in Warsaw. From the measured γ -ray yields combined with known spectroscopic data, a set of electromagnetic matrix elements was extracted using the GOSIA code [12]. In particular, the $B(E2)$ values in the decay of the 2_2^+ state have been precisely determined, yielding a lifetime of this state with a relative uncertainty of 3%. The literature values of this lifetime [6, 13–15] have uncertainties ranging from 22% to 37%. Accurate data for the 2_2^+ state — assigned as the γ bandhead in Ref. [6] — are important as we aim to distinguish between the existing interpretations of the 2_2^+ state, i.e. establish whether it results from a multi-phonon excitation or a non-axial rotation.

We report in Fig. 1 our experimental results, i.e., relative $B(E2)$ values between the lowest-lying states in ^{110}Cd , compared with predictions of two theoretical approaches: the simplest quadrupole harmonic vibrational model and the General Bohr Hamiltonian [16]. For the latter, two effective interactions from the Skyrme family were used, i.e., SLy4 and UNEDF0. The GBH model treats simultaneously and on equal footing both vibrational and rotational excitations and describes the full quadrupole dynamics including both of these degrees of freedom. It is worth emphasizing that in this approach no parameters are fitted to the properties of the nucleus under study.

Within the vibrational model, the absolute $B(E2)$ values for the decay of two-phonon states (2^+ , 4^+ , 0^+) to the one-phonon level (2_1^+) are twice as large as the $B(E2; 2_1^+ \rightarrow 0_1^+)$

value, while transitions changing the phonon number by more than one are prohibited (Fig. 1(b)). Our experimental results are in clear disagreement with this simple picture, as shown in Fig. 1(a). This observation agrees with conclusions drawn in Refs. [4–6].

The results obtained with the GBH model differ depending on the variant of the Skyrme interaction (SLy4 or UNEDF0) used in the calculations. This particularly concerns relative intensities of transitions deexciting the 2_2^+ state, which are in better agreement with the experimental findings when using the SLy4 interaction. The GBH (UNEDF0) predictions (Fig. 1(d)) closely resemble those obtained for a harmonic oscillator potential.

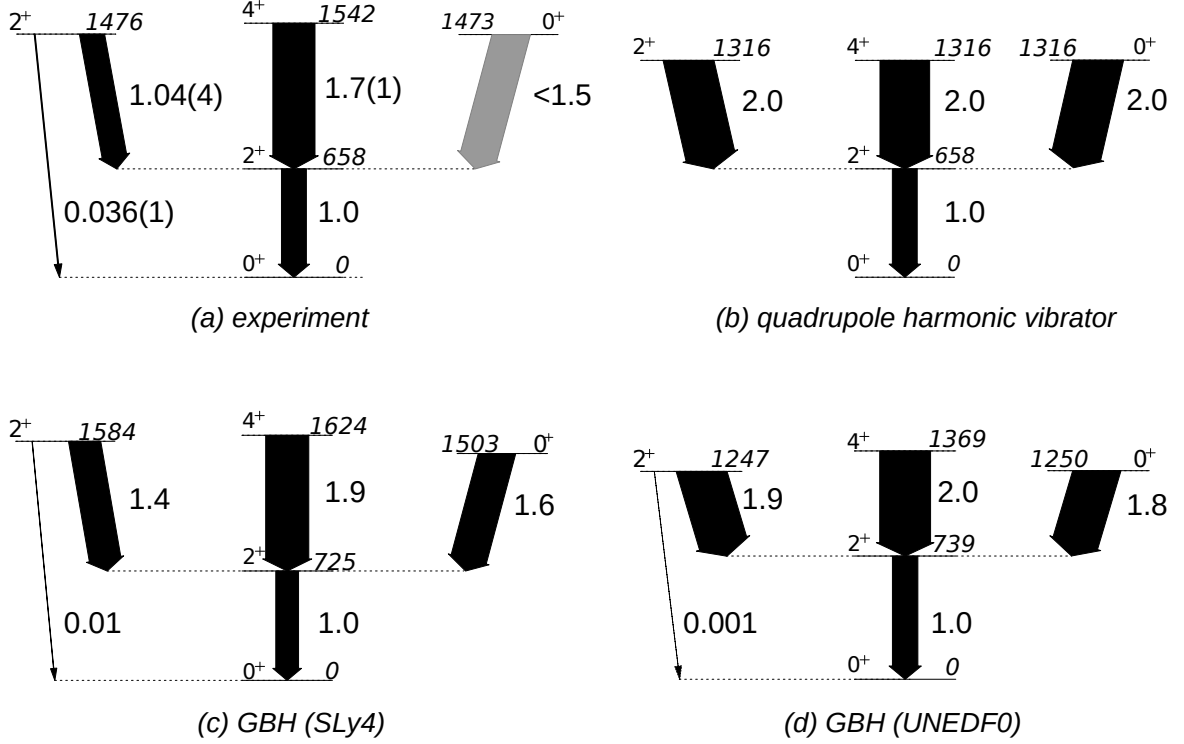


Figure 1: Low-energy portion of the ^{110}Cd level scheme resulting from (a) current Coulomb-excitation experiments [17] complemented by $(n,n'\gamma)$ studies [6]; (b) quadrupole harmonic vibrator model with the assumption that the energy of the first excited state (2_1^+) equals 658 keV; (c,d) calculations within the GBH approach using two variants of the Skyrme interaction: (c) SLy4 and (d) UNEDF0 [18]. Level energies are given in keV. $B(E2)$ values are given relative to $B(E2; 2_1^+ \rightarrow 0_1^+)$ and reflected in arrow widths. The gray arrow in panel (a) indicates that the corresponding $B(E2)$ value was obtained from a lifetime measured in a $(n,n'\gamma)$ study [6].

This analysis was the subject of the Master’s thesis of I. Piętko defended in September 2023 at the Faculty of Physics, University of Warsaw [17].

Bibliography

- [1] R.F. Casten, Nuclear Structure from a Simple Perspective (Oxford Univ. Press 1990).
- [2] B.L. Cohen and R.E. Price, Phys. Rev. **118** (1960) 1582.
- [3] R. Meyer and L. Peker, Zeitschrift für Physik **A283** (1977) 379.
- [4] P.E. Garrett and J.L. Wood, J. Phys. G: Nucl. Phys. **37** (2010) 064028.
- [5] P.E. Garrett *et al.*, Phys. Scr. **93** (2018) 063001.
- [6] P.E. Garrett *et al.*, Phys. Rev. C **86** (2012) 044304.
- [7] P.E. Garrett *et al.*, Phys. Rev. C **101** (2020) 044302.
- [8] P.E. Garrett *et al.*, Phys. Rev. Lett. **123** (2019) 142502.
- [9] K. Wrzosek-Lipska *et al.*, Acta Phys. Pol. **B51** (2020) 789.
- [10] M. Zielińska, Low-Energy Coulomb Excitation and Nuclear Deformation, in: The Euroschool on Exotic Beams, vol.VI, S.M. Lenzi and D. Cortina-Gil (eds.) Lecture Notes in Physics **1005**, pp. 43-86 (Springer, 2022).
- [11] I. Piętka *et al.*, HIL Annual Report 2022, page 63.
- [12] T. Czosnyka, D. Cline and C.Y. Wu, Bull. Amer. Phys. Soc. **28** (1983) 745.
- [13] Yu.N. Lobach *et al.*, Eur. Phys. J. **A6** (1999) 131.
- [14] M.F. Kudoyarov *et al.*, Proc. 45th Ann. Conf. Nucl. Spectr. Struct. At. Nuclei (St. Petersburg, 1995) 60.
- [15] J. Wesseling *et al.*, Nucl. Phys. A **535** (1991) 285.
- [16] L. Próchniak and S.G. Rohoziński, J. Phys. G: Nucl. Phys. **36** (2009) 123101.
- [17] I. Piętka, MSc. thesis, University of Warsaw, Poland (2023).
- [18] L. Próchniak, private communication.

C.9 Microscopic calculations of collective properties of the even-even $^{180-198}\text{Pt}$ isotopes.

L. Próchniak

Heavy Ion Laboratory, University of Warsaw, Warszawa, Poland

I present here a part of the theoretical results concerning collective properties of even-even Pt isotopes with mass numbers from 180 to 198. The lighter, neutron deficient, $^{180-188}\text{Pt}$ isotopes are unstable with half-lives from 56 s to 10.2 days. The other half of this set contains stable nuclei and for some of them experimental data are quite abundant. The applied theoretical framework consists of the General Bohr Hamiltonian model [1] with the potential energy and mass parameters calculated from the mean-field theory using the ATHFB approach. An accurate description of the evolution of the properties of the nuclei forming this long chain of isotopes is a challenge to theory. On the other hand, such a long chain of isotopes provides a good playground to test various aspects of the theory, in particular the consequences of a specific choice of effective nucleon-nucleon interaction used as a basis for the mean-field calculations. The ATDHFB calculations were done using four versions of a non-relativistic nucleon-nucleon interaction of the Skyrme type, namely SIII, SLy4, UNDEF0 and UNEDF1. The first two, well-known for many years, require the pairing interaction to be chosen. The strength of the pairing is determined by the mass differences in the considered region of nuclei. For the second pair, also called universal density functionals [2], all details of the interactions are fixed by a global fit. In both cases, no experimental spectroscopic data are used to determine the parameters of the theory.

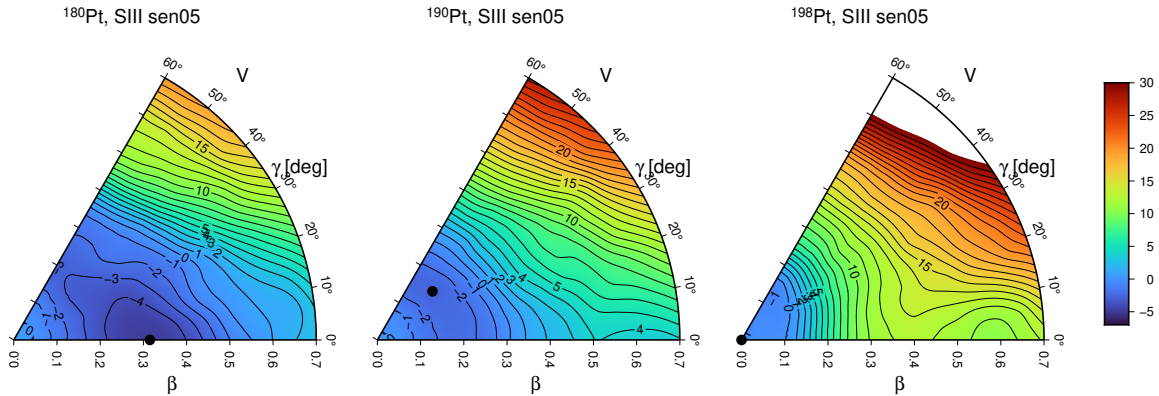


Figure 1: Theoretical potential energy relative to a spherical shape calculated with the SIII interaction.

To calculate energy levels and strengths of electromagnetic transitions, that is quantities directly comparable to experimental data, within the framework of the GBH theory one needs to know the collective potential energy and the so-called inertial functions (the moments of inertia included) as functions of the deformation variables (β , γ). These functions are obtained from the ATDHFB approach. As an illustration of the evolution of the potential energy I show in Fig. 1 plots of the collective potential energy for the chosen three isotopes: the lightest one, ^{180}Pt , the medium-mass ^{190}Pt , and the heaviest one, ^{198}Pt calculated with the SIII interaction. The transition from significant axial deformation in

the light isotopes to the almost spherical shape of ^{198}Pt is visible. The UNEDF1 and Sly4 interactions give even larger axial deformation for the lighter isotopes. The UNDEF0 interaction also predicts deformation for these isotopes but, a bit surprisingly, of the oblate type.

The next figures show a comparison of the results of calculations with experimental data. Again I chose the SIII interaction for the energy levels. The selected energy levels, namely the lowest yrast states (2_1 , 4_1) and the bandheads of quasi- γ and quasi- β Fig. 2. The agreement with experiment is remarkably good. Other interactions also gave good results, however, it is worth mentioning that UNEDF1 predicts yrast states lying systematically below the experimental ones.

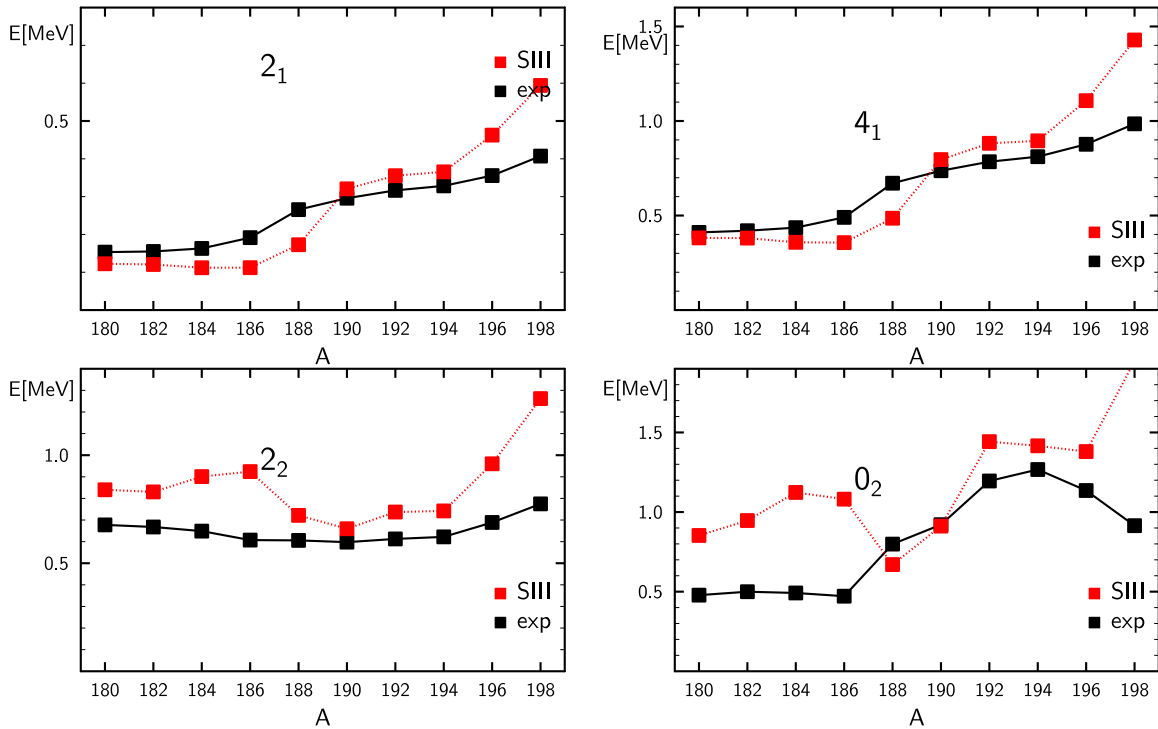


Figure 2: Selected (2_1^+ , 4_1^+ , 0_2^+ , 2_2^+) experimental [3] and theoretical levels in $^{180-198}\text{Pt}$.

The GBH approach provides us with detailed information on the electromagnetic properties of the excited levels without the need for additional parameters, e.g. effective charges. As seen in the upper panel of Fig. 3 the strength of the lowest yrast E2 transition ($2_1 \rightarrow 0_1$) is reproduced quite well by all the interactions. However, their predictions start to diverge when going to the lighter, unstable isotopes. This behaviour is even more visible for the $0_2 \rightarrow 2_2$ interband transition. The same can be said about other EM transitions not presented here.

Even though the E2 transitions are most frequently discussed in the framework of the GBH approach, the M1 transitions can also be considered. The $T(M1)$ operator has the form

$$T(M1)_k = G_k J_k, \quad k = 1, 2, 3$$

where J_k are the components of the collective angular momentum and $G_k(\beta, \gamma)$ are the gyromagnetic coefficients that may be calculated from the microscopic ATDHFB theory. In Fig. 4 I show results for the gyromagnetic factor for the 2_1 state. In contrast to the E2 case, all interactions give almost the same results that, moreover, are in excellent agreement with experiment.

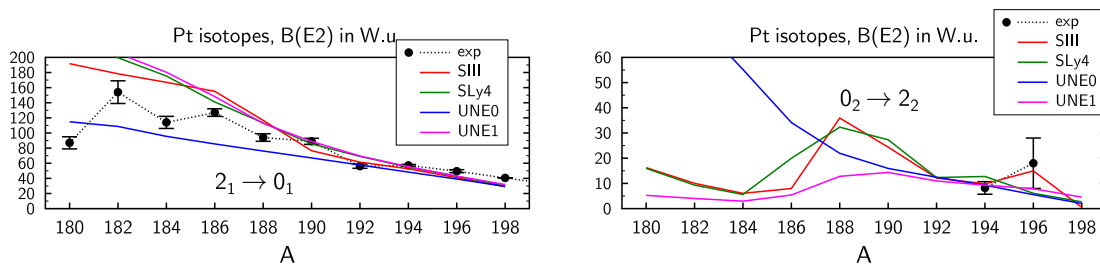


Figure 3: Experimental [3] and theoretical B(E2) probabilities for the $2_1 \rightarrow 0_1$ and $0_2 \rightarrow 2_2$ transitions in $^{180-198}\text{Pt}$.

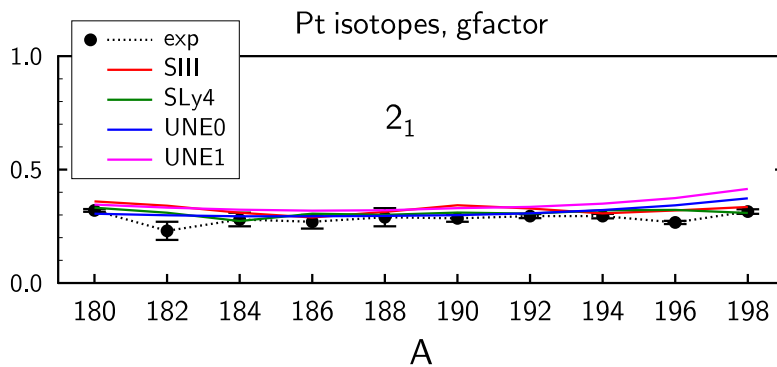


Figure 4: Experimental [3] and theoretical g-factor for the 2_1 state in $^{180-198}\text{Pt}$.

Bibliography

- [1] L. Próchniak, S.G. Rohoziński, J. Phys. G: Nucl. Phys. **36** (2009) 123101.
- [2] M. Kortelainen et al., Phys. Rev. C **82** (2010) 024313; M. Kortelainen et al., Phys. Rev. C **85** (2010) 024304.
- [3] Data from the NNDC database, revision as of October 2023.

C.10 Testing the values of the spectroscopic factors of single-neutron states in ^{11}B and ^{14}C .

A.T. Rudchik¹, S.Yu. Mezhevych¹, K. Rusek²

1) *Institute for Nuclear Research, National Academy of Sciences of Ukraine, Prospekt Nauky 47, 03028 Kyiv, Ukraine.*

2) *Heavy Ion Laboratory, University of Warsaw, Warszawa, Poland*

Experimental data for one-neutron transfer reactions induced by a ^{11}B beam incident on a ^{13}C target at a laboratory frame energy of 45 MeV were used to test spectroscopic factors for the $^{11}\text{B} = ^{10}\text{B}+n$, $^{11}\text{B} = ^{10}\text{B}_{0.718\text{MeV}}+n$ and $^{14}\text{C} = ^{13}\text{C}+n$ components of the ^{11}B and ^{14}C ground state wave functions. The experiment was performed at the Heavy Ion Laboratory of the University of Warsaw [1]. One-nucleon configurations of nuclei are among the most studied properties of nuclear structures, both experimentally and theoretically. For the light, 1p-shell nuclei, there exist two extensive sets of spectroscopic factors. S. Cohen and D. Kurath calculated spectroscopic factors for A=6–15 nuclei using shell-model wave functions obtained by fitting their energy levels (S(CK) in Table I) [2]. A.T. Rudchik and Yu.M. Tchuvilsky [3–5] used the translationally invariant shell model [4] for calculations of spectroscopic factors for the light nuclei (S(RU) in Table 1). More recently, N.K. Timofeyuk published two sets of spectroscopic factors for A=7–16 nuclei, together with the available experimental values [6]. One of these sets was calculated using her method of the Source Term Approach (S(TI^{STA}) in Table 1).

Table 1: Values of the spectroscopic factors (S) used in the CCBA calculations. The signs of the corresponding spectroscopic amplitudes are indicated in the last column.

	NLJ	S(CK) [2]	S(RU) [5]	S(TI ^{STA}) [6]	S(TI ^{DE}) [6]	sign
$^{14}\text{C}_{g.s.} = ^{13}\text{C}_{g.s.} + n$	1P1/2	1.7336	1.1968	1.573	1.87	+
$^{11}\text{B}_{g.s.} = ^{10}\text{B}_{g.s.} + n$	1P3/2	1.0943	1.8144	0.635	1.120	+
$^{11}\text{B}_{g.s.} = ^{10}\text{B}_{0.718\text{MeV}} + n$	1P1/2	0.1910	0.0718	0.069	0.106	-
$^{11}\text{B}_{g.s.} = ^{10}\text{B}_{0.718\text{MeV}} + n$	1P3/2	0.0715	0.0576	0.103	0.187	-

In the analysis presented in this contribution, we exploit the results of our earlier study of the α -transfer reaction $^{13}\text{C}(^{11}\text{B}, ^7\text{Li})^{17}\text{O}$. In that case, the coupled-channel Born approximation (CCBA) method was used, with coupling to the first excited state of ^{11}B included [1]. This method was also applied to the present analysis of the one-neutron transfer reaction $^{13}\text{C}(^{11}\text{B}, ^{10}\text{B})^{14}\text{C}$. Moreover, in the entrance channel the optical model potential found previously [1] was used. As previously, the coupling potential was taken as a simple derivative form.

The boron isotope ^{10}B is known to be “the most complicated 1p shell nuclei” [7]. Its ground state, apart from a large quadrupole deformation [9], has large spin, $J^\pi = 3^+$. In this work, the ground state and the three T=0 excited states at excitation energies of 0.72 MeV, 2.15 MeV and 3.59 MeV were assumed to be of collective nature, coupled by a potential having a derivative form, like for ^{11}B , multiplied by the quadrupole deformation length $\delta = 0.8$ fm, derived from the spectroscopic quadrupole moment of the ground state [9]. The optical model potential for $^{11}\text{B} + ^{14}\text{C}$ found at a similar energy [10] was adopted for the exit channel.

The binding potential of every single-neutron bound state used in the calculations was

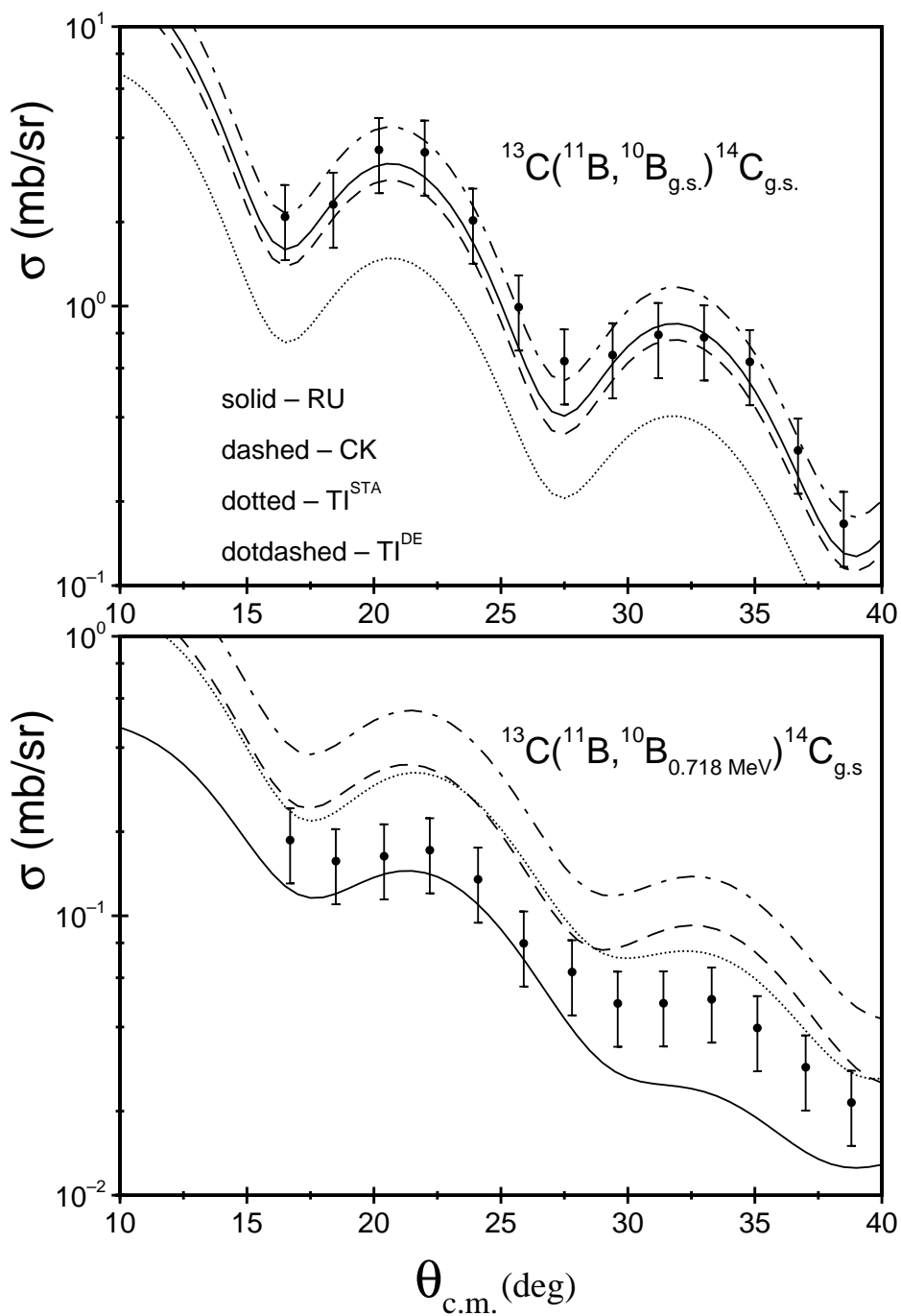
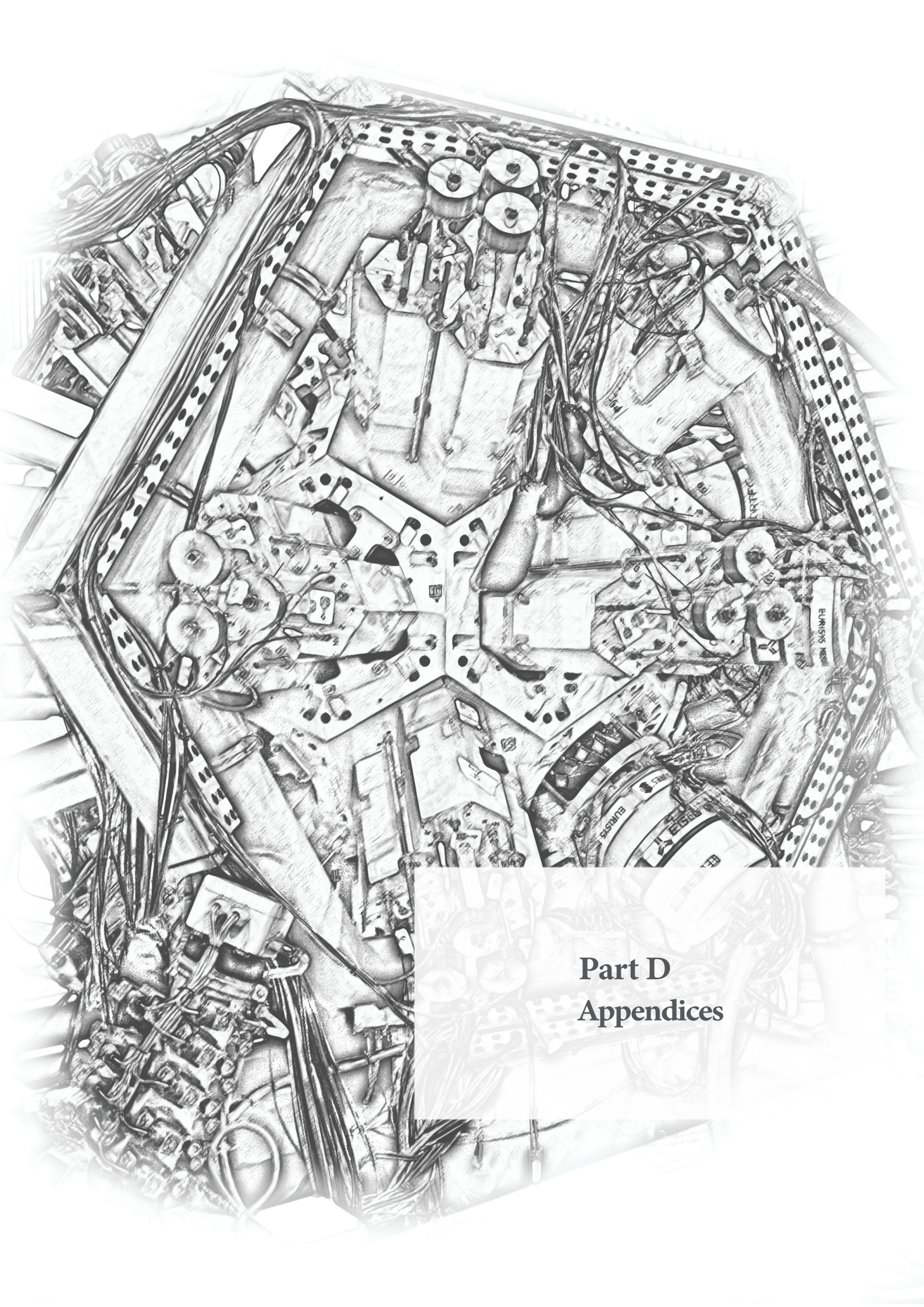


Figure 1: Angular distributions of the differential cross section for neutron transfer reactions induced by a ^{11}B beam incident on a ^{13}C target at 45 MeV, leading to ^{10}B in its ground and first excited states. The curves show results of the CCBA calculations with the four sets of spectroscopic factors listed in Table 1.

of Woods-Saxon form, with the standard geometry - $R = 1.30 A_{core}^{1/3}$ fm, $a_0 = 0.65$ fm. No parameter was adjusted in the course of the calculations. All the calculations presented in this paper were performed using the code Fresco [8]. The results of the CCBA calculations are plotted in Fig. 1, together with the experimental data. For the transfer leading to the ground state of ^{10}B (upper panel of 1), the three sets of spectroscopic factors (S(RU), S(CK) and S(TI DE)) give results close to the experimental values, while the one with the spectroscopic factors calculated using the Source Term Approach method underestimates the measured values of the differential cross section. For the transition to the first excited state of ^{10}B the agreement of the CCBA results with the data depends not only on the values of the spectroscopic factors but also on the signs of the spectroscopic amplitudes and is not so good (lower panel in 1). Here the calculations with the spectroscopic factors S(TI DE) significantly overestimate the data. In general, the results for the first excited state of ^{10}B suggest that this process could be two-step, with neutron transfer from the excited ^{11}B in the entrance channel. This effect will be the subject of further study.

Bibliography

- [1] S.Yu. Mezhevych *et al.*, Phys. Rev. C **88**, 034607 (2017).
- [2] S. Cohen, D. Kurath, Nucl. Phys. A **101**, 1 (1967).
- [3] A.T. Rudchik, Yu.M. Tchuvilsky, Ukr. Fiz. Zh. **30**, 819 (1985).
- [4] Yu.F. Smirnov, Yu.M. Tchuvilsky, Phys. Rev. C **15**, 84 (1977).
- [5] A.T. Rudchik, Yu.M. Tchuvilsky, A code DESNA, The Kiev Institute for Nuclear Research Report KIYAI-82-12, 1982.
- [6] N.K. Timofeyuk, Phys. Rev. C **88**, 044315 (2013).
- [7] D. Kurath, Nucl. Phys. A **317**, 175 (1979).
- [8] I.J. Thompson, Comput. Phys. Rep. **7**, 167 (1988).
- [9] R. Raghavan, At. Data and Nucl. Data Tables **42**, 189 (1989).
- [10] N. Keeley *et al.*, Phys. Rev. C **105**, 024615 (2022).



Part D
Appendices

D.1 List of experiments performed at HIL in 2023

A list of the experiments performed in 2023 is presented in the following pages. The following acronyms of institution names are used in the list:

- HIL — Heavy Ion Laboratory, University of Warsaw, Warszawa, Poland;
- ATOMKI — HUN-REN ATOMKI, Debrecen, Hungary;
- DFA USP — Dip. di Fisica e Astronomia, Univ. degli Studi di Padova, Padova, Italy;
- DP UL — Department of Physics, University of Liverpool, Liverpool, UK;
- DP UY — Department of Physics, University of York, York, UK;
- FC UW — Faculty of Chemistry, University of Warsaw, Warszawa, Poland;
- FP UW — Faculty of Physics, University of Warsaw, Warszawa, Poland;
- GSI — GSI Helmholtz Center for Heavy Ion Research, Darmstadt, Germany;
- IJCLab Orsay — Lab. de Physique des 2 infinis Irène Joliot-Curie, Orsay, France;
- IK UK Köln — Institut für Kernphysik, Universität zu Köln, Köln, Germany;
- IMP CAS — Inst. of Modern Physics, Chinese Academy of Science, Lanzhou, China;
- INFN-LNS Catania — LNS, INFN e Università di Catania, Catania, Italy;
- INP PAN Kraków — Institute of Nuclear Physics PAN, Kraków, Poland;
- INP UK Cologne — Institute for Nuclear Physics, University of Cologne, Germany;
- IZU Istanbul — Fac. of Engineering and Natural Sciences, Istanbul Sabahattin Zaim Univ. Istanbul, Turkey;
- KTH Stockholm — KTH Royal Institute of Technology, Stockholm, Sweden;
- LNL Legnaro — INFN, Laboratori Nazionali di Legnaro, Legnaro, Italy;
- NCNR Świerk — National Centre for Nuclear Research, Otwock, Poland;
- NU Nigde — Nigde Univ., Fen-Edebiyat Fakültesi, Fizik Bölümü, Nigde, Turkey;
- OLL LU — Oliver Lodge Laboratory, University of Liverpool, Liverpool, UK;
- PD UL — Physics Department, University of Lund, Lund, Sweden;
- SEC UWS — School of Engineering and Computing, University of the West of Scotland, Paisley, UK;
- U Ege Izmir — Physics Department, Ege University, Izmir, Turkey;
- UJ Jyväskylä — Department of Physics, University of Jyväskylä, Finland;
- U Sakaraya — Sakaraya University, Science and Literature Faculty, Physics Department, Sakaraya, Turkey;

For each experiment the following information is provided: ion, energy, setup/beam line information, date, proposal number, subject, spokespersons and institutions.

^{32}S — 86 MeV, 93 MeV — EAGLE-NEDA 30.01 – 03.02
HIL101 — Commissionings of EAGLE-NEDA and EAGLE-NEDA-DIAMANT setups. (G. Jaworski)

HIL, INP PAN Kraków, FP UW, NCNR Świerk

^{20}Ne — 50-75 MeV — CUDAC 06.02 - 17.02
HIL098 — Quasielastic barrier distributions for the $^{20}\text{Ne} + ^{92,94,95}\text{Mo}$: Influence of dissipation. (E. Piasecki, A. Trzcińska)

HIL, INFN-LNS Catania, UJ Jyväskylä, GSI

^{32}S — 147.2-160 MeV — EAGLE-NEDA 27.02 – 12.03
HIL099 — Lifetime measurement of excited states in ^{134}Sm . (B. Saygi)

U Ege Izmir, IK UK Köln, U Sakaraya, IZU Istanbul, NU Nigde, OLL LU, SEC UWS, HIL

^{16}O — 78.4-81.6 MeV — EAGLE-NEDA 22.03 – 04.04

HIL097 — *Shape coexistence and octupole correlations in the light Xe, Cs and Ba nuclei. (C. Petrache)*

IJCLab Orsay, INP UK Cologne, ATOMKI, UJ Jyväskylä, IMP CAS, DFA USP, HIL

^4He — 32 MeV — Internal beam irradiation station 22.05 – 26.05

HIL107 — *Commissioning of the research stand for irradiation with the internal beam of the cyclotron. (J. Choiński)*

HIL

^{20}Ne — 130-160 MeV — EAGLE-NEDA 29.05 – 02.06

HIL110 — *The effect of defects in the near-surface region on the oxidation mechanism of high-purity copper. (P. Horodek)*

INP PAN Kraków, HIL

^{20}Ne — 65-73 MeV — CUDAC 03.06 - 07.06

HIL098 — *Quasielastic barrier distributions for the $^{20}\text{Ne} + ^{92,94,95}\text{Mo}$: Influence of dissipation. (E. Piasecki, A. Trzcińska)*

HIL, INFN-LNS Catania, UJ Jyväskylä, GSI

^{32}S — 150 MeV — EAGLE-NEDA 14.06 – 27.06

HIL106 — *Shape coexistence and octupole correlations in the light Xe, Cs and Ba nuclei. (C. Petrache)*

IJCLab Orsay, ATOMKI, IMP CAS, DP UL, INP UK Cologne, UJ Jyväskylä, INP PAN Kraków, LNL Legnaro, FC UW, FP UW, HIL

^{32}S — 85 MeV — EAGLE-NEDA-DIAMANT 03.07 – 07.07

HIL101 — *Commissionings of EAGLE-NEDA and EAGLE-NEDA-DIAMANT setups. (G. Jaworski)*

HIL, INP PAN Kraków, ATOMKI, FP UW

^{20}Ne — EAGLE-NEDA, Radiobiology 22.10 – 25.10

HIL001 — *Student's Workshop.*

HIL

^{32}S — 80-89.6 MeV — EAGLE-NEDA 13.11 – 29.11

HIL105 — *Single-proton states and $N=Z=28$ core excitations in ^{57}Cu . (M. Palacz)*

HIL, FP UW, ATOMKI, INP PAN Kraków, IJCLab Orsay, GSI, PD UL, KTH Stockholm

^{32}S — 87-90 MeV — EAGLE-NEDA 05.12 – 20.12

HIL115 — *Study of the anomalous behavior of the Coulomb energy difference in the $A = 70, T = 1$ isobaric multiplet. (M. Matejska-Minda)*

INP PAN Kraków, HIL, FP UW, ATOMKI, NCNR Świerk, LNL Legnaro, DP UY

D.2 Degrees and theses completed in 2023 or in progress

D.2.1 DSc (habilitation) degrees of HIL staff members

Aleksandra Sentkowska

The degree was awarded in January 2023 by the Scientific Council of Chemical Science, University of Warsaw, for the work entitled

Methodological aspects in the determination of selenium speciation

Aspekty metodologiczne w oznaczaniu specjacji selenu

D.2.2 PhD theses of students affiliated to HIL, of HIL staff members, and supervised by HIL staff

Marcin Pietrzak, Faculty of Physics, University of Warsaw

Nanodosimetric characteristics of a carbon ion beam - experiments and Monte Carlo simulations

Supervisor: dr hab. Z. Szefliński. Thesis completed in January 2023

Lukasz Standyło, National Centre for Nuclear Research, Świerk

Badanie mechanizmu wychwytu i termalizacji strumieni jonów i atomów wprowadzonych do plazmy wytwarzanej metodą elektronowego rezonansu cyklotronowego

Investigation of capture and thermalization mechanisms of ions and atomic beams injected into plasma produced by the electron cyclotron resonance

Supervisor: prof. dr hab. K. Rusek, dr K. Sudlitz. Thesis completed in September 2023

Monika Mietelska, Faculty of Physics, University of Warsaw

Ionisation Detail Parameters for DNA Damage Evaluation in Charged Particle Radiotherapy: Simulation Study Based on Cell Survival Database

Supervisors: dr hab. Z. Szefliński and dr hab. B. Brzozowska, Expected completion date: 2024.

Bogumił Zalewski, Heavy Ion Laboratory, University of Warsaw

Study of the ${}^6\text{He}+d$ interaction

Supervisor: prof. dr hab. K. Rusek. Expected completion date: 2024

Adam Nałęcz-Jawecki, Graduate School of Physics and Chemistry, National Centre for Nuclear Research, Otwock, Poland

Search for nuclear chirality in low excitation energy states of odd-odd isotopes

Supervisors: dr hab. E. Grodner, dr J. Srebrny. Expected completion date: 2025.

Grzegorz Wałpuski, Faculty of Biology, University of Warsaw

Badanie wpływu promieniowania jonizującego na procesy fizjologiczne ujednokomórkowych glonów z gromady Cyanidiophyceae

Study of the influence of ionizing radiation on physiological processes in single-celled algae from the class Cyanidiophyceae

Supervisors: dr hab. Z. Szefliński - Faculty of Physic UW and dr hab. M. Zienkiewicz -

Faculty of Biology UW, Expected completion date: 2026

Mateusz Filipek, Faculty of Physics, University of Warsaw

From radiobiology to radiotherapy: dose homogeneity in cells after alpha irradiation in measurements and Monte Carlo simulations

Supervisors: dr hab. Z. Szepliński and dr hab. B. Brzozowska, Expected completion date: 2027.

Iwona Piętka, Heavy Ion Laboratory, University of Warsaw

Badanie współistnienia kształtów w jądrze ^{110}Cd metodą wzbudzeń kulombowskich

Study of multiple shape coexistence in ^{110}Cd using the Coulomb-excitation method

Supervisor: dr hab. L. Próchniak, dr K. Wrzosek-Lipska. Expected completion date: 2027

D.2.3 MSc and BSc theses supervised by HIL staff members

Kamila Żujewska, Faculty of Physics, University of Warsaw

Dozymetria stanowiska pomiarowego z powierzchniowym źródłem alfa do badań radiobiologicznych

Dosimetry of a measurement station with a surface alpha source for radiobiological research

Supervisors: prof. A. Korgul, dr hab. Z. Szepliński. Thesis completed in January 2023

Iwona Piętka, Faculty of Physics, University of Warsaw

Badanie struktury elektromagnetycznej jądra ^{110}Cd metodą wzbudzeń kulombowskich

Study of the electromagnetic structure of ^{110}Cd using the Coulomb excitation method

Supervisor: dr K. Wrzosek-Lipska. Thesis completed in September 2023.

Adam Malinowski, Faculty of Physics, University of Warsaw

Wydatność detekcji neutronów układu NEEDLE

Neutron detection efficiency of the NEEDLE array

Supervisor: dr G. Jaworski. Thesis completed in July 2023.

Justyna Sykuła, Faculty of Physics, University of Warsaw

Badanie zanieczyszczeń radionuklidowych w procesie produkcji radiofarmaceutyków znakowanych ^{18}F

Determination of radionuclidic impurities in the production of ^{18}F labelled radiopharmaceuticals.

Supervisor: dr hab. K. Kilian. Thesis completed in September 2023

Magda Bielecka, Faculty of Biology, University of Warsaw

Ocena powinowactwa terakarboxyfenyloporfiryryny i tetrasulfofenyloporfiryryny do komórek nowotworowych nabłonkowego raka szyjki macicy linii HeLa

Assessment of the affinity of teracarboxyphenylporphyrin and tetrasulfophenylporphyrin for HeLa cervical epithelial cancer cells

Supervisors: dr hab. K. Kilian, Expected completion date: 2024.

Ewa Bieniasz, Faculty of Chemistry, University of Warsaw

Synteza ^{18}F -fluoroetylotyrozyny (FET) na syntezerze Synthra RN

Synthesis of ^{18}F -fluoroethyltyrosine (FET) on the Synthra RN synthesizer

Supervisors: dr hab. K. Kilian, Expected completion date: 2024.

Krzysztof Domański, Faculty of Physics, University of Warsaw

Zastosowanie uczenia maszynowego do automatycznej analizy testu klonogenego przeprowadzonego na komórkach ssaków

Application of machine learning to automatic clonogenic test analysis of mammal cells

Supervisors: dr hab. Z. Szepliński, dr U. Kaźmierczak. Expected completion date: 2024.

Katarzyna Głazowska, Faculty of Chemistry, University of Warsaw

Synteza radiofarmaceutyku 18FAZA na syntezerze Synthra RN

Synthesis of the radiopharmaceutical 18FAZA on the Synthra RN synthesizer

Supervisors: dr hab. K. Kilian, Expected completion date: 2024.

Klaudia Koszel, Faculty of Physics, University of Warsaw

Oznaczanie pozostałości rozpuszczalników organicznych w radiofarmaceutyku ^{18}F -fluorocholina

Determination of organic solvent residues in the radiopharmaceutical ^{18}F -fluorocholine

Supervisor: dr hab. K. Kilian. Expected completion date: 2024.

Roman Kuczma, Applications of Physics in Biology and Medicine, University of Warsaw

Test klonogeny komórek glejaka napromienionych cząstkami alfa z powierzchniowego źródła Am-241

Clonogenic assay of glioma cells irradiated with alpha particles from a surface source of Am-241

Supervisors: dr B. Brzozowska, dr U. Kaźmierczak. Expected completion date: 2024.

Stanisław Bitner, Paweł Pilarski, Kamil Pilkiewicz, Marek Zbysiński, Faculty of Mathematics, Informatics, and Mechanics, University of Warsaw

Sterowanie zasilaczami cewek korekcyjnych w cyklotronie (16 x 300A)

Control of power supplies for correction coils in a cyclotron Supervisor: mgr. P. Gołąb

MIM UW, mgr.inż. J. Miszczak ŚLCJ UW, Expected completion date: 2024.

Agnieszka Klempis, Jacek Muszyński, Jan Rogowski, Marcin Żołek, Faculty of Mathematics, Informatics, and Mechanics, University of Warsaw

Sterowanie zasilaczami 200A oraz 100A w Cyklotronie Warszawskim (ŚLCJ UW)

Control of 200A and 100A power supplies in Cyklotron Warszawski (HIL UW)

Supervisor: dr J. Sroka MIM UW, mgr.inż. J. Miszczak ŚLCJ UW, Expected completion date: 2024.

D.3 Publications

- [1] I. Ahmed, R. Kumar, **K. Hadyńska-Klęk**, C. Qi. *Shell-model studies relevant for low-energy Coulomb excitation in Zn isotopes*. Eur. Phys. J. A **59**(2023) 306.
- [2] L. Al Ayoubi, I. Matea, A. Kankainen, D. Verney, H. Al Falou, G. Benzoni, V. Bozkurt, M. Ciemała, C. Delafosse, I. Deloncle, F. Didierjean, M. Fallot, C. Gaular, A. Gottardo, V. Guadilla, J. Guillot, **K. Hadyńska-Klęk**, F. Ibrahim, N. Jovancevic, F. Le Blanc, M. Lebois, R. Li, T. Martinez, **P. J. Napiorkowski**, B. Roussiere, Y. G. Sobolev, B. Sowicki, I. Stefan, S. Stukalov, D. Thisse, G. Tocabens. *Beta decay of ^{82}Ga studied at the alto facility*. Acta Phys. Pol. B Proc. Suppl **16**(2023) A35.
- [3] A. Amar, **K. Rusek**, S. Hamada. *Effects of deuteron breakup and nucleon-transfer reactions on $d+^{11}\text{B}$ elastic scattering*. Eur. Phys. J. A **59**(2023) 182.
- [4] C. Ciampi, S. Piantelli, G. Casini, G. Pasquali, L. Baldesi, S. Barlini, B. Borderie, R. Bougault, A. Camaiani, A. Chbihi, D. Dell'Aquila, M. Cicerchia, J. A. Duenas, Q. Fable, D. Fabris, J. D. Frankland, C. Frosin, T. Genard, F. Gramegna, D. Gruyer, M. Henri, B. Hong, S. Kim, **A. Kordyas**, T. Kozik, M. J. Kweon, J. Lemarie, N. Le Neindre, I. Lombardo, O. Lopez, T. Marchi, S. H. Nam, A. Ordine, P. Ottanelli, J. Park, J. H. Park, M. P. Parlog, G. Poggi, J. Quicray, A. Rebillard-Soulie, A. A. Stefanini, S. Upadhyaya, S. Valdre, G. Verde, E. Vient, M. Vigilante. *Nuclear symmetry energy at work in heavy ion reactions: new results from the INDRA-FAZIA apparatus*. J. of Physics Conf. Series **2586**(2023) 012039.
- [5] C. Ciampi, S. Piantelli, G. Casini, A. Ono, J. Frankland, L. Baldesi, S. Barlini, B. Borderie, R. Bougault, A. Camaiani, A. Chbihi, J. Dueñas, Q. Fable, D. Fabris, C. Frosin, T. Génard, F. Gramegna, D. Gruyer, M. Henri, B. Hong, S. Kim, **A. Kordyas**, T. Kozik, M. Kweon, N. Le Neindre, I. Lombardo, O. Lopez, T. Marchi, K. Mazurek, S. Nam, J. Park, M. Pârlog, G. Pasquali, G. Poggi, A. Rebillard-Soulié, A. Stefanini, S. Upadhyaya, S. Valdré, G. Verde, E. Vient, M. Vigilante. *Quasiprojectile breakup and isospin equilibration at fermi energies: Potential indication of longer projectile-target contact times*. Phys. Rev. C **108**(2023) 054611.
- [6] M. Ciemała, M. Kmiecik, A. Maj, B. Fornal, P. Bednarczyk, N. Cieplicka-Oryńczak, L. W. Iskra, M. Matejska-Minda, K. Mazurek, B. Wasilewska, M. Ziębliński, F. C. L. Crespi, A. Bracco, S. Bottoni, F. Camera, S. Leoni, G. Benzoni, B. Million, O. Wieland, S. Brambilla, J. Wilson, I. Matea, M. Lebois, N. Jovancevic, O. Dorvaux, C. Schmitt, J. Dudek, S. Kihel, **P. J. Napiorkowski**, M. Kicińska-Habior, I. Mazumdar, V. Nanal. *Feeding of the residual states with GDR gamma decay studied by nuBALL coupled with PARIS*. Acta Phys. Pol. B Proc. Suppl. **16**(2023) A14.
- [7] J. Diklic, S. Szilner, L. Corradi, T. Mijatovic, G. Pollarolo, P. Colovic, **G. Colucci**, E. Fioretto, F. Galtarossa, A. Goasduff, A. Gottardo, J. Grębosz, A. Illana, **G. Jaworski**, M. J. Gomez, T. Marchi, D. Mengoni, G. Montagnoli, D. Nurkic, M. Siciliano, N. Soic, A. M. Stefanini, D. Testov, J. J. Valiente-Dobon, N. Vukman. *Transfer reactions in $^{206}\text{Pb}+^{118}\text{Sn}$: From quasielastic to deep-inelastic processes*.

- Phys.Rev. C **107**(2023) 014619.
- [8] C. Frosin, S. Piantelli, G. Casini, A. Ono, A. Camaiani, L. Baldesi, S. Barlini, B. Borderie, R. Bougault, C. Ciampi, M. Cicerchia, A. Chbihi, D. Dell'Aquila, J. A. Duenas, D. Fabris, Q. Fable, J. D. Frankland, T. Genard, F. Gramegna, D. Gruyer, M. Henri, B. Hong, M. J. Kweon, S. Kim, **A. Kordyas**, T. Kozik, I. Lombardo, O. Lopez, T. Marchi, K. Mazurek, S. H. Nam, J. Lemarie, N. LeNeindre, P. Ottanelli, M. Parlog, J. Park, G. Pasquali, G. Poggi, A. Rebillard-Soulie, B. H. Sun, A. A. Stefanini, S. Terashima, S. Upadhyaya, S. Valdre, G. Verde, E. Vient, M. Vigilante. *Examination of cluster production in excited light systems at fermi energies from new experimental data and comparison with transport model calculations.* Phys. Rev. C **107**(2023) 044614.
- [9] L. Hariasz, M. Stukel, P. C. F. Di Stefano, B. C. Rasco, K. P. Rykaczewski, N. T. Brewer, D. W. Stracener, Y. Liu, Z. Gai, C. Rouleau, J. Carter, J. Kostensalo, J. Suhonen, H. Davis, E. D. Lukosi, K. C. Goetz, R. K. Grzywacz, M. Mancuso, F. Petricca, A. Fijałkowska, **M. Wolińska-Cichocka**, J. Ninkovic, P. Lechner, R. B. Ickert, L. E. Morgan, P. R. Renne, I. Yavin. *Evidence for ground-state electron capture of ^{40}K .* Phys. Rev. C **108**(2023) 014327.
- [10] A. Illana, M. Zielińska, M. Huyse, E. Rapisarda, P. Van Duppen, **K. Wrzosek-Lipska**, F. Nowacki, S. M. Lenzi, D. D. Dao, T. Otsuka, Y. Tsunoda, K. Arnsward, M. J. G. Borge, J. Cederkall, K. Chrysalidis, M. L. Cortes, D. M. Cox, T. D. Goodacre, H. De Witte, D. T. Doherty, V. Fedosseev, L. P. Gaffney, **K. Hadyńska-Klęk**, H. Hess, C. Henrich, M. Hlebowicz, **M. Komorowska**, W. Korten, T. Kroll, M. L. L. Benito, R. Lutter, B. Marsh, L. Martikainen, M. Matejska-Minda, P. L. Molkanov, E. Nacher, A. Nannini, **P. J. Napiorkowski**, J. Pakarinen, P. Papadakis, M. Queiser, P. Reiter, M. Rocchini, J. A. Rodriguez, T. Rolke, D. Rosiak, S. Rothe, M. Seidlitz, C. Seiffert, B. Siebeck, E. Siesling, J. Snaell, **J. Srebrny**, S. Thiel, F. Wenander, N. Warr. *Coulomb excitation of $^{74,76}\text{Zn}$.* Phys. Rev. C **108**(2023) 044305.
- [11] **G. Jaworski**, **M. Palacz**, A. Goasduff, **M. Kowalczyk**, P. Kulesa, I. Kuti, M. Matuszewski, **B. Radomyski**, N. Toniolo, **T. Abraham**, **G. Colucci**, A. Fijałkowska, **K. Hadyńska-Klęk**, **M. Komorowska**, R. Kopik, L. Lappo, A. Malinowski, **P. J. Napiorkowski**, W. Oklinski, A. Otreba, **S. Panasenko**, W. Poklepa, **J. Samorajczyk-Pyśk**, **K. Wrzosek-Lipska**, K. Zdunek. *Needle-the new setup to study neutron-deficient nuclei**. Acta Phys. Pol. B Proc. Suppl. **16**(2023) A36.
- [12] N. Keeley, I. Martel, K. W. Kemper, **K. Rusek**. *Breakup and transfer reactions in the $^{17}\text{Ne}+^{208}\text{Pb}$ system close to the Coulomb barrier.* Phys. Rev. C **108**(2023) 044603.
- [13] **K. Kilian**, K. Pyrzyńska. *Scandium radioisotopes-toward new targets and imaging modalities.* Molecules **28**(2023) 7668.
- [14] N. Marchini, A. Nannini, M. Rocchini, T. R. Rodriguez, M. Ottanelli, N. Gelli, A. Perego, G. Benzoni, N. Blasi, G. Bocchi, D. Brugnara, A. Buccola, G. Carozzi, A. Goasduff, E. T. Gregor, P. R. John, **M. Komorowska**, D. Mengoni, F. Recchia, S. Ricchetto, D. Rosso, A. Saltarelli, M. Siciliano, J. J. Valiente-Dobon, I. Zanon.

- Emergence of triaxiality in ^{74}Se from electric monopole transition strengths.* Phys. Lett. B **844**(2023) 138067.
- [15] M. Markova, A. Larsen, G. Tveten, P. Von Neumann-Cosel, T. Eriksen, F. Bello Garrote, L. Crespo Campo, F. Giaccoppo, A. Gorgen, M. Guttormsen, **K. Hadyńska-Klęk**, M. Klintefjord, T. Renstrom, E. Sahin, S. Siem, T. Tornyi. *Nuclear level densities and γ -ray strength functions of $^{111,112,113}\text{Sn}$ isotopes studied with the Oslo method.* Phys. Rev. C **108**(2023) 014315.
- [16] I. Martel, L. Acosta, J. L. Aguado, M. Assie, M. A. M. Al-Aqeel, A. Ballarino, D. Barna, R. Berjillos, M. Bonora, C. Bontoiu, M. J. G. Borge, J. A. Briz, I. Bustinduy, L. Bottura, L. Catalina-Medina, W. Catford, J. Cederkall, T. Davinson, G. de Angelis, A. Devred, C. Diaz-Martin, T. Ekelof, H. Felice, H. Fynbo, A. P. Foussat, R. Florin, S. J. Freeman, L. Gaffney, C. Garcia-Ramos, L. Gentini, C. A. Gonzalez-Cordero, C. Guazzoni, A. Haziot, A. Heinz, J. M. Jimenez, K. Johnston, B. Jonson, G. Kirby, O. Kirby, T. Kurtukian-Nieto, M. Labiche, M. Liebsch, M. Losasso, A. Laird, J. L. Munoz, B. S. N. Singh, G. Neyens, **P. J. Napiorkowski**, D. O'Donnell, R. D. Page, D. Perini, J. Resta-Lopez, G. Riddone, J. A. Rodriguez, V. Rodin, S. Russenschuck, V. R. Sharma, F. Salguero-Andujar, J. Sanchez-Segovia, K. Riisager, A. M. Sanchez-Benitez, B. Shepherd, E. Siesling, J. Smallcombe, M. Stanoiu, O. Tengblad, J. P. Thermeau, D. Tommasini, J. Uusitalo, S. Varnasseri, C. P. Welsch, G. Willering. *An innovative superconducting recoil separator for HIE-ISOLDE.* Nucl. Instrum. Methods Phys. Res. B **541**(2023) 176.
- [17] K. Masłowska, P. Redkiewicz, P. K. Halik, E. Witkowska, D. Tymecka, R. Walczak, **J. Choiński**, A. Misicka, E. Gniazdowska. *Scandium-44 radiolabeled peptide and peptidomimetic conjugates targeting neuropilin-1 co-receptor as potential tools for cancer diagnosis and anti-angiogenic therapy.* Biomedicines **11**(2023) 564.
- [18] L. Morrison, **K. Hadyńska-Klęk**, Z. Podolyak, L. P. Gaffney, M. Zieli, B. A. Brown, H. Grawe, P. D. Stevenson, T. Berry, A. Boukhari, M. Brunet, R. Canavan, R. Catherall, J. Cederkaell, S. J. Colosimo, J. G. Cubiss, H. De Witte, D. T. Doherty, C. Fransen, G. Georgiev, E. Giannopoulos, M. Gorska, H. Hess, L. Kaya, T. Kroell, N. Lalovic, B. Marsh, Y. M. Palenzuela, G. O'Neill, J. Pakarinen, J. P. Ramos, P. Reiter, J. A. Rodriguez, D. Rosiak, S. Rothe, M. Rudigier, M. Siciliano, E. C. Simpson, J. Snall, P. Spagnoletti, S. Thiel, N. Warr, F. Wenander, R. Zidarova. *Quadrupole and octupole collectivity in the semi-magic nucleus ^{206}Hg .* Phys. Lett. B **838**(2023) 137675.
- [19] M. Nassurlla, N. Burtebayev, S. B. Sakuta, **K. Rusek**, D. K. Alimov, M. Nassurlla, A. Sabidolda, R. Khojayevev, A. Urkinbayev, S. Hamada. *Investigation of scattering of deuterons on ^{10}B nucleus at 14.5 mev.* Acta Phys.Pol. B Proc. Suppl. **16**(2023) A11.
- [20] M. Nassurlla, N. Burtebayev, S. B. Sakuta, M. Nassurlla, A. Sabidolda, S. V. Artemov, E. T. Ruziev, F. K. Ergashev, O. R. Tojiboev, **K. Rusek**, **A. Trzcińska**, **M. Wolińska-Cichocka**, I. Boztosun, A. Amar. *$^{11}\text{B}(^{15}\text{N}, ^{14}\text{C})^{12}\text{C}$ reaction mechanisms and ANC for the $^{15}\text{N} \rightarrow ^{14}\text{C} + p$ configuration.* Acta Phys.Pol. B Proc. Suppl. **16**(2023) A14.

- [21] J. D. Ovejas, I. Martel, D. Dell'Aquila, L. Acosta, J. L. Aguado, G. de Angelis, M. J. G. Borge, J. A. Briz, A. Chbihi, **G. Colucci**, C. Diaz-Martin, P. Figuera, D. Galaviz, C. Garcia-Ramos, J. A. Gomez-Galan, C. A. Gonzales, N. Goyal, N. Keeley, K. W. Kemper, T. K. Nieto, D. J. Malenica, M. Mazzocco, D. Nurkic, A. K. Orduz, A. Ortiz, L. Palada, C. Parascandolo, A. Di Pietro, A. M. Rodriguez, **K. Rusek**, F. Salguero, A. M. Sanchez-Benitez, M. Sanchez-Raya, J. Sanchez-Segovia, N. Soic, F. Soramel, M. Stanoiu, O. Tengblad, N. Vukman, M. Xarepe. *Suppression of Coulomb-nuclear interference in the near-barrier elastic scattering of ^{17}Ne from ^{208}Pb* . Phys. Lett. B **843**(2023) 138007.
- [22] M. Pallas, A. Tarifeno-Saldivia, G. G. Kiss, J. L. Tain, A. Tolosa-Delgado, A. Vitez-Sveicz, F. Calvino, J. Agramunt, P. Aguilera, A. Algora, J. M. Allmond, H. Baba, N. T. Brewer, R. Caballero-Folch, P. J. Coleman-Smith, G. Cortes, T. Davinson, I. Dillmann, C. Domingo-Pardo, A. Estrade, N. Fukuda, S. Go, C. J. Griffin, R. K. Grzywacz, O. Hall, L. J. Harkness-Brennan, T. Isobe, D. Kahl, T. T. King, A. Korgul, S. Kovacs, S. Kubono, M. Labiche, J. Liu, M. Madurga, K. Miernik, F. Molina, N. Mont-Geli, A. I. Morales, E. Nacher, A. Navarro, N. Nepal, S. Nishimura, M. Piersa-Silkowska, V. Phong, B. C. Rasco, J. Romero-Barrientos, B. Rubio, K. P. Rykaczewski, Y. Saito, H. Sakurai, Y. Shimizu, M. Singh, T. Sumikama, H. Suzuki, T. N. Szegedi, H. Takeda, K. Wang, **M. Wolińska-Cichocka**, P. J. Woods, R. Yokoyama. *Study of decay properties of Ba to Nd nuclei ($A \sim 160$) relevant to the formation of the r-process rare-earth peak*. EPJ Web of Conferences **284**(2023) 02005.
- [23] **M. Pęgiel**, **K. Kilian**, K. Pyrżyńska. *Increasing reaction rates of water-soluble porphyrins for ^{64}Cu radiopharmaceutical labeling*. Molecules **28**(2023) 2350.
- [24] S. Piantelli, G. Casini, P. Ottanelli, L. Baldesi, S. Barlini, B. Borderie, R. Bougault, A. Camalani, A. Chbihi, C. Ciampi, J. A. Duenas, D. Fabris, Q. Fable, J. D. Frankland, C. Frosin, F. Gramegna, D. Gruyer, B. Hong, **A. Kordyasz**, T. Kozik, M. J. Kweon, J. Lemarie, N. LeNeindre, I. Lombardo, O. Lopez, T. Marchi, K. Mazurek, S. H. Nam, M. Parlog, J. Park, G. Pasquali, G. Poggi, A. Rebillard-Soulie, A. A. Stefanini, S. Upadhyaya, S. Valdre, G. Verde, E. Vient, M. Vigilante. *Characterization of the breakup channel in asymmetric systems*. Phys. Rev. **107**(2023) 044607.
- [25] K. Pyrżyńska, **A. Sentkowska**. *Selenium species in diabetes mellitus type 2*. Biol. Trace Elem. Res. (2023).
- [26] A. T. Rudchik, A. A. Rudchik, V. V. Khejlo, **K. Rusek**, K. W. Kemper, E. Piasecki, A. Stolarz, **A. Trzcińska**, V. M. Pirnak, O. A. Ponkratenko, E. I. Koshchy, O. E. Kutsyk, A. P. Ilyin, Y. M. Stepanenko, V. V. Uleshchenko, Y. O. Shyrma. *Reaction $^{10}\text{B}(^{15}\text{N}, ^{14}\text{C})^{11}\text{C}$ at energy 81 Mev, spectroscopic factors and interaction of ^{14}C* . Nucl. Phys. At. Energy (Iader. Fiz. Enerh.) **24**(2023) 22.
- [27] J. Saiz-Lomas, M. Petri, I. Y. Lee, I. Syndikus, S. Heil, J. M. Allmond, L. P. Gaffney, J. Pakarinen, H. Badran, T. Calverley, D. M. Cox, U. Forsberg, T. Grahm, P. Greenlees, **K. Hadyńska-Klęk**, J. Hilton, M. Jenkinson, R. Julin, J. Konki, A. O. Macchiavelli, M. Mathy, J. Ojala, P. Papadakis, J. Partanen, P. Rahkila, P. Ruotsalainen, M. Sandzelius, J. Saren, S. Stolze, J. Uusitalo, R. Wadsworth. *The spectroscopic quadrupole moment of the 2^+ state of ^{12}C : A benchmark of theoretical models*. Nat. Prod. Res. **845**(2023) 138114.

- [28] **A. Sentkowska**. *The potential of traditionally used medicinal plants for the synthesis of selenium nanoparticles*. Nat. Prod. Res. **37**(2023) 2055.
- [29] **A. Sentkowska**, K. Pyrzyńska. *Antioxidant properties of selenium nanoparticles synthesized using tea and herb water extracts*. Appl. Sci. **13**(2023) 1071.
- [30] **A. Sentkowska**, K. Pyrzyńska. *Old-fashioned, but still a superfood-red beets as a rich source of bioactive compounds*. Appl. Sci. **13**(2023) 7445.
- [31] **A. Sentkowska**, P. K. *Catechins and selenium species-how they react with each other*. Molecules **28**(2023) 5897.
- [32] A. M. Stefanini, G. Montagnoli, M. Del Fabbro, D. Brugnara, **G. Colucci**, L. Corradi, J. Diklic, E. Fioretto, F. Galtarossa, A. Goasduff, M. Mazzocco, J. Pellumaj, E. Pilotto, L. Zago, I. Zanon. *Sub-barrier fusion in $^{12}\text{C}+^{26,24}\text{Mg}$: Hindrance and oscillations*. Phys. Rev. C **108**(2023) 014602.
- [33] A. M. Stefanini, G. Montagnoli, M. Del Fabbro, **G. Colucci**, R. Depalo, A. Goasduff, I. Zanon. *Fusion of $^{12}\text{C}+^{24}\text{Mg}$ at far sub-barrier energies*. EPJ Web of Conferences **279**(2023) 11013.
- [34] M. Stryjczyk, B. Andel, J. G. Cubiss, K. Rezyunkina, T. R. Rodriguez, J. E. Garcia-Ramos, A. N. Andreyev, J. Pakarinen, P. Van Duppen, S. Antalic, T. Berry, M. J. G. Borge, C. Clisu, D. M. Cox, H. De Witte, L. M. Fraile, H. O. U. Fynbo, L. P. Gaffney, L. J. Harkness-Brennan, M. Huyse, A. Illana, D. S. Judson, J. Konki, J. Kurcewicz, I. Lazarus, R. Lica, M. Madurga, N. Marginean, R. Marginean, C. Mihai, P. Mosat, E. Nacher, A. Negret, J. Ojala, J. D. Ovejas, R. D. Page, P. Papadakis, S. Pascu, A. Perea, Z. Podolyak, **L. Próchniak**, V. Pucknell, E. Rapisarda, F. Rotaru, C. Sotty, O. Tengblad, V. Vedia, S. Vinals, R. Wadsworth, N. Warr, **K. Wrzosek-Lipska**. *Simultaneous gamma-ray and electron spectroscopy of $^{182,184,186}\text{Hg}$ isotopes*. Phys. Rev. C **108**(2023) 014308.
- [35] M. Stukel, L. Hariasz, P. C. F. D. Stefano, B. C. Rasco, K. P. Rykaczewski, N. T. Brewer, D. W. Stracener, Y. Liu, Z. Gai, C. Rouleau, J. Carter, J. Kostensalo, J. Suhonen, H. Davis, E. D. Lukosi, K. C. Goetz, R. K. Grzywacz, M. Mancuso, F. Petricca, A. Fijałkowska, **M. Wolińska-Cichocka**, J. Ninkovic, P. Lechner, R. B. Ickert, L. E. Morgan, P. R. Renne, I. Yavin. *Rare ^{40}K decay with implications for fundamental physics and geochronology*. Phys. Rev. Lett. **131**(2023) 052503.
- [36] O. R. Tojiboev, S. V. Artemov, F. K. Ergashev, A. A. Karakhodjaev, E. T. Ruziev, E. S. Ikromkhonov, I. Z. Tursunboyev, **K. Rusek**, **M. Wolińska-Cichocka**, N. Burtebayev, S. B. Sakuta, M. Nassurlla, M. Nassurlla, I. Boztosun, S. Hamada. *Asymptotic normalization coefficients of $^{28}\text{Si} \rightarrow ^{27}\text{Al} + p$ configurations from the proton transfer reaction*. Acta Phys. Pol. B Proc. Suppl. **16**(2023) A4.
- [37] A. Vitez-Sveiczler, S. Kovacs, G. G. Kiss, Y. Saito, A. Tarifeno-Saldivia, M. Pallas, J. L. Tain, L. Dillmann, J. Agramunt, A. Algora, C. Domingo-Pardo, A. Estrade, C. Appleton, J. M. Allmond, P. Aguilera, H. Baba, N. T. Brewer, C. Bruno, R. Caballero-Folch, F. Calvino, P. J. Coleman-Smith, G. Cortes, T. Davinson, N. Fukuda, Z. Ge, S. Go, C. J. Griffin, R. K. Grzywacz, O. Hall, A. Horvath, J. Ha, L. J. Harkness-Brennan, T. Isobe, D. Kahl, T. T. King, A. Korgul, R. Krucken,

- S. Kubono, M. Labiche, J. Liu, J. Liang, M. Madurga, K. Miernik, F. Molina, A. I. Morales, M. R. Mumpower, E. Nacher, A. Navarro, N. Nepal, S. Nishimura, M. Piersa-Silkowska, V. Phong, B. C. Rasco, B. Rubio, K. P. Rykaczewski, J. Romero-Barrientos, H. Sakurai, L. Sexton, Y. Shimizu, M. Singh, T. Sprouse, T. Sumikama, R. Surman, H. Suzuki, T. N. Szegedi, H. Takeda, A. Tolosa-Delgado, K. Wang, **M. Wolińska-Cichocka**, P. Woods, R. Yokoyama, Z. Xu. *Half-life measurement using implant- $(\beta - \gamma)$ time correlations in the region of neutron-rich lanthanides*. Acta Phys. Pol. B Proc. Suppl. **16**(2023) A8.
- [38] **M. Wolińska-Cichocka**, B. C. Rasco, K. P. Rykaczewski, N. T. Brewer, A. Fijałkowska, M. Karny, R. K. Grzywacz, K. C. Goetz, C. J. Gross, D. W. Stracener, E. F. Zganjar, J. C. Batchelder, J. C. Blackmon, S. Go, B. Heffron, J. Johnson, T. T. King, J. T. Matta, K. Miernik, M. Madurga, E. A. McCutchan, D. Miller, C. D. Nesaraja, S. V. Paulauskas, M. M. Rajabali, S. Taylor, A. A. Sonzogni, E. H. Wang, J. A. Winger, Y. Xiao, C. J. Zachary. *Complete gamma-decay patterns of ^{142}Cs , ^{142}Ba , and ^{142}La determined using total absorption spectroscopy*. Phys. Rev. C **107**(2023) 034303.
- [39] R. Yokoyama, R. Grzywacz, B. C. Rasco, N. Brewer, K. P. Rykaczewski, I. Dillmann, J. L. Tain, S. Nishimura, D. S. Ahn, A. Algora, J. M. Allmond, J. Agramunt, H. Baba, S. Bae, C. G. Bruno, R. Caballero-Folch, F. Calvino, P. J. Coleman-Smith, G. Cortes, T. Davinson, C. Domingo-Pardo, A. Estrade, N. Fukuda, S. Go, C. J. Griffin, J. Ha, O. Hall, L. J. Harkness-Brennan, J. Heideman, T. Isobe, D. Kahl, M. Karny, T. Kawano, L. H. Khiem, T. T. King, G. G. Kiss, A. Korgul, S. Kubono, M. Labiche, I. Lazarus, J. Liang, J. Liu, G. Lorusso, M. Madurga, K. Matsui, K. Miernik, F. Montes, A. I. Morales, P. Morrall, N. Nepal, R. D. Page, V. H. Phong, M. Piersa-Silkowska, M. Prydderch, V. F. E. Pucknell, M. M. Rajabali, B. Rubio, Y. Saito, H. Sakurai, Y. Shimizu, J. Simpson, M. Singh, D. W. Stracener, T. Sumikama, H. Suzuki, H. Takeda, A. Tarifeno-Saldivia, S. L. Thomas, A. Tolosa-Delgado, **M. Wolińska-Cichocka**, P. J. Woods, X. X. Xu. *β -delayed neutron emissions from $n > 50$ gallium isotopes*. Phys. Rev. C **108**(2023) 064307.

D.4 Seminars

D.4.1 Seminars organised at HIL

- M. Pęgiel — Heavy Ion Laboratory, University of Warsaw, 18 January 2023
Warszawa, Poland
Wydzielanie i zateżnianie jonów skandiu przy pomocy ekstrakcji do fazy stałej
Separation and concentration of scandium ions using solid phase extraction
- L. Standylo — Heavy Ion Laboratory, University of Warsaw, 22 February 2023
Warszawa, Poland
Badanie mechanizmu wychwytu jonów i atomów wprowadzanych do plazmy wytwarzanej metodą ECR
Separation and concentration of scandium ions using solid phase extraction
- R. Wolski — Flerov Laboratory of Nuclear Reactions, JINR, 19 April 2023
Dubna
Observation of the ${}^7\text{He}$ system vs. direct reactions approach
- J. Choiński — Heavy Ion Laboratory, University of Warsaw, 26 April 2022
Warszawa, Poland
Informacje o aparaturze pozyskanej z Uppsali
Information about the apparatus acquired from Uppsala
- M. Paluch-Ferszt — Heavy Ion Laboratory, University of Warsaw, 07 June 2023
Warszawa, Poland
Różne oblicza mechaniki kwantowej w filmowym obiektywie.
Different faces of quantum mechanics through a film lens.
- A. Sentkowska — Heavy Ion Laboratory, University of Warsaw, 21 June 2023
Warszawa, Poland
Przypadki chodzą po ludziach
Nieoznaczony Heisenberg. Naukowcy w obliczu II Wojny Światowej.
Accidents happen.
Uncertain Heisenberg. Scientists facing World War II.
- G. Colucci — Heavy Ion Laboratory, University of Warsaw, 18 October 2023
Warszawa, Poland
Barrier distribution studies at HIL: from most recent results to future plans.
- R. Wolski — Institute of Nuclear Physics PAN, Kraków, 06 November 2023
Poland
The presence of s-wave in low energy ${}^7\text{He}$ spectrum seen by the ${}^6\text{He}(d,p){}^7\text{He}$ reaction.

Z. Szeffiński — Heavy Ion Laboratory, Univ. of Warsaw, 13 December 2023
Warszawa, Poland

Słońce, Atom czy Wiatr

Sun, Atom or Wind

D.4.2 Seminars co-organised by HIL

Warsaw Nuclear Physics Seminar

Seminars organised jointly by the divisions of Nuclear Physics and Nuclear Structure Theory of the Faculty of Physics, University of Warsaw and the Heavy Ion Laboratory, University of Warsaw

T. Matulewicz — Inst. of Exp. Physics, University of Warsaw, 12 January 2023
Warszawa, Poland

Konferencja CPOD-2022 – wybrane wrażenia

CPOD-2022 conference – selected impressions

J. Rzadkiewicz — National Centre for Nuclear Research 19 January 2023

Proces wzbudzenia jądra atomowego poprzez wychwyty elektronu do powłoki elektronowej atomu

The process of exciting atomic nuclei by electron capture into the electronic shell of an atom.

J. Golak — Zakład Teorii Układów Jądrowych, Instytut 02 March 2023
Fizyki im. Mariana Smoluchowskiego,
Uniwersytet Jagielloński

Teoretyczne badania układów trzynukleonowych

Theoretical studies of three-nucleon systems

W. Wiślicki — National Centre for Nuclear Research 09 March 2023

Łamanie CP w elektrosłabych oddziaływaniach ciężkich kwarków

CP breaking in electroweak interactions of heavy quarks

L. Zdunik — Centrum Astronomiczne Mikołaja Kopernika 16 March 2023
PAN

Gwiazdy neutronowe jako laboratorium gęstej materii

Neutron stars as a laboratory of dense matter

M. Kowal — National Centre for Nuclear Research 23 March 2023

Wybrane problemy syntezy jąder superciężkich

Selected problems in the synthesis of superheavy nuclei

E. Janiak — National Centre for Nuclear Research 30 March 2023

Pomiar czasu połowicznego zaniku stanu izomerycznego ^{184}Re

Measurement of the half-life of the isomeric state of ^{184}Re

K. Kolos McCubbin — Lawrence Livermore National Laboratory, USA 13 April 2023

Nuclear structure and isomer studies in neutron-rich Sb/Sn isotopes

- I. Dedes — Institute of Nuclear Physics Polish Academy of Sciences, Kraków, Poland 20 April 2023
Exotic Shape Systematics in the $N = 136$ Region: Tracing Predicted Molecular Symmetries in Sub-Atomic Physics: Example of the Actinides
- M. Block — GSI and University of Mainz, Germany 27 April 2023
Structure of heavy nuclei investigated by laser spectroscopy and mass spectrometry at GSI/SHIP
- K. K. KIM — KINGS, Republic of Korea 11 May 2023
Introduction to SMART
- E. V. Pagano — INFN - Laboratori Nazionali del Sud, Catania, Italy 18 May 2023
Isospin influence on nuclear reaction dynamics: firsts results of the CHIFAR experiment at LNS and future perspectives on neutron detection
- R. Lalik — M. Smoluchowski Institute of Physics, Jagiellonian University, Kraków, Poland 25 May 2023
Review of the strangeness physics programme at HADES - past and future perspectives
- H. P. Zbroszczyk — Warsaw University of Technology, Warszawa, Poland 01 June 2023
Strong final state interactions seen by femtoscopy
- M. Fila — Inst. of Exp. Physics, University of Warsaw, Warszawa, Poland 15 June 2023
Investigating photodisintegration reactions with the Warsaw TPC
- A. Kubiela — Inst. of Exp. Physics, University of Warsaw, Warszawa, Poland 05 October 2023
Neutrono-deficytowe izotopy cynku - produkcja, promieniotwórczość dwuprotonowa i inne kanały rozpadu
Neutron-deficient zinc isotopes - production, two-proton radioactivity and other decay channels
- K. Pomorski — Dep. of Theoretical Physics, Inst. of Physics, Maria Curie-Skłodowska Univ., Lublin, Poland 12 October 2023
Low energy nuclear fission dynamics within the 3D Langevin model
- V. G. Gomez — Inst. of Exp. Physics, University of Warsaw, Warszawa, Poland 19 October 2023
Gamma spectroscopy at ISOLDE for isospin mirror asymmetry studies

N. Cieplicka-Oryńczak — Institute of Nuclear Research, Kraków, Poland 26 October 2023
“Stretched” state decays studied at CCB IFJ PAN by gamma-particle coincidences

M. Kubkowska — Instytut Fizyki Plazmy i Laserowej Mikrosyntezy, 09 November 2023
 Warszawa
Obecny stan badań nad syntezą jądrową
The current state of research on nuclear fusion

J. Dobaczewski — Inst. of Exp. Physics, University of Warsaw, 16 November 2023
 Warszawa, Poland
Nuclear DFT electromagnetic moments in heavy deformed open-shell odd nuclei

K. Kacperski — National Centre for Nuclear Research 23 November 2023
Nowa metoda obrazowania za pomocą promieniowania rentgenowskiego rozproszonego wstecznie
A new imaging method using backscattered X-rays

M. Csanad — Eötvös Loránd University, Budapest 14 December 2023
Femtoscscopy with Lévy-stable sources from SPS through RHIC to LHC

Y. Balkova — Uniwersytet Śląski 21 December 2023
Exploring Strangeness: Lambda Baryon Production in Heavy-Ion Collisions with the NA61/SHINE experiment

D.4.3 External seminars given by HIL staff

K. Wrzosek-Lipska 07 February 2023
Probing multiple shape coexistence in ^{110}Cd with Coulomb excitation
 VI Topical Workshop on Modern Aspects in Nuclear Structure, Bormio, Italy

Z. Szeffiński 09 March 2023
Jak zlekceważyć Nagrodę Nobla. Test nierówności Bella dla splątanych kwantów gamma
How to disregard the Nobel Prize. Bell’s inequality test for entangled gamma quanta
 Zakład Fizyki Biomedycznej, UW

K. Hadyńska-Klęk 29 March 2023
SilCA - a new COULEX array at HIL
 4th GOSIA Workshop 2023

M. Palacz 19 April 2023
Direct measurement of proton-neutron matrix elements with respect to the ^{100}Sn core by studying excited states in ^{100}In .
 AGATA zero-degree workshop LNL Legnaro, LNL Legnaro, Italy

- K. Kilian 21 April 2023
Czy w badaniach przedklinicznych jest miejsce dla technik izotopowych?
Is there a place for isotope techniques in preclinical research?
 Konferencja MiDoK'23 Warszawa
- K. Wrzosek-Lipska 04 May 2023
Probing multiple shape coexistence in ^{110}Cd with Coulomb excitation
 Workshop on Shape Coexistence, E0 Transitions, and Related Topics, University of Guelph, Canada
- G. Jaworski 05 May 2023
Gamma spectroscopy studies of neutron-deficient nuclei at HIL
 International Symposium on Physics of Unstable Nuclei 2023 (ISPUN23), Phu Quoc, Vietnam
- K. Hadyńska-Klęk 14 May 2023
Signatures of shape coexistence in $N=Z$ nuclei – studies of nuclear deformation in the vicinity of ^{40}Ca and ^{56}Ni
 ISTROS, Casta Papernicka, Slovakia
- K. Wrzosek-Lipska 14 May 2023
Shape coexistence studied with Coulomb excitation in the ($Z=80$, $N=104$) and ($Z=48$, $N=60$) regions
 ISTROS, Casta-Papiernicka, Slovakia
- P. J. Napiorkowski 17 May 2023
Isospin, Structure, Reactions and energy Of Symmetry
 Častá-Papiernička, ISTROS 2023, Slovakia
- G. Jaworski 28 June 2023
NEEDLE
 International Conference on Proton-Emitting Nuclei, Warsaw
- J. Srebrny 08 July 2023
Experimental proof of chirality by absolute transition probabilities
 Chirality and Wobbling in Atomic Nuclei- CWAN'23 in Huizhou, China
- K. Hadyńska-Klęk 01 September 2023
Studium deformacji jądrowych narzędziami spektroskopii gamma
Study of nuclear deformations using gamma spectroscopy tools
 48 Zjazd Fizyków Polskich
- G. Jaworski 04 September 2023
Sailing with Needle beyond the horizon
 Mazurian Lake Conference on Physics, Piaski
- Z. Szeffiński 07 September 2023
An irradiation system for studying biological effects in glioblastoma cell lines

after exposure to high LET α -particles appearing in BNCT therapy

Mazurian Lake Conference on Physics, Piaski

G. Colucci 07 September 2023

Quasielastic barrier distributions for the $^{20}\text{Ne}+^{92,94,95}\text{Mo}$ systems: Influence of dissipation

Mazurian Lake Conference on Physics, Piaski

I. Piętka 19 September 2023

Study of the electromagnetic structure of ^{110}Cd using the Coulomb excitation method

Badanie struktury elektromagnetycznej jądra ^{110}Cd metodą wzbudzeń kulombowskich

Symposium Młodych Naukowców Wydziału Fizyki UW

K. Kilian 29 September 2023

Determination of radionuclidic impurities in the production of ^{18}F labeled radiopharmaceuticals

V Konferencja Radiofarmaceutyczna, Toruń

G. Colucci 07 September 2023

Barrier distributions studies at HIL: influence of dissipation

II Otwarte Zebranie Sekcji Fizyki Jądrowej Polskiego Towarzystwa Fizycznego, Warszawa

K. Hadyńska-Klęk 20 November 2023

Status of the experimental campaign: nuBall2+PARIS+SiLCA at ALTO

IN2P3-COPIN Workshop, SLCJ UW, Warszawa

G. Colucci 22 November 2023

Dissipation by transfer and its influence on fusion

FUSION23, Shizuoka, Japonia

D.4.4 Poster presentations

B. Zalewski 04 June 2023

Elastic scattering of $^6\text{He}+d$ at 26 MeV/A

ARIS conference, Avignon, France

G. Colucci 07 September 2023

Quasielastic barrier distributions for the $^{20}\text{Ne}+^{92,94,95}\text{Mo}$ systems: Influence of dissipation

Mazurian Lake Conference on Physics, Piaski

G. Jaworski 07 September 2023

Sailing with Needle beyond the horizon

Mazurian Lake Conference on Physics, Piaski

D.4.5 Lectures for students and student laboratories

- K. Hadyńska-Klęk October 2023
Spektroskopia gamma na wiązce
Gamma spectroscopy- beam measurements
XVIII Warsztaty Akceleracji i Zastosowań Ciężkich Jonów, ŚLCJ UW
- O. Nassar October 2023
Akceleracja ciężkich jonów i elementy optyki jonowej
Heavy ion acceleration and elements of ion optics
XVIII Warsztaty Akceleracji i Zastosowań Ciężkich Jonów, ŚLCJ UW
- U. Kaźmierczak October 2023
Gamma kamera – narzędzie do obrazowania medycznego
Gamma camera – a medical imaging tool
XVIII Warsztaty Akceleracji i Zastosowań Ciężkich Jonów, ŚLCJ UW
- U. Kaźmierczak summer semester of the academic year 2022/2023
Laboratorium Techniki Obrazowania- ćwiczenia
Imaging Techniques Laboratory- exercises
- K. Kilian summer semester of the academic year 2022/2023
Radiofarmaceutyki, synteza, wytwarzanie i zastosowania
Radiopharmaceuticals, synthesis, production and applications
Faculty of Chemistry, University of Warsaw, Warszawa, Poland
- K. Kilian summer semester of the academic year 2022/2023
Badania przedkliniczne radiofarmaceutyków
Preclinical testing of radiopharmaceuticals
Faculty of Chemistry, University of Warsaw, Warszawa, Poland
- K. Kilian summer semester of the academic year 2022/2023
Pracownia radiofarmaceutyków
Laboratory of Radiopharmaceuticals
Faculty of Physics, University of Warsaw, Warszawa, Poland
- K. Kilian winter semester of the academic year 2022/2023
Metody izotopowe i chemia radiofarmaceutyków
Radiochemistry and radiopharmacy
Faculty of Physics, University of Warsaw, Warszawa, Poland
- M. Palacz October 2023
Detekcja promieniowania gamma, cząstek naładowanych i neutronów
Detection of gamma radiation, charged particles and neutrons
XVIII Warsztaty Akceleracji i Zastosowań Ciężkich Jonów, ŚLCJ UW

M. Palacz 22 December 2023
Prezentacja ŚLCJ dla studentów Politechniki Warszawskiej
presentation of HIL for students of the Warsaw University of Technology
 Heavy Ion Laboratory, University of Warsaw, Warszawa, Poland

K. Rusek October 2023
Wstęp do fizyki reakcji jądrowych
Introduction to the physics of nuclear reactions
 XVIII Warsztaty Akceleracji i Zastosowań Ciężkich Jonów, ŚLCJ UW

J. Samorajczyk-Pyśk summer semester of the academic year 2022/2023
Pracownia Technik Pomiarowych dla astronomów - ćwiczenia
Laboratory of Measurement Techniques for astronomers - exercises
 Faculty of Physics, University of Warsaw, Warszawa, Poland

A. Sentkowska winter semester of the academic year 2022/2023
Spektrofotometryczna różnicowa metoda oznaczania acylowanych antocyjanów w bluszczu
Differential spectrophotometric method for the determination of acylated anthocyanins in ivy
 Faculty of Chemistry, University of Warsaw, Warszawa, Poland

Z. Szefliński summer semester of the academic year 2022/2023
Laboratorium technik obrazowania. Narzędzia diagnostyki medycznej
Laboratory imaging technics. Medical diagnostic tools.
 Faculty of Physics, University of Warsaw, Warszawa, Poland

Z. Szefliński Summer 2023
Fizyka w diagnostyce i terapii medycznej, PET – wiązki terapeutyczne
Physics in medical diagnosis and therapy, PET – therapeutic beams
 Faculty of Physics, University of Warsaw, Warszawa, Poland

Z. Szefliński May 2023
Fizyka w diagnostyce medycznej PET-SPECT
Physics in PET-SPECT medical diagnostics
 Faculty of Physics, University of Warsaw, Warszawa, Poland

K. Wrzosek-Lipska 27 March 2023
Normalisation in Coulomb excitation experiments
 4th GOSIA Workshop, Heavy Ion Laboratory, University of Warsaw, Warszawa, Poland

D.4.6 Science popularization lectures

K. Hadyńska-Klęk Polish Physical Society

Woda - co o niej wiesz? Fizyczna Karuzela oraz POWER
Water - what do you know about it? Physical Carousel and POWER

- P. J. Napiorkowski II LO im. Marii Skłodowskiej-Curie 31.05.2023
Gdzie się kończy tablica Mendelejewa?
Where does Mendeleev's table end?
- P. J. Napiorkowski II LO im. Marii Skłodowskiej-Curie 08.11.2023
Reaktory jądrowe: inspiracje i nadzieje
Nuclear reactors: inspirations and hopes
- A. Sentkowska 27 Festiwalu Nauki 27.09.2023
Przypadki chodzą po ludziach czyli o przypadkowych odkryciach w chemii
Accidents happen to people, i.e. accidental discoveries in chemistry
- A. Sentkowska 27 Festiwalu Nauki 28.09.2023
Nieoznaczony Heisenberg. Naukowcy w obliczu II Wojny Światowej
Uncertain Heisenberg. Scientists facing World War II
- Z. Szeffiński CLVII LO im. Marii Skłodowskiej-Curie 7.06.2023
Radon wokół nas
Radon around us
- Z. Szeffiński XLVIII LO im. Edwarda Dembowskiego 4.10.2023
Radon wokół nas
Radon around us
- Z. Szeffiński Festiwal Nauki 16.09.2023
Słońce atom czy wiatr
Sun, atom or wind
- Z. Szeffiński Festiwal Nauki 27.09.2023
Słońce atom czy wiatr
Sun, atom or wind
- G. Colucci Meeting of the Heavy Ion Laboratory Council 18.12.2023
Barrier distributions studies at HIL

D.5 Honours and Awards

Rector's distinction for scientific achievements 2023 received

Dr. Eng. Grzegorz Maria Jaworski.

Individual awards of the 3rd degree Rhetor of the University of Warsaw for scientific achievements were awarded to:

Ph.D. Marcin Palacz - for organizing and managing the successful international NEEDLE measurement campaign using the NEDA detection system and the EAGLE gamma-ray spectrometer,

Ph.D. Aleksandra Sentkowska - for research entitled: "Methodological aspects in determining selenium speciation" resulting in obtaining a habilitated doctor's degree.

The Rector of the University of Warsaw awards in 2023 received the following employees of the Heavy Ion Laboratory:

Tomasz Abraham,
Mariusz Antczak,
Eliza Balcerowska,
Tomasz Braha,
Jarosław Choiński,
Antoni Dąbkowski,
Piotr Jasiński,
Wiesław Kalisiewicz,
Robert Kopik,
Marian Kopka,
Michał Kowalczyk,
Mariusz Matuszewski,
Jan Miszczak,
Anna Odziemczyk,
Bogdan Radomyski,
Anna Ratyńska,
Justyna Samorajczyk-Pyśk,
Nurullo Sobirov,
Lidia Strzelczyk,
Edyta Szelaąg,
Mariusz Szperkiewicz,
Marzena Wolińska-Cichocka.

D.6 Laboratory staff

Director: Paweł Napiorkowski
Deputy directors: Jarosław Choiński, Leszek Próchniak
Financial executive: Eliza Balcerowska

Senior scientists:

Krzysztof Kilian, Andrzej Kordyasz^a, Marcin Palacz, Ernest Piasecki^a, Krzysztof Rusek^a, Aleksandra Sentkowska, Anna Stolarz, Zygmunt Szeffiński^a

Scientific staff and engineers:

Tomasz Abraham, Andrzej Bednarek, Giulia Colucci, Przemysław Gmaj, Katarzyna Hadyńska-Klęk, Grzegorz Jaworski, Grzegorz Kamiński^b, Urszula Kaźmierczak, Maciej Kisieliński, Michalina Komorowska, Marian Kopka, Michał Kowalczyk, Katarzyna Krutul-Bitowska^c, Ireneusz Mazur, Jan Miszczak, Olga Nassar, Wojciech Okliński^a, Monika Paluch-Ferszt, Serhii Panasenko, Mateusz Pęgier, Bogdan Radomyski, Justyna Samorajczyk-Pyśk, Paulina Sekrecka^d, Andrej Špaček^e, Julian Srebrny^a, Łukasz Standyło, Roman Tańczyk^f, Agnieszka Trzcińska, Andrzej Tucholski, Marzena Wolińska-Cichocka, Katarzyna Wrzosek-Lipska

Doctoral candidates:

Patrycja Chuchala^g, Patrycja Kamińska^g, Iwona Piętka^g, Bogumił Zalewski

Technicians:

Mariusz Antczak, Tomasz Bracha, Piotr Jasiński, Wiesław Kalisiewicz, Robert Kopik, Wojciech Kozaczka, Zbigniew Kruszyński^a, Piotr Krysiak, Krzysztof Łabęda, Kamil Makowski, Mariusz Matuszewski, Bogusław Paprzycki, Krzysztof Pietrzak, Robert Ratyński, Mariusz Szperkiewicz, Łukasz Świątek

Administration and support:

Anna Błaszczuk-Duda, Antoni Dąbkowski, Maciej Durkiewicz, Andrzej Giziński, Radosław Jaielski, Tadeusz Jagielski, Rafał Klęk, Joanna Kowalska, Jolanta Matuszczak, Aleksander Morantowicz, Anna Odziemczyk, Jolanta Ormaniec^c, Anna Ratyńska, Mirosław Rogalski, Ewa Sobańska, Nurullo Sobirov, Lidia Strzelczyk, Edyta Szela^a, Lech Szela^a, Katarzyna Włodarczyk^a, Magdalena Zawal

Voluntary scientists:

Jędrzej Iwanicki, Jan Kownacki, Andrzej Wojtasiewicz.

^apart time

^bon leave

^con maternity leave

^dsince 15 November

^esince 16 October

^funtil 30 April

^gsince 1 October

D.7 Laboratory Council

1. Prof. dr hab. Józef Andrzejewski
Nuclear Physics Division
University of Łódź, Łódź
2. Prof. dr hab. Mieczysław Budzyński
Institute of Physics
Maria Curie-Skłodowska University, Lublin
3. Prof. dr hab. Ewa Bulska
Biological and Chemical Research Centre
University of Warsaw, Warszawa
4. Dr Jarosław Choiński
Heavy Ion Laboratory
University of Warsaw, Warszawa
5. Prof. dr hab. Zbigniew Czerski
Institute of Physics
University of Szczecin, Szczecin
6. Prof. dr hab. inż. Andrzej Chmielewski
(Member of the Council Presidium)
Institute of Nuclear Chemistry
and Technology, Warszawa
7. Prof. dr hab. Bogdan Fornal
The Henryk Niewodniczański
Institute of Nuclear Physics
Polish Academy of Sciences, Kraków
8. Dr hab. Krzysztof Kilian
Heavy Ion Laboratory
University of Warsaw, Warszawa
9. Prof. dr hab. Stanisław Kistryn
(Member of the Council Presidium)
M. Smoluchowski Institute of Physics
Jagiellonian University, Kraków
10. Dr hab. Agnieszka Korgul, prof. UW
Faculty of Physics
University of Warsaw, Warszawa
11. Dr hab. Michał Kowal, prof. NCBJ
The National Centre for Nuclear Research
Świerk
12. Prof. dr hab. n. med Leszek Królicki
Department of Nuclear Medicine
Medical University of Warsaw, Warszawa
13. Prof. dr hab. inż. Krzysztof Kurek
(Member of the Council Presidium)
The National Centre for Nuclear Research
Świerk
14. Prof. dr hab. Adam Maj
(Chairman of the Council)
The Henryk Niewodniczański
Institute of Nuclear Physics
Polish Academy of Sciences, Kraków
15. Prof. dr hab. inż. Piotr Magierski
Faculty of Physics
Warsaw University of Technology,
Warszawa
16. Dr hab. Krzysztof Miernik, prof. UW
Faculty of Physics
University of Warsaw, Warszawa
17. Dr Paweł Napiorkowski
(Director of HIL)
Heavy Ion Laboratory
University of Warsaw, Warszawa
18. Dr hab. Marcin Palacz
Heavy Ion Laboratory
University of Warsaw, Warszawa
19. Dr hab. Leszek Próchniak
Heavy Ion Laboratory
University of Warsaw, Warszawa
20. Prof. dr hab. Krzysztof Rusek
Heavy Ion Laboratory
University of Warsaw, Warszawa
21. Prof. dr hab. Wojciech Satuła
(Deputy Chairman of the Council)
Faculty of Physics
University of Warsaw, Warszawa
22. Dr hab. Elżbieta Stephan, prof. US
Institute of Physics
University of Silesia, Katowice
23. Dr Agnieszka Trzecińska
(representative of the HIL staff)
Heavy Ion Laboratory
University of Warsaw, Warszawa

D.8 Programme Advisory Committee

PAC members

- Piotr Bednarczyk (Institute of Nuclear Physics Polish Academy of Sciences, Kraków, Poland)
- Gilles de France (GANIL, Caen, France)
- Nicholas Keeley (National Centre for Nuclear Research, Otwock, Poland)
- Marco Mazzocco (Padova University, Padova, Italy)
- Chiara Mazzocchi (Faculty of Physics, University of Warsaw, Warszawa, Poland)
- Leszek Próchniak (Heavy Ion Laboratory, University of Warsaw, Warszawa, Poland)
- **Władysław Trzaska (Department of Physics, University of Jyväskylä, Finland) - Chair**

The international Programme Advisory Committee of the Heavy Ion Laboratory usually meets twice a year, in spring and autumn. The deadline for submitting proposals is 3 - 4 weeks before a PAC meeting. PAC approved experiments are scheduled at the meetings of the Users' Committee, which also serves as a link between cyclotron users and the Laboratory. The Users' Committee is chaired by Jarosław Perkowski (University of Łódź).

D.9 External HIL users

From 2023, external HIL users must register before arrival. In 2023 there were **84** external HIL users and visitors from **39** scientific institutions, including 38 people from 12 institutes in Poland, 30 people from 13 institutions in the European Union and associated countries and 16 people from 8 institutes in other countries.

External HIL users and visitors were from:

Poland

- AGH University of Science and Technology, Kraków, Poland
- Faculty of Biology, University of Warsaw, Warszawa, Poland
- Faculty of Chemistry, University of Warsaw, Warszawa, Poland
- Faculty of Physics, University of Warsaw, Warszawa, Poland
- Institute of Nuclear Physics Polish Academy of Sciences, Kraków, Poland
- Faculty of Physics, Astronomy and Applied Computer Science, Jagiellonian University, Kraków, Poland
- Faculty of Physics and Applied Computer Science, University of Lodz, Łódź, Poland
- Faculty of Science and Technology, University of Silesia, Chorzów, Poland
- National Centre for Nuclear Research, Otwock, Poland
- Poznań University of Technology, Poznań, Poland
- University of Silesia, Katowice, Poland
- Warsaw University of Technology, Warszawa, Poland

European Union and associated countries

- Department of Physics, University of Jyväskylä, Finland
- Department of Physics and Astronomy, University of Catania, Catania, Italy
- Dipartimento di scienze MIFT, Università di Messina, Messina, Italy
- GSI Helmholtz Center for Heavy Ion Research, Darmstadt, Germany
- HUN-REN Institute for Nuclear Research (HUN-REN ATOMKI), Debrecen, Hungary
- Institute for Nuclear Physics, University of Cologne, Germany
- Institut für Kernphysik, Universität zu Köln, Köln, Germany
- INFN Sezione di Catania, Catania, Italy
- INFN, Laboratori Nazionali di Legnaro, Legnaro, Italy
- IRFU, CEA, Université Paris-Saclay, Gif-sur-Yvette, France
- KTH Royal Institute of Technology, Stockholm, Sweden
- Laboratoire de Physique des 2 infinis Irène Joliot-Curie – IJCLab, Orsay, France
- Physics Department, University of Lund, Lund, Sweden

Other countries

- Department of Physics, University of Liverpool, Liverpool, UK
- Department of Chemistry, Simon Fraser University, Burnaby, Canada
- Department of Physics, University of York, York, UK
- Fac. of Engineering and Natural Sciences, Istanbul Sabahattin Zaim Univ. Istanbul, Turkey
- Institute of Modern Physics, Chinese Academy of Science, Lanzhou, China
- Nigde Univ., Fen-Edebiyat Fakültesi, Fizik Bölümü, Nigde, Turkey
- Physics Department, Ege University, Izmir, Turkey
- University of the West of Scotland, Paisley, UK

List of Authors

- Abraham T., 18, 22, 59
Ahlgren Cederlöf E., 47
Andreoiu C., 56
Antczak M., 13, 14
Astier A., 56
- Beckers M., 56, 59
Bednarczyk P., 47, 52
Bednarek A., 9, 17
Bilewicz A., 40
Bracha T., 9, 14, 17, 19, 40
Briscoe A., 56
- Cap T., 52
Chen Q.B., 59
Choiński J., 9, 11, 13, 14, 19, 40
Chuchała P., 27
Ciemala M., 47, 52
Cieplicka-Oryńczak N., 52
Colucci G., 27, 47, 62
- Dedes I., 52
de Angelis G., 52
Droste Ch., 59
Dunkel F., 56
- Fijałkowska A., 47
Fransen C., 56, 59
- Gajewska I., 52
Garrett P.E., 68
Geraci E., 62
Gmaj P., 9
Gniazdowska E., 40
Gnoffo B., 62
Goasduff A., 47, 50
Grahm T., 56
Grodner E., 56, 59
Grudniak A., 33
Gryczka U., 27
Grębosz J., 47, 52, 56
Guadilla V., 47
Guo S., 56
Górska M., 47
- Hadyńska-Klęk K., 22, 27, 47, 52, 56, 62, 65
Hiver C., 47, 65
Hrabar Y., 47
- Iskra L., 52
- Jasiński P., 9, 13, 14
Jaworski G., 22, 27, 47, 50, 52, 56, 59, 62
Jodidar P.M., 56
- Kalisiewicz K., 9, 13
Kamińska P., 27
Kaźmierczak U., 27
Kilian K., 27, 35, 38
Kisieliński M., 22, 47, 62
Kmieciak M., 52
Koczoń P., 62
Komorowska M., 22, 27, 47, 52, 56
Konarska J., 33
Kopeć M., 52
Kopik R., 13, 14, 19
Kopka M., 9, 14
Korgul A., 47
Kornweibel L., 56
Kowalczyk M., 22, 27, 47, 52, 56, 59, 62
Kowalska J.A., 19, 24, 27, 40, 47, 52, 62
Kozaczka W., 9
Kožmiński P., 40
Krakó A., 47, 52, 56
Krutul-Bitowska K., 56
Kruzsicz B., 47, 52
Krysiak P., 9, 14
Kulesa P., 47
Kuti I., 22, 47, 50, 52, 56
Kwiatkowska A., 59
- Lakenbrink C., 56, 59
Leifels Y., 62
Lommel B., 62
Loriggiola M., 52
Lv B.F., 56
Łabęda K., 9, 13, 14
- Macdonalds N., 56
Makowski K., 9, 11, 18

- Malinowski A., 22, 47, 52
Masłowska K., 40
Matejska-Minda M., 47, 52
Matuszewski M., 14, 22, 47, 50, 52
Mazurek K., 52
Mazur I., 9
Mazzocchi C., 47
McCarter A., 56
Mezhevych S.Yu., 74
Miernik K., 47
Miszczak J., 9, 14
Molnár J., 22, 47, 50, 52

Napiorkowski P.J., 22, 27, 52, 56, 65, 68
Nassar O., 9, 11, 19, 27, 40
Nałęcz-Jawecki A., 47, 56, 59

Okliński W., 22, 47
Orliński J., 59
Otręba A., 52

Pęgiel M., 35, 38
Palacz M., 14, 22, 24, 27, 47, 50, 52, 56, 59
Palkowski M.M., 56
Paluch-Ferszt M., 27, 59
Panassenko S., 22, 47
Paprzycki B., 9, 13
Pasqualato G., 65
Petrahe C.M., 56
Piasecki E., 62
Pietrzak K., 9
Piętka I., 22, 27, 47, 68
Podwysocka A., 59
Poklepa W., 52, 56
Próchniak L., 68
Pyrzyńska K., 31, 35, 38

Radomyski B., 9, 13, 14, 19
Ratyński R., 14
Razzaq N., 40
Regulska M., 47, 52
Risitano F., 62
Rudchik A.T., 74
Rusek K., 27, 74

Samorajczyk-Pyśk J., 22, 27, 47, 52, 56, 59,
62
Sarén J., 56
Sekrecka P., 22, 47, 52
Sentkowska A., 31, 33

Skwira-Chalot I., 59
Smolira O., 59
Sohler D., 56
Sosnowski K., 17
Spagnoletti P., 56
Srebrny J., 56, 59
Standyło Ł., 9, 11, 18
Stolarz A., 19, 24, 27, 40, 47, 52, 59, 62
Strawski M., 24
Sudlitz K., 11
Szeffiński Z., 27
Szmytke J., 33
Szymanek A., 47
Świątek Ł., 19, 40
Špaček A., 22, 27, 47, 52

Tańczyk R., 19, 40
Toniolo N., 47
Towers J., 52
Trimarchi M., 62
Trzaska W.H., 62
Trzcińska A., 27, 62
Tucholski A., 22, 47, 56, 59, 62

Uusikyla E., 56
Uusitalo J., 56

von Spee F., 56, 59

Walczak R., 40
Wilson J., 65
Wolińska-Cichocka M., 27, 62
Wrzosek-Lipska K., 22, 47, 56, 68
Wu F., 56

Zagami C., 62
Zalewski B., 62
Zheng K.K., 56
Zielińska M., 68